INCORPORATING ACOUSTICAL CONSISTENCY IN THE DESIGN FOR MANUFACTURING OF WOODEN GUITARS

Patrick Dumond

A thesis submitted to the Faculty of Graduate and Postdoctoral Studies
in partial fulfillment of the requirements for the

DOCTORATE IN PHILOSPHY

degree in Mechanical Engineering

Ottawa-Carleton Institute for Mechanical and Aerospace Engineering
Faculty of Engineering
University of Ottawa

Abstract

As a musical instrument construction material, wood is both musically and aesthetically pleasing. Easy to work and abundant, it has traditionally been the material of choice. Unfortunately, wood is also a very inconsistent material. Due to great environmental and climatic variations, wooden specimens present large variations in their mechanical properties, even within species of a similar region. Surprisingly, an industry based entirely on acoustics has done very little to account for these variations. For this reason, manufactured wooden guitars are acoustically inconsistent.

Previous work has shown that varying the dimensions of a guitar soundboard brace is a good method for taking into account variations in the mechanical properties of the wooden soundboard plate. In this thesis, the effects of a scalloped-shaped brace on the natural frequencies of a brace-plate system have been studied and tools have been developed in order to calculate the dimensions of the brace required to account for variations in the mechanical properties of the plate.

It has been shown that scalloped braces can be used to modify two natural frequencies of a brace-plate system simultaneously. Furthermore, the most important criteria in modifying any given frequency of a brace-plate system is the mass and stiffness properties of the brace at the antinode of the given frequency's associated modeshape.

Subsequently, designing a brace for desired system natural frequencies, by taking into account the mechanical properties of the wooden plate, is an inverse eigenvalue problem. Since few methods exist for solving the inverse eigenvalue problem of general matrices, a new method based on the generalized Cayley-Hamilton theorem was proposed in the thesis. A further method, based on the determinant of the generalized eigenvalue problem was also presented. Both methods work well, although the determinant method is shown to be more efficient for partially described systems.

Finally, experimental results were obtained for the natural frequencies of simply supported wooden plates, with and without a brace, as well as the inverse eigenvalue determinant method. Good correlation was found between theoretical and experimental results.

***

Le bois, ressource abondante et matière facile à travailler, représente un matériau de construction agréable tant sur le plan musical qu'esthétique. Pour cette raison, il a été traditionnellement le matériau de choix pour les instruments de musique. Malheureusement, en raison des grandes variations climatiques et environnementales, le bois représente aussi d'importantes variations dans ses propriétés mécaniques, et ce, même pour le bois provenant de régions semblables. Fait étonnant, une industrie axée complètement sur l'acoustique ne prend même pas en compte ces variations. C'est pourquoi les guitares acoustiques faites de bois ont des propriétés acoustiques variables.

Des études antérieures ont démontré qu'en changeant les dimensions des barres de la table d'harmonie d'une guitare, il est possible de tenir compte des variations dans les propriétés mécaniques de la table d'harmonie. Dans la présente thèse, les effets d'une barre festonnée sur les fréquences naturelles d'une plaque à barre ont été étudiés et des outils ont été développés pour calculer les dimensions de la barre nécessaire pour tenir compte des variations dans les propriétés mécaniques de la plaque.

Il a été démontré que les barres festonnées peuvent être utilisés pour modifier simultanément deux fréquences naturelles de la plaque à barre. De plus, pour modifier n'importe quelle fréquence de la plaque à barre, les critères les plus importants sont les propriétés de masse et de rigidité de la barre au ventre du mode vibratoire associé à la fréquence spécifiée.

Par la suite, le problème inverse des valeurs propres est développé pour la conception de la barre à partir des fréquences naturelles du système désiré en prenant en compte les propriétés mécaniques de la plaque de bois. Une nouvelle méthode basée sur le théorème général de Cayley-Hamilton est proposée dans cette thèse puisqu'il existe très peu de méthodes pour des matrices de forme générale. Une autre méthode basée sur le déterminant du problème des valeurs propres général est également présentée. Il est démontré que les deux méthodes fonctionnent bien; cependant, la méthode du déterminant s'annonce plus efficace pour les systèmes partiellement décrits.

Finalement, des résultats expérimentaux ont été obtenus pour les fréquences naturelles d'une plaque de bois à appui simple, avec et sans barre. Une comparaison entre les résultats théoriques et expérimentaux démontre une bonne corrélation.

Acknowledgments

First and foremost, I would like to thank my whole family for helping me through and putting up with yet another one of my crazy projects. You are all very patient and understanding. I would especially like to thank my lovely wife, Geneviève, to whom I owe more than I can acknowledge with words, especially a few home cooked meals.

I would like to thank my supervisor, Dr. Natalie Baddour, for being an awesome supervisor and knowing exactly what I need to git'er done. Everyone knows that you are "brilliant" (it says so on your mug), but you also know how to inspire us to find all the solutions to our problems. I would also like to thank Dr. Baddour for giving me the opportunity to attend many conferences, which have allowed me to gain a tremendous amount of experience, expand my knowledge and increase my worldly view. Finally, I must thank her for believing in my capabilities from day one when I first presented this zany idea.

I would like to thank all my officemates in the dungeons of CBY B08D including, Zach, Peter, Nick, Shaun, Véro, Scott, Frank, Lucas, Farhad, Aslan and Sanaz, as well as all my fellow MCG grad students over the course of the last seven years. You made it all fun and worthwhile. I would especially like to thank Farhad for working on inverse eigenvalue problems with me, even if your paper using my method got published before my method did! ;)

I would like to thank all the professors, administrative staff and shop guys for making my life easier, wiser and overall more enjoyable.

Finally, I would like to thank my son, Theodore, to whom this PhD is dedicated. I hope that when you grow up, you will be inspired to do exactly what it is you want to do. Don't ever let anyone tell you what you can or can't do. I will love you forever.

Table of Contents

Chapter 1 Introduction 1

1.1 Literature Review 3

1.2 Motivation 12

1.3 Outline of the Thesis 13

Chapter 2 Effects of Using Scalloped Shape Braces on the Natural Frequencies of a Brace-Soundboard System 15

2.1 Abstract 16

2.2 Introduction 16

2.3 Analytical Model 18

2.4 Results 22

2.5 Discussion 28

2.6 Conclusions 29

2.7 Acknowledgment 30

2.8 References 30

Chapter 3 Effects of a Scalloped and Rectangular Brace on the Modeshapes of a Brace-Plate System 33

3.1 Abstract 34

3.2 Introduction 34

3.3 Model 37

3.4 Results 41

3.5 Conclusion 47

3.6 References 47

Chapter 4 A Structured Approach to Design-for-Frequency Problems Using the Cayley-Hamilton Theorem 50
4.1 Abstract 51
4.2 Introduction 51
4.3 Problem Definition 54
4.4 Cayley-Hamilton Theorem 55
4.5 Analysis 60
4.6 Discussion 64
4.7 Conclusion 67
4.8 Appendix - Example of using the Cayley-Hamilton inverse method for brace design 67
4.9 Acknowledgments 73
4.10 References 73
Chapter 5 A Structured Method for the Design-for-Frequency of a Brace-Soundboard System Using a Scalloped Brace 78
5.1 Abstract 79
5.2 Introduction 79
5.3 Model 81
5.4 Results 89
5.5 Discussion 97
5.6 Conclusion 100
5.7 Acknowledgments 101
5.8 References 101
Chapter 6 Experimental Investigation of the Mechanical Properties and Natural Frequencies of Simply Supported Sitka Spruce Plates 103
6.1 Abstract 104
6.2 Introduction 105
6.3 Specimen Samples 106
6.4 Methods 107
6.5 Results 115
6.6 Conclusion 122

6.7 Acknowledgements 122
6.8 References 123
Chapter 7 Natural Frequencies and Modeshapes of Simply Supported Sitka Spruce Plates With and Without a Brace 125
7.1 Dimensions 125
7.2 Mechanical Properties 126
7.3 Natural Frequencies and Modeshapes 127
7.4 Discussion 129
7.5 Measurement errors 131
Chapter 8 Summary, Conclusions and Future Work 132
8.1 Summary 132
8.2 Conclusions 133
8.3 Recommendations for Future Work 134
Appendix A Maple Code for the Assumed Shape Method Scalloped Braced-Plate Model 136
Appendix B Maple Code for the Cayley-Hamilton Inverse Eigenvalue Method 142
Appendix C Maple Code for the Determinant Inverse Eigenvalue Method 144
Appendix D ANSYS Code for the Finite Element Method Scalloped Braced-Plate Model 146
References 149

List of Figures

Figure 1. Quality control measurement of soundboard plate used in industry. 3
Figure 2. Underside of braced guitar soundboards. 9
Figure 3. Plainsawn versus quartersawn wood. 11
Figure 4. Orthogonal properties of quartersawn wood. 11
Figure 5. Shape of a scalloped brace 18
Figure 6. Orthotropic plate reinforced with a scalloped brace..... 19
Figure 7. Location of cross-section for modeshape comparison. 27
Figure 8. Section "A-A" comparison of $m_x \times m_y$ modeshapes: a. 1×1, b. 2×1 and c. 1×2. 27
Figure 9. Scalloped brace with affected frequencies. 28
Figure 10. Effect of a negative peak height adjustment factor. 29
Figure 11. Shape of a scalloped brace. 37
Figure 12. Orthotropic plate reinforced by a scalloped brace..... 37
Figure 13. Location of cross-section for modeshape comparison. 42
Figure 14. Section "A-A" comparison of modeshapes: a. 1×1, b. 2×1, c. 1×2. 43
Figure 15. Location of cross-section for modeshape comparison. 43
Figure 16. Section "B-B" comparison of modeshapes: a. 1×1, b. 2×1, c. 1×2. 44
Figure 17. Location of cross-section for modeshape comparison. 44
Figure 18. Section "C-C" comparison of modeshapes: a. 1×1, b. 2×1, c. 1×2. 45
Figure 19. 2DOF spring-mass system. 58
Figure 20. Orthotropic plate reinforced with a rectangular brace. 68
Figure 21. Cross section of the brace-plate system's fundamental modeshape. 69
Figure 22. Orthotropic plate reinforced with a scalloped brace..... 82
Figure 23. Shape of a scalloped brace. 82
Figure 24. Quartersawn Sitka spruce plate. 89

Figure 25. The effect of a negative peak height adjustment factor. 97
Figure 26. Sectioned soundboard. 107
Figure 27. Three point bending test rig. 108
Figure 28. Two point plate twist test rig. 110
Figure 29. Tension test rig. 111
Figure 30. Experimental simply supported boundary conditions. 113
Figure 31. Experimental frequency test frame. 114
Figure 32. Frequency tests experimental setup. 115
Figure 33. Experimental modeshapes for the simply supported plates. 128
Figure 34. Experimental modeshapes for the simply supported plate with scalloped brace. 129
Figure 35. FEA modeshapes for the simply supported plate with scalloped brace. 129

List of Tables

Table 1. Material properties for Sitka spruce as an orthotropic material..... 23
Table 2. Model dimensions..... 23
Table 3. First 5 natural frequencies of the benchmark soundboard..... 24
Table 4. Natural frequency variation with changes in E_R..... 25
Table 5. Natural frequency variation with changes in h_{bo} ($\lambda = 1$)..... 25
Table 6. Compensation for variations in soundboard stiffness..... 26
Table 7. Orthotropic material properties of Sitka spruce..... 41
Table. 8. Model dimensions..... 41
Table 9. Material properties..... 71
Table 10. Dimensions of brace-plate model..... 71
Table 11. Results of the inverse model analysis..... 72
Table 12. Calculated frequencies of the inverse model analysis..... 72
Table 13. Alternate brace thickness solution satisfying the physical constraints..... 72
Table 14. Material properties for Sitka spruce as an orthotropic material..... 89
Table 15. Model geometric dimensions..... 90
Table 16. First five natural frequencies of the benchmark system..... 91
Table 17. Results of the Cayley-Hamilton method..... 93
Table 18. Other calculated partial frequencies..... 94
Table 19. Results of the determinant method..... 95
Table 20. Results of a previous study using trial and error..... 95
Table 21. Alternate solutions found by expanding the constraints..... 97
Table 22. Measured dimensions of the test specimens..... 116
Table 23. Experimentally measured mechanical properties of Sitka spruce..... 116
Table 24. Mechanical property ratios with regards to E_L..... 118

Table 25. Calculated fundamental frequencies of the simply supported spruce plates. . 119
Table 26. Partial frequencies calculated using mechanical property simplifications (Hz). 120
Table 27. Theoretical and experimental frequencies for the 1x1, 1x2 and 2x1 modes (Hz). 120
Table 28. Theoretical and experimental frequencies for the 1x3 and 2x2 modes (Hz). . 121
Table 29. Measured dimensions of the test plates. 126
Table 30. Measured dimensions of the test brace. 126
Table 31. Experimentally measured mechanical properties of the plates. 127
Table 32. Experimental and approximate values for the mechanical properties of the brace. 127
Table 33. Theoretical and experimental frequencies for the simply supported plates (Hz). 128
Table 34. Theoretical and experimental frequencies for the simply supported plates (Hz). 129

Nomenclature

a: Variable

A: Variable matrix

b: depth

b: Variable

B: Variable matrix

C: Polynomial coefficients

D: Stiffness function

D: Diagonal length

E: Young's modulus

G: Shear modulus

GF: Gauge factor

h: Thickness

i: Counter

I: Identity matrix

I: Second moment of area

j: Counter

k: Stiffness

K: Stiffness matrix

K: Point of application correction factor

l: length

L: Longitudinal axis parallel to the wood grain

L_x: Length along the x axis

L_y: Length along the y axis

m: Mode number

m: Mass

M: Mass matrix

MC: Moisture content

n: Trial function number

n: System order

p: Polynomial equation

P: Load

q: Time function

R: Radial axis normal to the growth rings and perpendicular to the wood grain

R: Electrical resistance

s: Span

S: Span at points of application

S: Stiffness components

t: Time

T: Kinetic energy of the system

T: Tangential axis tangent to the growth rings and perpendicular to the wood grain

U: Strain energy of the system

V: Volume

w: Displacement along the z axis

x: Axis direction and position

y: Axis direction and position

z: Axis direction and position

ε: Strain

λ: Peak height adjustment factor

λ: Eigenvalue

μ: Density

ν: Poisson's ratio

ρ: Mass per area

σ: Standard deviation

φ: Trial function

ω: Natural frequency

Chapter 1

Introduction

Unlike other engineering materials, consistency is something that eludes wood. While inconsistencies in other materials are often due to processes which have the ability to be controlled, wood is created via a natural and uncontrollable process, with a variable climate taking a large toll on wood's material properties. This is clearly evidenced by the heavy use of statistical averages in the wood industry as demonstrated in [1]. While wood does demonstrate certain favourable properties, such as being a renewable resource, having high strength-to-weight ratios and being easy to work with, its lack of engineering consistency has proven to be problematic when used in design. The structural wood industry has overcome this deficiency by using the statistical 5^{th} percentile in wood's strength properties in order to ensure adequate design specifications of structures [2]. Combined with the stress-sharing nature of today's engineered structures, wood has proven itself to be a versatile structural material.

Although wood has been used in acoustic applications for as long as it has been used in structural applications, its ability to be acoustically engineered is not as refined. The primary reason is that while variations in wood's properties can be accommodated in a structural application by over-designing the structure, acoustical frequencies are precisely controlled by the properties of the wood itself. Therefore, a variation in material properties correlates directly to a variation in acoustical frequencies. It is thus necessary to compensate for the variation in the physical properties of the wood by modifying its dimensional properties. Musical instrument makers have been accounting for these variations empirically for centuries using various techniques [3]. Typically, a very stiff

wood specimen producing higher frequencies will be made thinner and thus less stiff, lowering its natural frequencies. This is true since the stiffness is related to the square of the depth [4]. Mass also has a significant effect on the natural frequencies. Therefore, it is important to ensure that material is removed in a way which will reduce the stiffness of the specimen more than the mass or vice-versa. A previous study has also demonstrated that frequencies can be controlled by modifying the dimensions of a brace in a brace plate system [5].

Great strides have been made recently in the manufacturing of wooden musical instruments. Dimensional tolerances and quality control have increased significantly due to the introduction of computer controlled machinery and through the use of laser cutting. These advances have significantly increased the output dimensional consistency of wooden musical instruments [6]. However, it is commonly observed that no two manufactured instruments sound alike. Although empirical methods for adjusting the frequencies of a musical instrument have been used for years by luthiers [7], these techniques are generally considered too time-consuming and require highly skilled labour. For these reasons, including acoustical consistency in the mass-manufacture of wooden musical instruments is not considered to be cost effective. Regardless, if any progress is to be made in improving acoustical consistency during manufacturing, knowledge of the mechanical properties of the wood used during construction would be an asset. Measurements of any mechanical properties of the wood is uncommon during manufacturing and still somewhat primitive [8]. Godin Guitars take a rough measure of the guitar's soundboard stiffness in the radial direction, as shown in Figure 1, and then decides for which instrument line it is most suited, based on the result of the plate's displacement under a known force in a three point bending test.

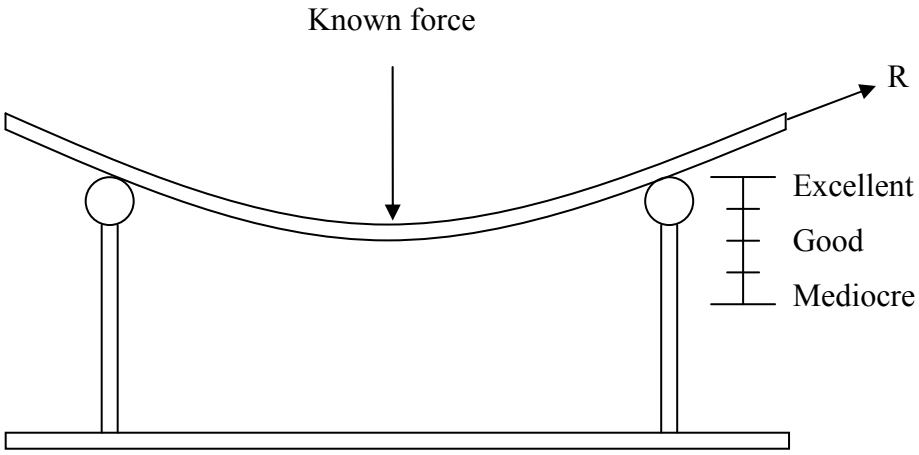

Figure 1. Quality control measurement of soundboard plate used in industry.

For the wooden guitar manufacturing industry to improve acoustical consistency during production, exact knowledge of the wood's mechanical properties will be required.

1.1 Literature Review

1.1.1 Musical Acoustics

Over the last half century, a great deal of research has been done to advance the science of musical acoustics. A large focus of this research has been on understanding the fundamental principles of sound generation in musical instruments [9] and also how these affect the resulting sound field. Most research on guitars and other musical instruments has focused on their modal properties, as well as their radiated sound field (what is perceived by the listener). Recently, the numerical and experimental modeling of guitars, and their soundboards in particular, have been rigorously studied. Techniques using holography and laser interferometry for visualizing the soundboard and box of guitars have proven particularly useful in studying their resonant properties [10]–[14].

The numerical and experimental study of the radiation fields of the guitar have also been of great interest [15]–[18]. Recently, it has been demonstrated that a relatively small number of measured parameters are required to predict the sounds radiated by a guitar [13], [18], [19]. It is also interesting to note that Brooke and Richardson have concluded

that the "quality" of an instrument cannot be estimated from its modal properties [15]. Although surprising, this may in fact simply be the scientific equivalent of stating that even though an instrument is in tune, "quality" sound cannot be guaranteed. Conversely, out-of-tune musical instruments will be rejected by musicians as unplayable, thereby inferring that "good" modal properties are necessary but not sufficient to ensure a decent instrument. What constitutes "good" modal properties is still nonetheless a heavily discussed topic. Interestingly enough, a recent study on the natural frequencies of various musical instruments has demonstrated that although physical changes to the instruments have occurred over the years, the lowest five or six eigenvalues have moved around with relative positions which are "musically pleasing" [20], reinforcing the requirement for consistent acoustic properties.

Extensive numerical and experimental studies have been conducted by Elejabarrieta, Ezcurra, and Santamaría throughout the entire construction process of a guitar by a master luthier. As modifications to the guitar were made by the luthier, experimental tests on the soundboard were performed at each manufacturing step in order to better understand the effect of the modification on the vibration properties of the soundboard [21]. Finite element analysis of this same data followed [22]. As the guitar neared completeness, further analysis of the resonance box and its modes of vibrations were performed, as well as a study of the effect of the sound-hole on the acoustic modes of the box [23]. Once the box of the guitar had been assembled, an experimental and finite element analysis of the coupling between the structural (soundboard and back-plate) and acoustic (the box as a Helmholtz resonator) vibration modes was performed [24]. Finally, the fluid-air interaction in the guitar box was investigated by numerically and experimentally changing the interior gas [25]. This extensive set of work greatly contributed to the understanding of the contribution to the frequency response and vibration properties of each component of the guitar, but offered no insight into how desired acoustical properties could be achieved by an instrument designer by modifying these components.

Radiation efficiency and frequency content in the vibrations of classical guitars was performed by Boullosa [26], [27] but also stopped short of offering insight into which components of the guitar or which modifications could contribute to either. The effects of

the bridge on the vibration properties of the soundboard were studied by Torres and Boullosa using both finite element analysis and laser vibrometry [28]. In order to better understand the vibroacoustical behaviour of the guitar, Chaigne and various collaborators focused their research on time-domain modeling via physical parameters [29]–[31]. The goal of their research was to create a tool for the estimation of physical quantities that are difficult to measure experimentally. Examples include the estimation of the relative structural losses and radiation losses in the sounds generated by the guitar.

Thomas Rossing gives an excellent overview of the current state of musical acoustic research for string instruments in his recent book [32].

1.1.2 Braced Plates

Since the soundboard of the guitar is considered to be the most acoustically active part of the guitar [3], great focus must be spent on understanding this component. Based on its general design, it can usually be considered as a thin plate. It is made thin so that it can vibrate and amplify the frequencies produced by the strings of the guitar. Large stresses are also applied to the soundboard through the highly tensioned strings. These stresses are structurally resisted by adding braces on the underside of the soundboard at key locations. This gives the soundboard enough flexibility to produce the desired frequencies while being structurally strong enough to resist the large string tension. The application of these braces to the soundboard creates a stiffened plate, as shown in Figure 2.

The vibrational study of stiffened plates has been a topic of great interest in structural applications. In this case, stiffened plates have been modeled by various methods [33]–[38], including finite elements, finite difference, mesh-free galerkin, trigonometric interpolation methods, as well as many other numerical methods. In most cases, the goal was to give a new modeling method for these plates and demonstrate the method's limits and bounds. Other studies have looked at ways of modeling stiffened plates with braces of various lengths and positions [39]–[42]. These models give results which allow a much greater flexibility in design. Recently, Dozio and Ricciardi have used a unique analytical-numerical method based on the assumed modes method to model stiffened plates more efficiently for parametric and optimization problems [43]. This presents a potentially

interesting approach for those wishing to deliberately design the frequency spectrum of a stiffened plate. However, these studies have focused primarily on the structural properties of such systems rather than the acoustical properties of the interaction between the beam and plate elements. Very little information in the literature can be found on the effect of a bracing beam element on the frequency and modal spectrum of the plate. Additionally, Amabili appears to be the only researcher to have studied the natural frequencies of rectangular plates using an experimental setup for simply supported boundary conditions [44], [45]. On the other hand, the effect of shaping a beam on its acoustic properties has been diligently studied by Orduna-Bustamante [46]. In this study, the effect of undercutting a xylophone bar on its tuning was modeled and analyzed analytically. Moreover, brace shapes in acoustic guitars has long been a controversial topic and very little scientific research has looked at how the shape of the brace affects the natural frequencies of a brace-plate system.

1.1.3 Inverse Eigenvalue Problems

The study of stiffened plates has focussed primarily on various modeling approaches. Any engineering design using stiffened plates has drawn on past experience and empirical trial and error methods. This is especially true for plates requiring a certain frequency spectrum, as demonstrated in [5]. One area that could potentially hold great promise for addressing the problem of frequency spectrum design of stiffened plates is that of inverse eigenvalue problems. Although not currently used for such purpose, the theory could potentially be applied to these problems. A rather broad field covering many subjects, such as control systems, structural analysis, particle physics and vibrations, inverse eigenvalue problems have an interesting and large field of application. While continuous inverse theories have been studied such as the classical Sturm-Liouville problem [47]–[49], a more interesting approach for the purpose of design is to use discrete theory. For the application of inverse eigenvalue theory to the field of vibrations, this typically involves the use of a discrete matrix representation of a real system. This approach presents greater value to the problem since many numerical and analytical tools already exist for the solution of discrete problems.

A great deal of focus has been applied to the study of discrete inverse eigenvalue problems. This has been made clear by a thorough review of the topic by Chu and Golub [50], [51]. Gladwell takes a more direct route where he considers specific inverse problems and matrix structures related to mechanical vibrations [52]. Particularly, it appears that most of the literature focuses on system identification. One of the most common techniques in inverse eigenvalue problems is to use the system's spectrum and then constrain the system in some fashion in order to get a second spectrum [53]–[57]. This clearly indicates that a system usually exists and that it can be tested to obtain data that will be used in the inverse problem of mathematically reconstructing the system. Although interesting, this approach cannot be used for engineering design to construct a system having a specific spectrum without another system on which to base the design.

In most cases, the solution to the inverse problem begins by writing the known eigenvalues along the diagonal entries of the diagonal matrix Λ. Additionally, any invertible matrix P can be used to obtain another solution (matrix) with the same spectrum, namely $P\Lambda P^{-1}$. Since $P\Lambda P^{-1}$ is the trivial solution, restrictions are required on the P matrix so that certain structural requirements of the system can be satisfied. Various methods can be used to impose such structure. According to Chu, these methods can be distinguished by the types of procedures used in imposing structure to the matrix [50]. Structuring matrices by prescribing specific entries has been studied in [58], [59]. Modifying the matrix through the addition of another matrix has also been studied in [60]–[62]. Dias de Silva, de Oliveira, and others have studied how multiplying the discrete system by another matrix can affect its structure [63]–[65]. The use of the well-developed field of matrix theory for structured matrices, such as Jacobi or band matrices, as applied to inverse problems has also been investigated [66]–[69]. Finally, applying least square methods has shown to be an effective method for finding an approximate solution to inverse eigenvalue problems and has been considered in [70], [71].

In most cases, the research on inverse eigenvalue problems has focused on the existence, uniqueness and computability of the solution. Other studies are typically variations on those described above, including partially described problems, where not all spectral information is known. These types of problems have been considered in [72],

[73], and are of great interest for problems requiring only certain frequencies to be specifically determined.

Once an inverse eigenvalue problem has been set up and the type of solution has been chosen, various algorithms can be used in order to numerically solve the problem. These include orthogonal polynomials methods, the block Lanczos algorithm, the Newton method and the divide and conquer method, as well as several others [66], [74]–[78]. Forward iterative methods using some form of optimization method have been around for many years and could also be used [79]. However, since the problem of solving a pair of system matrices from a set of eigenvalues is ill-posed (meaning lacking a unique solution), an optimization approach may miss out on some good alternative solutions since these methods only seek one solution. Although broad in scope, very little has been done to apply inverse eigenvalue theory to actual engineering design problems. In the case of wooden stringed musical instruments such as the guitar, the potential advantage of using such theory when designing a frequency spectrum into a material that is inherently inconsistent appears to be immense.

1.1.4 Guitar Bracing Patterns

In order to apply such design theories to the soundboard of guitars, an understanding of their bracing patterns must be explored. Very little scientific research on this subject exists. However, a very good historical timeline exists for their development [80], [81]. It is clear that bracing patterns of the soundboard emerged out of the need to allow the soundboard to vibrate as easily as possible while still maintaining structural integrity under string tension. Early guitars had gut strings which applied less tension to the soundboard. Early brace designs typically searched for ways of distributing this local load over the entire soundboard. By doing so, the effectiveness of the bracing pattern was judged not only by how well it resisted the local string tension, but also by how clearly and how well the musical instrument projected its sound. Early designs included simple ladder bracing. Eventually, a fan design was developed by A. de Torres as shown in Figure 2b. Since the design proved to be very effective, it was adopted by many other instrument makers. Its widespread use eventually made it the industry standard. When classical and flamenco guitars started using nylon strings, tension in the strings remained

similar, therefore tradition dictated the continued use of fan bracing. Although various builders have introduced small variations to brace structure over the years, very little has changed in the design of most instruments. In parallel, musicians started to seek larger and louder guitars. This led to the use of steel strings which produce much greater tensions. Typical fan bracing could not support this extra load. The solution came from an X-brace design, as shown in Figure 2a, developed by C. F. Martin many years before.

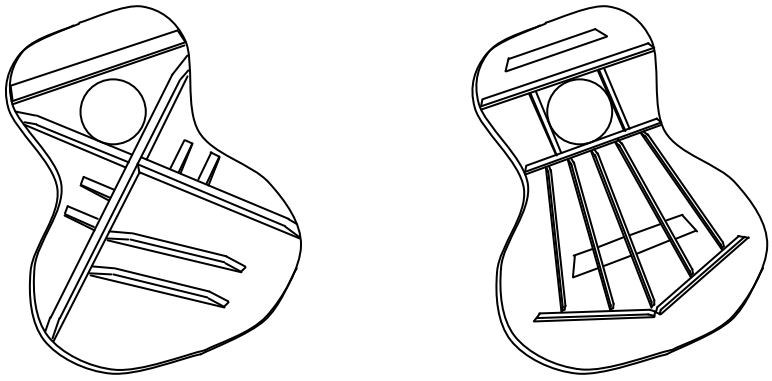

a. X-brace design ***b.*** fan-brace design

Figure 2. Underside of braced guitar soundboards.

This design proved highly effective and has been the standard for steel string guitars ever since. The efficiency of these designs has been optimized empirically over the years with subjective analysis coming from critical musicians. More recently, lattice type bracing and Nomex double-top soundboards have seen a surge of interest among luthiers, however their advantages are still under review by the musical community.

Very little scientific study has been performed on the effects that various brace patterns and placements have on the sound of the musical instrument. In fact, the references in Fletcher and Rossing's review of musical acoustics show little to indicate otherwise [82]. Conversely, many renowned luthiers, including Cumpiano and Natelson, as well as Somogyi, believe, based on many years of experience, that it is not so much the bracing pattern itself that has the greatest effect on the sound quality of the instrument but rather the skill in which varying wood properties are accounted for in the construction of the instrument [80], [83]. Most knowledge of soundboard physics comes from technical articles, such as the article by Somogyi [83], written by luthiers trying to explain what

they have come to grasp naturally. In these articles, the dynamics of the soundboard motion are based on physical observation alone.

A few other works have looked at how different bracing patterns change the modal properties of the soundboard using Chladni's method for modeshape visualization, and have then attempted to model the differences using finite element modal analysis [84]–[86]. A good description of Chladni's method is provided by Jensen [87]. None of these papers, however, explain how to bring about specific changes in the bracing in order to produce specific modal patterns. An interesting paper by Lawther addresses the issue of avoiding certain frequency ranges in the context of braced structures through a modification of the bracing [88]. However, the goal was to avoid resonance rather than to tune the structure. In many ways, the behaviour of the bracing structure of a guitar is poorly understood and must credit its success to the generations of empirical evidence, rather than scientific analysis. Although a good general idea of the physics behind the structure exists, no mapping of its dynamics has been thoroughly carried out. Without this information, a scientific approach to its design for manufacturing cannot be completely achieved.

1.1.5 Wood

The wood used for guitar making is typically quartersawn so that the grain lines are as normal to the surface of the plate as possible (Figure 3).

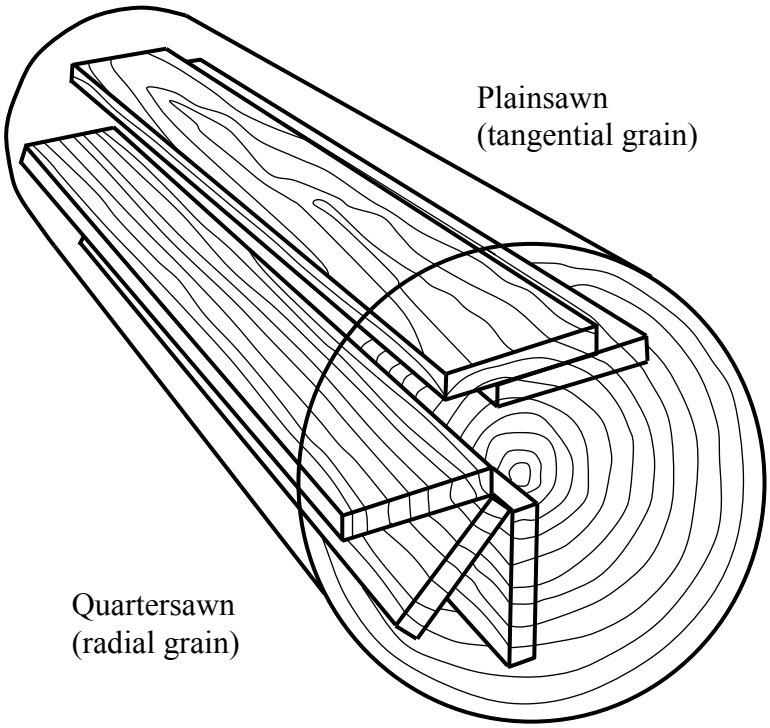

Figure 3. Plainsawn versus quartersawn wood.

This leads to a wooden plate which can be represented using orthotropic material properties such as shown in Figure 4.

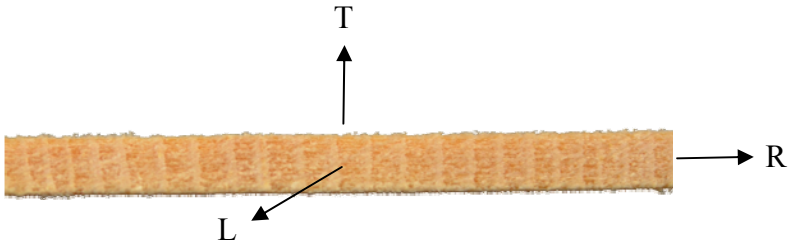

Figure 4. Orthogonal properties of quartersawn wood.

Many wood scientists would agree that most variability comes from the ratio of earlywood (early season growth) versus latewood (growth which occurs later in the season) rather than the properties of each on their own. Many studies have measured the range of mechanical properties for a number of different types of wood, where each measurement was made on separate pieces of wood of the same species and subsequently averaged [1], [89]–[91]. A method for measuring the elastic and damping constants by

interpreting the frequencies and Q-factors of the lowest modes of vibration of a wooden plate is provided by McIntyre and Woodhouse [92], [93]. Other papers have approached the study of the mechanical properties of wood by taking a look at their microstructure [94], [95]. Nonetheless, very little is known with regards to the relationship between mechanical properties within the same wooden specimen.

1.2 Motivation

The goal of this thesis is not to understand every aspect of the guitar's soundboard physics, but rather to create a foundation on which a better understanding can be achieved. Evidently, a general idea of how the braces interact with the soundboard in creating natural frequencies and modeshapes must be formed. Headway was made in this area during the previous study on the subject [5]. However, much more work remains to be completed in order to gain a complete picture of this interaction. On the other hand, in order to design for manufacture, control of the eigenvalues (frequencies) must be accomplished through modifications of the shape and/or the placement of the braces on the soundboard. Once the ability to control the important eigenvalues has been established, a design tool must be developed in order to determine brace geometry and position from spectral and material property information. Since current inverse eigenvalue theory focuses on building a mathematical model from a pre-existing system by obtaining additional information through various system constraints, new tools must be developed using similar theory. Once created, these tools can aid in the design of brace-plate systems and feed valuable information into the manufacturing process. This information could be used via CNC machinery in order to compensate for the highly variable material properties of the wood which is currently being used. Experimental investigation of the proposed methods must also be used to validate the results. The ultimate goal is to have the facts and tools required to design the spectrum of the guitar's soundboard, given knowledge of the mechanical properties of the wood specimens being used.

1.3 Outline of the Thesis

The thesis begins in Chapter 2 with a paper published in Applied Acoustics [96] considering the effects that the brace shape has on a brace-soundboard system. In particular, this paper investigated how the scalloped shape of a brace can be used to control two frequencies simultaneously. It was successful in demonstrating that this shape of brace, which has been used by luthiers for centuries, can control two separate system frequencies by simple adjustment of the base thickness of the brace or the height of the scalloped peaks. It also described a method for adjusting these physical dimensions and the specific frequencies which would be affected.

Chapter 3 is a follow-up paper published in the International Journal of Mechanical Engineering and Mechatronics (IJMEM) [97] which looked at the effects of the scalloped-shaped brace on the modeshapes of the system. In this study, the modeshapes were analysed by looking at a number of cross-sections along the length of the brace. It was shown that the scalloped peaks had the greatest effect on the modeshapes which had their antinode (maximum amplitude) located at the exact location of these peaks. As could be expected, the brace had very little effect on modeshapes which had a nodal line coincident with the length of the brace.

Chapter 4 is a paper published in SpringerPlus [98] which solves design-for-frequency problems by proposing an inverse eigenvalue method for general matrices using the Cayley-Hamilton theorem. Mathematical details of the method for both the simple and generalized cases are presented along with a number of examples. The need to implement structural constraints in the forward problem is discussed and solutions for partially described systems are also described.

Chapter 5 is a paper published in Applied Acoustics [99] which applies the Cayley-Hamilton method developed in [98] to the scalloped-shaped brace-plate model of [96]. Particularly, it calculated the dimensions of the scalloped brace necessary so that the brace plate system achieves a desired pair of natural frequencies. Moreover, it presents a new inverse eigenvalue method, based on solving the determinant of the generalized eigenvalue problem, which is found to be more efficient than the Cayley-Hamilton method for partially-described problems.

Chapter 6 is an unpublished paper which experimentally measured the mechanical properties of Sitka spruce wood specimens in order to investigate the possibility of relating the mechanical properties amongst each other. Assumptions made in the other papers with regards to the mechanical properties are verified. The natural frequencies of the simply supported plates were also calculated analytically and then compared to those obtained experimentally. Additionally, this study looked at how variations of the mechanical properties affected the natural frequencies.

Chapter 7 gives the experimental results of the natural frequency investigation of a simply supported Sitka spruce plate, to which is attached a scalloped brace similar to the model used in [96].

Finally, a summary of the results, concluding remarks and recommendations for future work are given in Chapter 8.

It is hoped that this research sets the fundamental framework on which a complete and efficient method for incorporating acoustical consistency in the design for manufacturing of wooden guitars can eventually be developed.

Chapter 2

Effects of Using Scalloped Shape Braces on the Natural Frequencies of a Brace-Soundboard System

Applied Acoustics

DOI: 10.1016/j.apacoust.2012.05.015

Volume 73, Issue 11, November 2012, Pages 1168–1173

2.1 Abstract

Many prominent musical instrument makers shape their braces into a scalloped profile. Although reasons for this are not well known scientifically, many of these instrument makers attest that scalloped braces can produce superior sounding wooden musical instruments in certain situations. The aim of this study is to determine a possible reason behind scalloped-shaped braces. A simple analytical model consisting of a soundboard section and a scalloped brace is analyzed in order to see the effects that changes in the shape of the brace have on the frequency spectrum of the brace-soundboard system. The results are used to verify the feasibility of adjusting the brace thickness in order to compensate for soundboards having different mass properties or stiffness in the direction perpendicular to the wood grain. It is shown that scalloping the brace allows an instrument maker to independently control the value of two natural frequencies of a combined brace-soundboard system. This is done by adjusting the brace's base thickness in order to modify the 1st natural frequency and by adjusting the scalloped peak heights to modify the 3rd natural frequency, both of which are considered along the length of the brace. By scalloping their braces, and thus controlling the value of certain natural frequencies, musical instrument makers can improve the acoustic consistency of their instruments.

2.2 Introduction

Like most musical instruments, stringed instruments are designed and built to produce sound by allowing their body to vibrate when excited by some outside force. In the case of stringed musical instruments, a set of strings are usually plucked, strummed or tapped by the musician in order to set these in motion. The vibrating motion of the strings is then transmitted to the body of the instrument through the soundboard which in turn displaces the air around it, creating pressure waves perceived by the listener to be the characteristic tones of a particular instrument. Certain stringed musical instruments such as the flat top guitar, the mandolin or the piano use braces on the underside of their soundboard so that it remains thin enough to be within the desired natural frequency range while still maintaining the structural integrity required to withstand the large string tension.

Effects of Using Scalloped Shape Braces on the Natural Frequencies of a Brace-Soundboard System

Although the braces are structural in nature, their shape and size greatly affect the vibrational behaviour and thus, the frequency spectrum of the soundboard system. The braces modify the frequency spectrum of the soundboard by locally modifying its mass and stiffness.

The physics of musical instruments have been thoroughly studied over the last half century, with most research focusing on understanding the key elements of sound production and radiation as can be seen in various books published over the past few decades [1]–[3]. With the growth in popularity and capabilities of numerical simulation, many researchers have focused on trying to reproduce parts or whole instruments as accurately as possible [4]–[8]. However, due to the variable nature of wood, it is often necessary to adjust a numerical model's parameters based on those of actual material specimens used in instrument construction. As such, other studies have produced numerical simulations which parallel the construction of an instrument so as to be as accurate as possible while verifying the effects of various construction stages on the frequency spectrum of the instrument [9], [10]. These studies in particular have helped verify the effects of the addition or removal of material on an instrument's spectrum. These results have also allowed researchers to create repeatable construction methods and instruments of more consistent acoustic quality [11], [12]. More recently, instrument makers have also attempted to share and explain their empirical expertise gained over years of construction and fine tuning experience [13]–[15]. However, their explanations are not always scientific in nature. It is clear that a certain gap still exists between the scientific understanding of musical instrument construction and the nature of hand-built instruments.

One such unexplored example is the reason why many prominent instrument makers shape the braces on their instrument's soundboard. While most instrument makers disagree on the reasons behind the shaping of braces, many will agree that it can improve an instrument's sound. Known as scalloped braces, they have a shape similar to those of Figure 5.

Figure 5. Shape of a scalloped brace

This paper seeks to justify the use of scalloped braces by determining why, in certain situations, they appear to improve the sound of a musical instrument. Based on previous research, it was thought that it may be possible to independently control the value of two natural frequencies using a scalloped-shaped brace [16]. The goal of this paper is to verify this hypothesis.

Current research shows that it is the first few natural frequencies of the soundboard that have the largest impact on its acoustic properties [11]. Therefore, we focus our attention on the first few eigenvalues of the combined brace-soundboard system and our solution approach will exploit this (although any set of eigenvalues could be analysed using a similar approach). Previous research also suggests that the required frequency accuracy for a musical instrument must fall within a 1% margin due to the ear's sensitivity to pitch [17]. Although this figure may be reduced when looking at the soundboard's acoustic properties, rather than the instrument's radiated sound. Common practice in the industry is to use the stiffness perpendicular to the wood grain as a measure of the acoustical quality of a soundboard [18]. In this paper, we determine if it is possible to compensate for the variance in the mass and stiffness perpendicular to the grain (Young's modulus in the wood's radial direction) by adjusting the thickness at various points along the brace.

2.3 Analytical Model

A simple model is created in order to investigate whether or not the value of two natural frequencies can be controlled using a scalloped brace. The model of Figure 6 represents a section of musical instrument soundboard generally supported by a single brace.

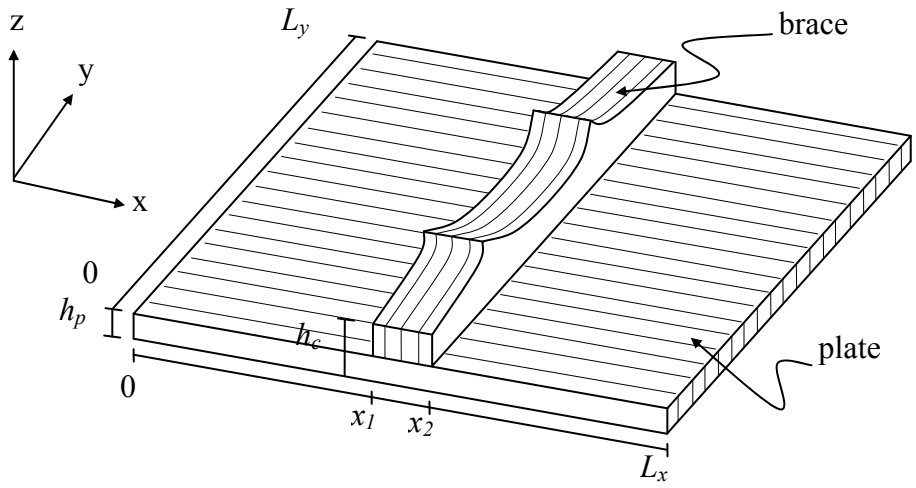

Figure 6. Orthotropic plate reinforced with a scalloped brace.

The assumed shape method is the method chosen for investigating the effects of changes in the thickness of the brace. The method itself is well explained in [19]. This method is chosen because it allows us to use the flat-plate modeshapes as the fundamental building blocks of the solution, thereby permitting observation of how the addition of the scalloped brace affects those fundamental modeshapes. This method also permits greater flexibility in analyzing the effects of the scalloping since it enables the creation of an analytical solution from which numerical solutions can be quickly obtained for various parameter modifications including changes in the thickness of the scalloped brace. The method uses 3×3 trial functions during the analysis. The equations of motion are derived using a computer algebra system (Maple). This yields mass and stiffness matrices where each matrix entry is a function of *all* physical parameters (dimensions, density, stiffness, etc.). The effect of any parameter on the system's eigenvalues can then be easily examined without having to re-establish the entire system model.

2.3.1 Modeling Assumptions

The soundboard is modeled as a thin rectangular plate and the brace is modeled as a thicker section of the same plate. A simple rectangular geometry is assumed in order to enable the closed-form solution of a simple plate (without the brace) to be used as the trial functions for the assumed shape method. The plate is assumed thin so that linear

Kirchhoff plate theory can be used. The Kirchhoff assumptions state that when compared to the plate's thickness, deflections are small. Kirchhoff plate theory also neglects transverse normal and shear stresses, as well as rotary inertia. Although this is an accurate assumption for the plate, due to the brace's thickness-to-width aspect ratio, it may imply a certain error in that region of the soundboard. Also, because of the method in which the brace thickness is added to that of the plate in the kinetic and strain energy expressions, it was necessary to change the direction of the grain of the plate, in this region only, to match that of the brace. This is a reasonable assumption since the plate is thin in comparison to the brace and there is a solid link of wood glue which bonds them together. Since the stiffness and mass of the brace is much greater than that of the plate in this region, it is the brace which dominates these properties. The plate is also assumed to be simply supported all around, although in reality it is somewhere between simply supported and clamped [3]. It has been assumed that the system is conservative in nature, which allows damping to be neglected. Although there is a certain amount of damping found in wood, its effects on the lower natural frequencies is considered minimal and has been neglected. This is justified because the lower frequencies have a larger effect on the soundboard's perceived pitch than do the higher frequencies [11].

2.3.2 Kinetic and Strain Energies

Because the brace is modeled as a thicker section of the plate between x_1 and x_2, the standard kinetic and strain energies must be modified accordingly by breaking them down into three distinct sections. For an orthotropic plate, the kinetic and strain energies can be found in [20].

With the addition of the brace, the kinetic energy for the soundboard and brace system becomes

$$T = \frac{1}{2}\int_0^{x_1}\int_0^{L_y} \dot{w}^2 \rho_p \, dy dx + \frac{1}{2}\int_{x_1}^{x_2}\int_0^{L_y} \dot{w}^2 \rho_c \, dy dx + \frac{1}{2}\int_{x_2}^{L_x}\int_0^{L_y} \dot{w}^2 \rho_p \, dy dx \qquad (1)$$

where L_x and L_y are the dimensions of the plate in the x and y directions respectively, the dot above the transverse displacement variable w represents the time derivative, ρ is the mass per unit area of the plate such that

$$\rho_p = \mu \cdot h_p \text{ and } \rho_c = \mu \cdot h_c, \tag{2}$$

μ is the material density and h_p and h_c are the thickness of the plate and combined brace-plate sections respectively.

The strain energy is also modified by the addition of the brace and becomes

$$\begin{aligned} U = &\frac{1}{2}\int_0^{x_1}\int_0^{L_y}\left[D_{xp}w_{xx}^2 + 2D_{xyp}w_{xx}w_{yy} + D_{yp}w_{yy}^2 + 4D_{kp}w_{xy}^2\right]\mathrm{d}y\mathrm{d}x \\ &+\frac{1}{2}\int_{x_1}^{x_2}\int_0^{L_y}\left[D_{xc}w_{xx}^2 + 2D_{xyc}w_{xx}w_{yy} + D_{yc}w_{yy}^2 + 4D_{kc}w_{xy}^2\right]\mathrm{d}y\mathrm{d}x \\ &+\frac{1}{2}\int_{x_2}^{L_x}\int_0^{L_y}\left[D_{xp}w_{xx}^2 + 2D_{xyp}w_{xx}w_{yy} + D_{yp}w_{yy}^2 + 4D_{kp}w_{xy}^2\right]\mathrm{d}y\mathrm{d}x \end{aligned} \tag{3}$$

where the subscripts on w refer to partial derivatives in the given direction, as per standard notation, the stiffnesses D are section-specific because of the change in thickness h from x_1 to x_2:

$$D_{xp} = \frac{S_{xx}h_p^3}{12}, \quad D_{yp} = \frac{S_{yy}h_p^3}{12}, \quad D_{xyp} = \frac{S_{xy}h_p^3}{12}, \quad D_{kp} = \frac{G_{xy}h_p^3}{12}, \tag{4}$$

and

$$D_{xc} = \frac{S_{xx}h_c^3}{12}, \quad D_{yc} = \frac{S_{yy}h_c^3}{12}, \quad D_{xyc} = \frac{S_{xy}h_c^3}{12}, \quad D_{kc} = \frac{G_{xy}h_c^3}{12}, \tag{5}$$

where G is the shear modulus and the S are stiffness components that are defined as

$$S_{xx} = \frac{E_x}{1-\nu_{xy}\nu_{yx}}, \qquad S_{yy} = \frac{E_y}{1-\nu_{xy}\nu_{yx}}, \qquad S_{xy} = S_{yx} = \frac{\nu_{yx}E_x}{1-\nu_{xy}\nu_{yx}} = \frac{\nu_{xy}E_y}{1-\nu_{xy}\nu_{yx}}. \tag{6}$$

Here, the subscripts represent the direction of the plane in which the material properties act. Therefore, E_x is the Young's modulus along the *x*-axis, E_y along the *y*-axis and ν_{xy} and v_{yx} are the major Poisson's ratios along the *x*-axis and *y*-axis respectively.

2.3.3 Scalloped Brace Shape

To accommodate the scalloped-shaped brace in the energy equations, the variable thickness of the brace h_b such that $h_c = h_p + h_b$ must be taken into account. In order to model the scalloped shape, a second-order piece-wise polynomial function is chosen and

applied along the *y*-direction between x_1 and x_2. This polynomial function puts the peaks of the scallops at ¼ and ¾ of the brace. The function is given by

$$h_b = \begin{cases} \lambda \cdot y^2 + h_{bo} & \text{for} \quad y < \dfrac{L_y}{4} \\ \lambda \cdot \left(y - \dfrac{L_y}{2} \right)^2 + h_{bo} & \text{for} \quad \dfrac{L_y}{4} \le y \le \dfrac{3L_y}{4} \\ \lambda \cdot \left(y - L_y \right)^2 + h_{bo} & \text{for} \quad y > \dfrac{3L_y}{4} \end{cases} \tag{7}$$

where h_{bo} is the height of the brace at its ends and centre and λ is the scallop peak height adjustment factor which is a real value whose range is the subject of investigation. For the purpose of dimensioning, the width of the brace is identified as L_b.

2.4 Results

2.4.1 Material Properties

The material chosen for analysis of the soundboard is Sitka spruce due to its common usage in the industry. Material properties for Sitka spruce are obtained from the U.S. Department of Agriculture, Forest Products Laboratory [21]. Since properties between specimens of wood have a high degree of variability, the properties obtained from the Forest Products Laboratory are an average of specimen samplings. The naturally occurring properties of wood cause it to act as an orthotropic material. Material properties of Sitka spruce are seen in Table 1. The subscripts '*R*' and '*L*' refer to the radial and longitudinal property directions of wood respectively. These property directions are adjusted accordingly for both the plate and the brace.

Table 1. Material properties for Sitka spruce as an orthotropic material.

Material properties	Values
Density – μ (kg/m^3)	403.2
Young's modulus – E_R (MPa)	850
Young's modulus – E_L (MPa)	E_R / 0.078
Shear modulus – G_{LR} (MPa)	E_L × 0.064
Poisson's ratio – v_{LR}	0.372
Poisson's ratio – v_{RL}	$v_{LR} \times E_R / E_L$

2.4.2 Soundboard Dimensions

A typical section of a soundboard structurally reinforced by a single brace is modeled using the same dimensions throughout the analysis. The pertinent dimensions are given in Table 2. In order to avoid confusion, subscript '*p*' stands for plate, '*b*' for brace and '*c*' for combined plate and brace.

Table 2. Model dimensions.

Dimensions	Values
Length – L_x (m)	0.24
Length – L_y (m)	0.18
Length – L_b (m)	0.012
Reference – x_1 (m)	$L_x / 2 - L_b / 2$
Reference – x_2 (m)	$x_1 + L_b$
Thickness – h_p (m)	0.003
Thickness – h_{bo} (m)	0.012
Thickness – h_c (m)	$h_p + h_b$

2.4.3 Benchmark Values

To set a benchmark for further investigation, a set of values for the natural frequencies are computed and will be used for comparison purposes. This benchmark is based on a Young's modulus of 850 MPa in the soundboard's radial direction, a brace base height of 0.012 m and a scallop peak height adjustment factor of 1. The first 5 natural frequencies and their modeshapes are found in Table 3.

Table 3. First 5 natural frequencies of the benchmark soundboard.

m_x	m_y	Natural frequency (Hz)	Modeshape
1	1	619	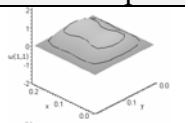
2	1	820	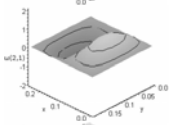
1	2	1131	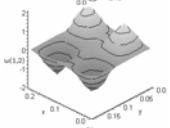
1	3	1346	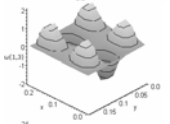
2	2	1400	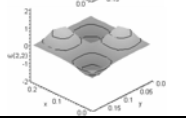

In Table 3, m_x and m_y represent the mode numbers in the x and y directions respectively. Also, the dip in the centre of x-axis of the modeshapes represents the location of the brace, which locally stiffens the area and limits the maximum amplitude possible.

2.4.4 Effects of the Soundboard Stiffness and Brace Thickness

We consider the effects of a change in both the Young's modulus in the radial direction E_R and of the brace base thickness h_{bo}, on the scalloped brace-soundboard system. Although several of the lowest natural frequencies carry importance, only two will be observed during the variation in structural properties. This is because frequencies that have a mode of vibration which contain a node at the location of the brace are not as affected by the brace as those which have a mode which passes through it. Therefore the two frequencies observed during this analysis are the 1st and 3rd natural frequencies of the system. The 2nd and 5th modeshapes have a node at the location of the brace and are not as affected by the brace, contrary to the 1st and 3rd modeshapes which do not, as seen from the figures in Table 3. Although the 4th natural frequency does not contain a node at

the location of the brace, the brace's current scalloped design of Equation (7) is not well suited to adjust this frequency and will therefore not be held constant. This is because the scalloped shape's peaks do not correspond with the maximum amplitudes of the fourth modeshape.

In order to see what effects changes in the soundboard's stiffness and brace's base thickness have on the overall natural frequencies of the system, each of soundboard stiffness and brace base thickness is varied from its benchmark value. When one is varied, the other is held constant at the benchmark value. As can been seen in Table 4 and Table 5, the natural frequencies increase when both the soundboard's stiffness and scalloped brace base thickness increase respectively.

Table 4. Natural frequency variation with changes in E_R.

Young's modulus E_R (MPa)	1st natural frequency ω_1 (Hz)	3rd natural frequency ω_3 (Hz)
750	582	1062
800	601	1097
850	619	1131
900	637	1164
950	655	1196

Table 5. Natural frequency variation with changes in h_{bo} ($\lambda = 1$).

Brace thickness h_{bo} (m)	1st natural frequency ω_1 (Hz)	3rd natural frequency ω_3 (Hz)
0.0110	579	1085
0.0115	599	1108
0.0120	619	1131
0.0125	640	1155
0.0130	661	1180

2.4.5 Previous Results

It was shown in [16] that by adjusting the thickness of a rectangular brace, one can control the value of the fundamental frequency of the brace-soundboard system. The rectangular brace achieves this by limiting the maximum amplitude of the dome shaped fundamental frequency. Reducing the stiffness of the brace increases the vibration amplitude of the fundamental modeshape. The value of other natural frequencies, which

have maximum amplitudes along the length of the brace, can also be controlled. However, a rectangular brace alone does not offer enough freedom to control the value of more than one frequency independently.

2.4.6 Controlling the Value of Two Natural Frequencies

In order to control the value of two natural frequencies independently, a modification to the shape of the brace is made. The resulting scalloped-shaped brace increases the freedom with which frequencies can be controlled. The 1st natural frequency is adjusted by changing the base thickness of the brace, h_{bo}. The 3rd natural frequency is adjusted by changing the scallop peak heights of the brace by modifying the peak height adjustment factor, λ. The natural frequencies are adjusted to within 1% of those calculated at the benchmark of $E_R = 850\,\text{MPa}$. Table 6 shows these natural frequencies which have been made consistent by compensating for variations in the soundboard's cross-grain stiffness.

Table 6. Compensation for variations in soundboard stiffness.

Young's modulus E_R (MPa)	Brace base thickness h_{bo} (m)	Peak height adjustment factor λ	1st natural frequency ω_1 (Hz)	3rd natural frequency ω_3 (Hz)
750	0.0123	2.0	619	1128
800	0.0121	1.6	620	1133
850	0.0120	1.0	619	1131
900	0.0118	0.6	618	1134
950	0.0120	-0.2	620	1134

2.4.7 Effects of the brace on the modeshapes

By adjusting the shape of the brace, two natural frequencies of the soundboard system can be controlled simultaneously. However, by changing the shape of the brace, the modeshapes are also affected, Figure 7 and Figure 8.

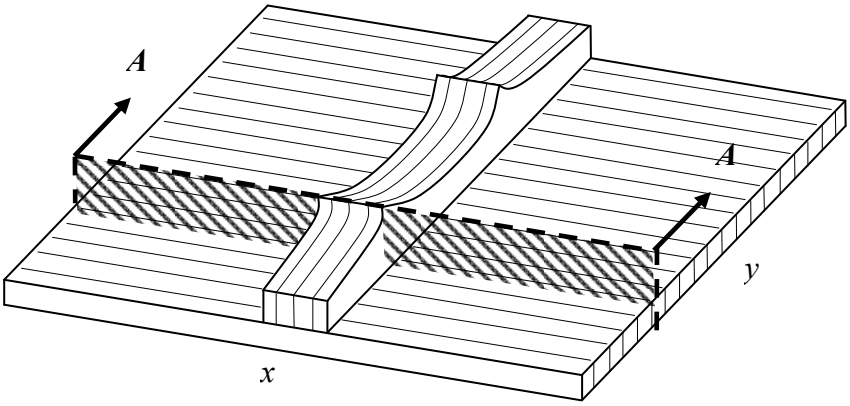

Figure 7. Location of cross-section for modeshape comparison.

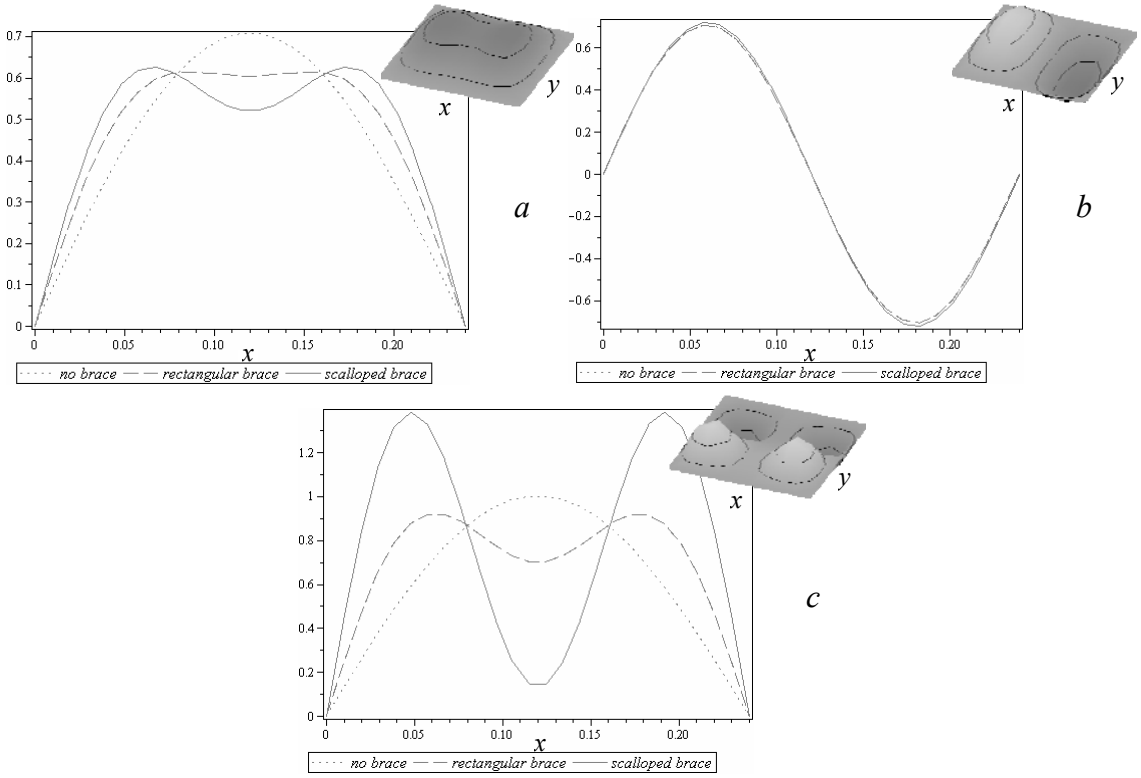

Figure 8. Section "A-A" comparison of $m_x \times m_y$ modeshapes: a. 1×1, b. 2×1 and c. 1×2.

To demonstrate the effect of the scalloped brace on each modeshape, a cross section of the three lowest modeshapes is taken and analyzed. Figure 7 shows the location in the plate where the cross-section is taken, while Figure 8 demonstrates the effect on that (cross-section of) modeshapes. Figure 8, part (a) shows a cross-section of modeshape 1 × 1 for the plate without a brace, with a rectangular brace as in [16] and with the scalloped

brace. The 3D shape of the modeshape is shown in the top right corner of the figure, and shows that the 1 × 1 modeshape is a dome. It can be observed that adding a brace flattens out the dome shape but changing the rectangular brace to a scalloped brace does not have a significant effect on the average shape for this particular mode. Looking at the second (2 × 1) modeshape, shown in part (b) of Figure 8, it is clear that the brace has very little effect on the modeshape due to its location along the nodal line of that modeshape. Finally, looking at the 1 × 2 modeshape in Figure 8 (c), it is clear that adding peaks on the brace at the location of the soundboard's maximum amplitude of vibration significantly affects the modeshape and therefore also its frequency.

2.5 Discussion

Based on the results, it becomes clear that it is possible to adjust two natural frequencies at once by modifying the shape of only one brace. This is made evident by Figure 9. This is not possible with a single rectangular brace [16]. Therefore, the scalloping of the brace allows for greater control over two values in the frequency spectrum of the system.

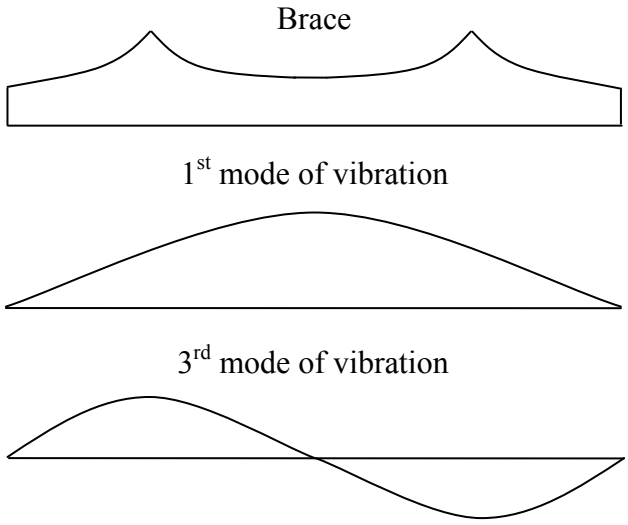

Figure 9. Scalloped brace with affected frequencies.

Figure 9 demonstrates that the maximum amplitude of the 1st natural frequency occurs at the centre of the brace where the base thickness of the scalloped brace is the predominant

factor in determining the magnitude of this natural frequency. Conversely, the maximum amplitude of the 3rd natural frequency occurs at the location of the scalloped shape's peaks. Therefore the height of these peaks becomes the predominant factor in determining the magnitude of this natural frequency. Also interesting is the fact that if the soundboard stiffness is high enough, an inverted scalloped brace may be required as seen by the negative peak height adjustment factor required to keep the 3rd natural frequency constant for a soundboard having a stiffness of $E_R = 950\,\text{MPa}$ in Table 6. This negative peak height adjustment factor would cause the brace to look like the one in Figure 10.

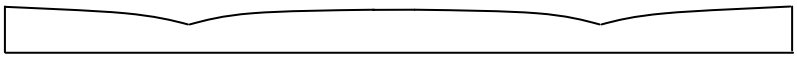

Figure 10. Effect of a negative peak height adjustment factor.

It is then evident that what a musical instrument maker is doing when shaping his braces, is in fact empirically controlling the value of multiple natural frequencies so as to optimize the acoustic quality and consistency of his instrument. Without a scientific understanding of the process, the methods used are those developed from years of experience. Although a great understanding of the scientific principles behind the construction of musical instruments is not a prerequisite to producing great sounding instruments, tradition and history have repeatedly proven that a good ear and loads of experience go a long way. However, these attributes are not always available to mass-manufacturers at a reasonable cost.

2.6 Conclusions

In this paper, the effects and reasoning behind using scalloped braces to acoustically modify a brace-soundboard system were modeled and analyzed in order to better understand how musical instrument makers control the sound of their musical instruments. The assumed shape method was used in the analysis and the insight gained by using this approach was tremendous.

This study has demonstrated that it is possible to modify a scalloped-shaped brace in order to control the values of two distinct natural frequencies in a wooden brace-

soundboard system. This is done by adjusting the base thickness and scallop peak heights of the brace in order to compensate for the 1st and 3rd natural frequencies respectively, since the maximum amplitudes of each of these frequencies occurs at these locations.

It is therefore likely that when musical instrument makers shape their braces, they are in fact controlling the value of multiple natural frequencies in order to improve the overall acoustic quality and consistency of their instruments. This helps clarify the reasons behind why so many instrument makers have been shaping their braces.

2.7 Acknowledgment

Special thanks go out to Dr. Frank Vigneron for help with certain aspects of this study and Robert Godin of Godin Guitars for giving important insight into the guitar manufacturing industry.

2.8 References

[1] C. M. Hutchins, "Musical Acoustics, Part 2," in *Benchmark Papers in Acoustics*, vol. 6, Stroudsburg, Pennsylvania: Hutichinson and Ross, Inc., 1975, pp. 88–208.

[2] A. H. Benade, *Fundamentals of Musical Acoustics*. New York, NY: Dover Publications, 1990.

[3] N. H. Fletcher and T. D. Rossing, *The Physics of Musical Instruments*, 2nd ed. Springer, 1998.

[4] G. A. Knott, Y. S. Shin, and M. Chargin, "A modal analysis of the violin," *Finite Elements in Analysis and Design*, vol. 5, no. 3, pp. 269–279, Oct. 1989.

[5] J. Bretos, C. Santamaría, and J. A. Moral, "Vibrational patterns and frequency responses of the free plates and box of a violin obtained by finite element analysis," *J. Acoust. Soc. Am.*, vol. 105, no. 3, p. 1942, 1999.

[6] M. J. Elejabarrieta, A. Ezcurra, and C. Santamaría, "Vibrational behaviour of the guitar soundboard analysed by the finite element method," *Acta Acustica united with Acustica*, vol. 87, no. 1, pp. 128–136, 2001.

[7] E. Bécache, A. Chaigne, G. Derveaux, and P. Joly, "Numerical simulation of a guitar," *Computers & Structures*, vol. 83, no. 2–3, pp. 107–126, Jan. 2005.

[8] J. A. Torres and R. R. Boullosa, "Influence of the bridge on the vibrations of the top plate of a classical guitar," *Applied Acoustics*, vol. 70, no. 11–12, pp. 1371–1377, Dec. 2009.

[9] M. J. Elejabarrieta, A. Ezcurra, and C. Santamaría, "Evolution of the vibrational behavior of a guitar soundboard along successive construction phases by means of the modal analysis technique," *J. Acoust. Soc. Am.*, vol. 108, no. 1, p. 369, 2000.

[10] A. Okuda and T. Ono, "Bracing effect in a guitar top board by vibration experiment and modal analysis," *Acoustical Science and Technology*, vol. 29, no. 1, pp. 103–105, 2008.

[11] C. Hutchins and D. Voskuil, "Mode tuning for the violin maker," *CAS Journal*, vol. 2, no. 4, pp. 5–9, 1993.

[12] G. Caldersmith, "Designing a guitar family," *Applied Acoustics*, vol. 46, no. 1, pp. 3–17, 1995.

[13] J. Natelson and W. Cumpiano, "Guitarmaking: Tradition and Technology: A Complete Reference for the Design & Construction of the Steel-String Folk Guitar & the Classical Guitar," San Francisco, CA: Chronicle Books, 1994, pp. 93–113.

[14] R. H. Siminoff, *The Luthier's Handbook: A Guide to Building Great Tone in Acoustic Stringed Instruments*. Milwaukee, WI: Hal Leonard, 2002.

[15] R. H. Siminoff, *Art of Tap Tuning How to Build Great Sound into Instruments Book*. Milwaukee, WI: Hal Leonard, 2002.

[16] P. Dumond and N. Baddour, "Toward improving the manufactured consistency of wooden musical instruments through frequency matching," in *Transactions of the North American Manufacturing Research Institution of SME*, 2010, vol. 38, pp. 245–252.

[17] A. Chaigne, "Recent advances in vibration and radiation of musical instruments," *Flow, Turbulence and Combustion*, vol. 61, pp. 31–34, 1999.

[18] R. M. French, "Engineering the Guitar: Theory and Practice," 1st ed., New York: Springer, 2008, pp. 159–208.

[19] L. Meirovitch, "Principles and Techniques of Vibrations," Upper Saddle River, NJ: Prentice Hall, 1996, pp. 542–543.

[20] S. P. Timoshenko and S. W.- Kreiger, "Theory of Plates and Shells," 2nd ed., New York: McGraw-Hill Higher Education, 1964, pp. 364–377.

[21] Forest Products Laboratory (US), "Wood Handbook, Wood as an Engineering Material," Madison, WI: U.S. Department of Agriculture, Forest Service, 1999, pp. 4.1–13.

Chapter 3

Effects of a Scalloped and Rectangular Brace on the Modeshapes of a Brace-Plate System

International Journal of Mechanical Engineering and Mechatronics
DOI: 10.11159/ijmem.2012.001
Volume 1, Issue 1, December 2012, Pages 1-8

3.1 Abstract

Shaping the soundboard braces on a wooden stringed musical instrument has long been a way in which instrument makers optimize their musical instruments. Reasons for these methods are scientifically not well understood. Various bracing patterns have successfully been used to create different-sounding wooden stringed musical instruments. These bracing patterns stimulate the modeshapes that are specific to the soundboard of the instrument. However, a higher adjustment resolution is required in order to specify the frequency spectrum of the musical instrument. This paper demonstrates how the shape of the braces affects the modeshapes of the vibrating system. A simple analytical model composed of a plate and brace is analyzed in order to see these effects. The results are plotted together for three cases: the plate by itself, the plate with a rectangular brace and the plate with a scalloped brace. For clarity, the modeshapes are analysed in 2D at different locations and along both the x and y directions of the plate. It is shown that any brace affects modeshapes for which the brace does not run along a nodal line. The different shapes of the brace are shown to affect different modeshapes by various degrees. If braces are stiffened at locations of maximum amplitude for a given modeshape, then that modeshape will be significantly affected. It is clear that by properly designing the shape of a brace, instrument makers can exert great control over the shape of the instrument's modeshapes and therefore also their frequencies.

3.2 Introduction

For centuries, stringed wooden musical instrument makers have been optimizing the sound of their musical instruments. Separately, the study of the physics of musical instruments has been on-going for some time. These studies have generally looked at sound production and sound radiation in musical instruments [1]–[5]. Other studies have looked into modeling the instrument in order to better understand its function. The typical numerical approach is to use finite element analysis, but other methods are also used [6]–[9]. Since wood is a naturally inconsistent material, numerical models are often compared to real counterparts and parameters are adjusted to match experimental results [10], [11]. In parallel with these developments, the ability to achieve high dimensional tolerances

has also been achieved in the instrument manufacturing industry. In spite of this, acoustical consistency is still lacking in manufactured wooden instruments [12]. The primary reason for this is a lack of scientific understanding of the methods used by musical instrument makers in optimizing the sound of their instruments.

The soundboard of a stringed musical instrument is considered to be the most acoustically active part of a stringed musical instrument [13]. Therefore, when optimizing the sound of the instrument, the soundboard becomes the most interesting component. Although it is clear that the bracing pattern of the soundboard has a significant effect on its modeshapes, very little scientific research on this subject exists. However, a very good historical timeline exists for its development [14], [15]. It is clear that bracing patterns of the soundboard emerged out of the need to allow the soundboard to vibrate as easily as possible while still maintaining structural integrity under string tension. Early guitars had gut strings which applied less tension to the soundboard. Early brace designs typically searched for ways of distributing this local string load over the entire soundboard. By doing so, the effectiveness of the bracing pattern was judged not only on how well it resisted the local string tension but also based on how clearly and how well the musical instrument projected its sound. Early designs included simple ladder bracing. Eventually, a fan design was developed by A. de Torres. Since the design proved to be very effective, it was adopted by many other instrument makers. Its widespread use eventually made it the industry standard. When classical and flamenco guitars started using nylon strings, tension in the strings remained similar, therefore tradition dictated the continued use of fan bracing. Although various builders have introduced small variations to brace structure over the years, very little has changed in the design of most instruments. In parallel, musicians started to seek larger and louder guitars. This led to the use of steel strings which produce much greater tensions. Typical fan bracing could not support this higher load. The solution came in the form of an X-brace design developed by C. F. Martin many years before. This design proved highly effective and has been the standard for steel string guitars ever since. The efficiency of these designs has been optimized empirically over the years with subjective analysis coming from critical musicians. More recently, lattice type bracing and double-top soundboards, where Nomex honeycomb paper is sandwiched between two thin layers of wood laminate, have seen a surge of

interest among instrument makers. However, their advantages are still under review by the community.

Very little scientific study has actually been performed on the effects of the various brace patterns and placements on the sound of the musical instrument. In fact, a look at the references in Fletcher and Rossing's review of musical acoustics shows little to indicate otherwise [3]. Conversely, based on years of experience, many renowned instrument makers including Cumpiano and Natelson as well as Somogyi believe that it is not so much the bracing pattern itself that has the greatest effect on the sound quality of the instrument but rather the skill in which inconsistent wood properties are accounted for in the construction of the instrument [14], [16]. Most knowledge of soundboard physics comes from technical articles, such as the article by Somogyi [16], written by instrument makers trying to explain what they have come to grasp naturally. In these articles, the dynamics of the soundboard motion are based on physical observation alone.

A few other works have looked at how different bracing patterns change the modal properties of the soundboard using Chladni's method and have then attempted to model the differences using finite element modal analysis [17], [18]. However, none of these papers explain how to affect specific changes in the bracing in order to produce specific modal patterns. An interesting paper by Lawther addresses the issue of avoiding certain frequency ranges in the context of braced structures through a modification of the bracing [19]. However, the goal was to avoid resonance rather than to tune the structure. In many ways, the bracing structure of a guitar is a scientifically misunderstood phenomenon which has built its success on the back of generations of practical experience. Although a good general idea of the physics behind the structure exists, no mapping of its dynamics has been thoroughly carried out.

However, it is clear that while bracing patterns have a direct effect on the modeshapes they cannot directly be used to choose the frequency spectrum of the soundboard. In most cases, bracing patterns completely reorganise the set of modeshapes. Thus a finer adjustment is necessary if only a change in frequency is sought. The most common way in which instrument makers adjust and optimize their musical instruments is by shaping the soundboard braces. Typically, the braces end up with what is known as a scalloped shape, as shown in Figure 11.

Figure 11. Shape of a scalloped brace.

Very little is known scientifically as to why instrument makers shape their braces and much debate still exists about the usefulness of scalloped braces. Although musical instrument makers have attempted to share their vast knowledge, a large gap still exists between their empirical methods and the scientific understanding and reasoning behind such methods. Thus, the goal of this paper is to demonstrate the effects of using a shaped brace on the modeshapes of a soundboard. A previous study has looked at the effects of brace shape on the frequencies of the system [20], but to the best of the author's knowledge, the effect of brace shape on the system's modeshapes has not been previously explored in the literature.

3.3 Model

A simple analytical model is used to investigate the effects of a shaped brace on the modeshapes of a rectangular plate. Figure 12 shows a typical soundboard section supported by a single brace. The brace is used to reinforce the structurally-weaker direction of the plate.

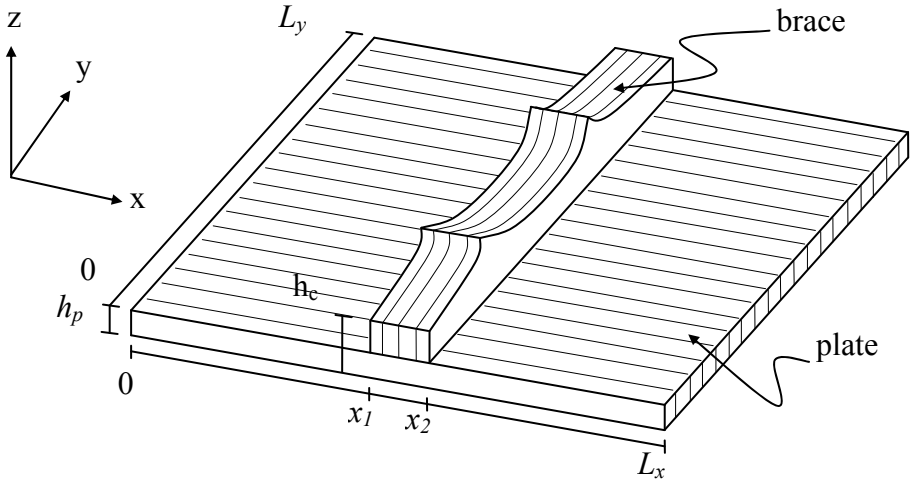

Figure 12. Orthotropic plate reinforced by a scalloped brace.

The assumed shape method is used in the analysis [21]. Since this is an energy method, the kinetic and strain energies of the plate must be developed. Certain assumptions are made in creating the model. The brace is modeled as a thicker section of the plate. The plate is considered thin and linear Kirchhoff plate theory is used. Although, as shown in Figure 12, the grain of the plate and brace are perpendicular to each other, the way in which the kinetic and strain energy are added force the grain of the plate to be parallel to the brace between x_1 and x_2 in the analytical model. This is justifiable since brace properties dominate this region. The plate is modeled as being simply supported, although a more accurate analysis would find it to be somewhere between simply supported and clamped [3]. Finally, the system has been modeled as being conservative in nature which is accurate based on the lower frequency range being used [22].

The assumed shape method is favoured for this study because it uses global elements based on the modeshapes of the rectangular plate such that

$$\phi_{n_x n_y} = \sin\left(n_x \cdot \pi \cdot \frac{x}{L_x}\right) \cdot \sin\left(n_y \cdot \pi \cdot \frac{y}{L_y}\right) \tag{8}$$

where L_x and L_y are the dimensions of the plate in the x and y directions respectively and n_x and n_y are the trial function numbers in these same directions. Therefore any physical modifications made to the plate by the addition of some form of bracing will be reflected directly in the method's choice and summation of trial functions used to represent any given modeshape. In this way, the effects of the shape of the brace can be seen not only by analysing the final model but also when building the model, thereby significantly increasing insight into the problem.

3.3.1 Kinetic and Strain Energies

The kinetic and strain energy are separated into three distinct sections along the *x*-axis, as shown in Figure 12. Kinetic and strain energies of an orthotropic plate are used [23]. The kinetic energy for the plate and brace system is thus given by

$$T = \frac{1}{2}\int_0^{x_1}\int_0^{L_y} \dot{w}^2 \rho_p \, \mathrm{d}y\mathrm{d}x + \frac{1}{2}\int_{x_1}^{x_2}\int_0^{L_y} \dot{w}^2 \rho_c \, \mathrm{d}y\mathrm{d}x + \frac{1}{2}\int_{x_2}^{L_x}\int_0^{L_y} \dot{w}^2 \rho_p \, \mathrm{d}y\mathrm{d}x \tag{9}$$

where the dot above the transverse displacement variable w represents the time derivative and ρ is the mass per unit area of the plate such that

$$\rho_p = \mu \cdot h_p \text{ and } \rho_c = \mu \cdot h_c, \tag{10}$$

μ is the material density and h_p and h_c are the thickness of the plate alone and combined brace-plate sections, respectively. The brace modifies the expression for strain energy which becomes

$$\begin{aligned} U = {} & \frac{1}{2}\int_0^{x_1}\int_0^{L_y} \left\{ D_{xp} w_{xx}^2 + 2D_{xyp} w_{xx} w_{yy} + D_{yp} w_{yy}^2 + 4D_{kp} w_{xy}^2 \right\} \mathrm{d}y\mathrm{d}x \\ & + \frac{1}{2}\int_{x_1}^{x_2}\int_0^{L_y} \left\{ D_{xc} w_{xx}^2 + 2D_{xyc} w_{xx} w_{yy} + D_{yc} w_{yy}^2 + 4D_{kc} w_{xy}^2 \right\} \mathrm{d}y\mathrm{d}x \\ & + \frac{1}{2}\int_{x_2}^{L_x}\int_0^{L_y} \left\{ D_{xp} w_{xx}^2 + 2D_{xyp} w_{xx} w_{yy} + D_{yp} w_{yy}^2 + 4D_{kp} w_{xy}^2 \right\} \mathrm{d}y\mathrm{d}x \end{aligned} \tag{11}$$

where the subscripts on w refer to partial derivatives in the given direction, as per standard notation. The stiffnesses D are section-specific because of the change in thickness h from x_1 to x_2 so that for the plate-only (no brace) section it follows that

$$D_{xp} = \frac{S_{xx} h_p^3}{12}, \quad D_{yp} = \frac{S_{yy} h_p^3}{12}, \quad D_{xyp} = \frac{S_{xy} h_p^3}{12}, \quad D_{kp} = \frac{G_{xy} h_p^3}{12}, \tag{12}$$

and similarly for the combined brace-plate section where the subscript 'p' is replaced with 'c'. Also, G is the shear modulus and the S are stiffness components that are defined as

$$S_{xx} = \frac{E_x}{1 - \nu_{xy}\nu_{yx}}, \qquad S_{yy} = \frac{E_y}{1 - \nu_{xy}\nu_{yx}}, \qquad S_{xy} = S_{yx} = \frac{\nu_{yx} E_x}{1 - \nu_{xy}\nu_{yx}} = \frac{\nu_{xy} E_y}{1 - \nu_{xy}\nu_{yx}}. \tag{13}$$

Here, the subscripts represent the direction of the plane in which the material properties act. Therefore, E_x is the Young's modulus along the *x*-axis, E_y along the *y*-axis and ν_{xy} and ν_{yx} are the major Poisson's ratios along the *x*-axis and *y*-axis, respectively.

3.3.2 Brace Shape

Although an argument could certainly be made for many other brace shapes, this study looks at the most common shape used by musical instrument makers. Furthermore, in order to fully understand the effects of brace shape, only a single brace is considered in this paper. The scalloped peaks are placed at locations of importance, as pointed out in the discussion.

The scalloped brace shape is defined as a second-order piece-wise polynomial function applied along the *y*-direction between x_1 and x_2. This positions the peaks of the scallops at ¼ and ¾ of the length of the brace. The thickness of the brace, h_b, is then defined as

$$h_b = \begin{cases} \lambda \cdot y^2 + h_{bo} & \text{for} \quad y < \dfrac{L_y}{4} \\ \lambda \cdot \left(y - \dfrac{L_y}{2} \right)^2 + h_{bo} & \text{for} \quad \dfrac{L_y}{4} \le y \le \dfrac{3L_y}{4} \\ \lambda \cdot \left(y - L_y \right)^2 + h_{bo} & \text{for} \quad y > \dfrac{3L_y}{4} \end{cases} \tag{14}$$

Here, h_{bo} is the height of the brace at its ends and centre and λ is the scallop peak height adjustment factor which is a real value whose range can be any value within physical reason. Within physical reason implying that the scalloped peaks can be made from the available bracing material being used, fit within the musical instrument's soundbox and does not interfere with the vibration of the musical instrument. Finally, the length of the brace is defined as L_y.

Since the rectangular brace has uniform thickness along its entire length, h_b remains a constant equal to h_{bo} during the analysis of the rectangular brace-plate system.

3.4 Results

3.4.1 Wood Properties

The material used in the analysis is Sitka spruce. This is the most common material used for soundboards in the stringed musical instrument industry. Properties of Sitka spruce are obtained from [24] and can be seen in Table 7.

Table 7. Orthotropic material properties of Sitka spruce.

Material properties	Values
Density – μ (kg/m^3)	403.2
Young's modulus – E_R (MPa)	850
Young's modulus – E_L (MPa)	E_R / 0.078
Shear modulus – G_{LR} (MPa)	$E_L \times 0.064$
Poisson's ratio – v_{LR}	0.372
Poisson's ratio – v_{LR}	$v_{LR} \times E_R / E_L$

In Table 7, the subscripts '*R*' and '*L*' refer to the radial and longitudinal directions of the wood respectively. These property directions are adjusted accordingly for both the plate and brace as shown in Figure 12.

3.4.2 Soundboard Dimensions

The dimensions given to the model for analysis are found in Table. 8. The subscript '*p*' stands for plate dimensions, '*b*' for the brace and '*c*' for the combined plate and brace.

Table. 8. Model dimensions

Dimensions	Values
Length – L_x (m)	0.24
Length – L_y (m)	0.18
Brace width – L_b (m)	0.012
Reference – x_1 (m)	$L_x / 2 - L_b / 2$
Reference – x_2 (m)	$x_1 + L_b$
Thickness – h_p (m)	0.003
Thickness – h_{bo} (m)	0.012
Thickness – h_c (m)	$h_p + h_b$

3.4.3 Analysis

In order to perform the analysis and derive the modeshapes (eignenvectors) of the system, a computer algebra system was used (Maple). Maple is a mathematical software package produced by Maplesoft which solves analytical equations such as those stipulated above. Modeshapes for the plate with a scalloped brace are compared to those of the plate alone and those of a plate with a rectangular brace. The effects of the brace shape can then be observed. In order to get a good understanding of the effect on modeshapes, 2D plots are given at three different cross sections (slices) of the plate along two directions. These can be observed in Figures 13 through 18. Each 2D plot contains the corresponding 3D modeshape in the top-right corner, obtained from the plate with a scalloped brace, for reference.

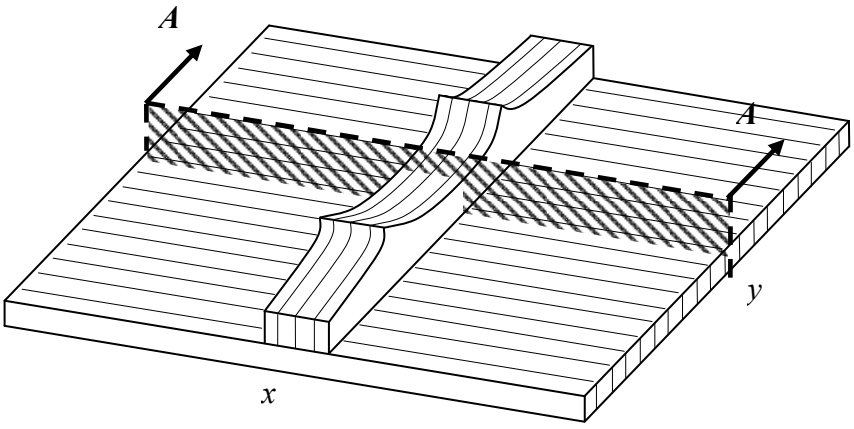

Figure 13. Location of cross-section for modeshape comparison.

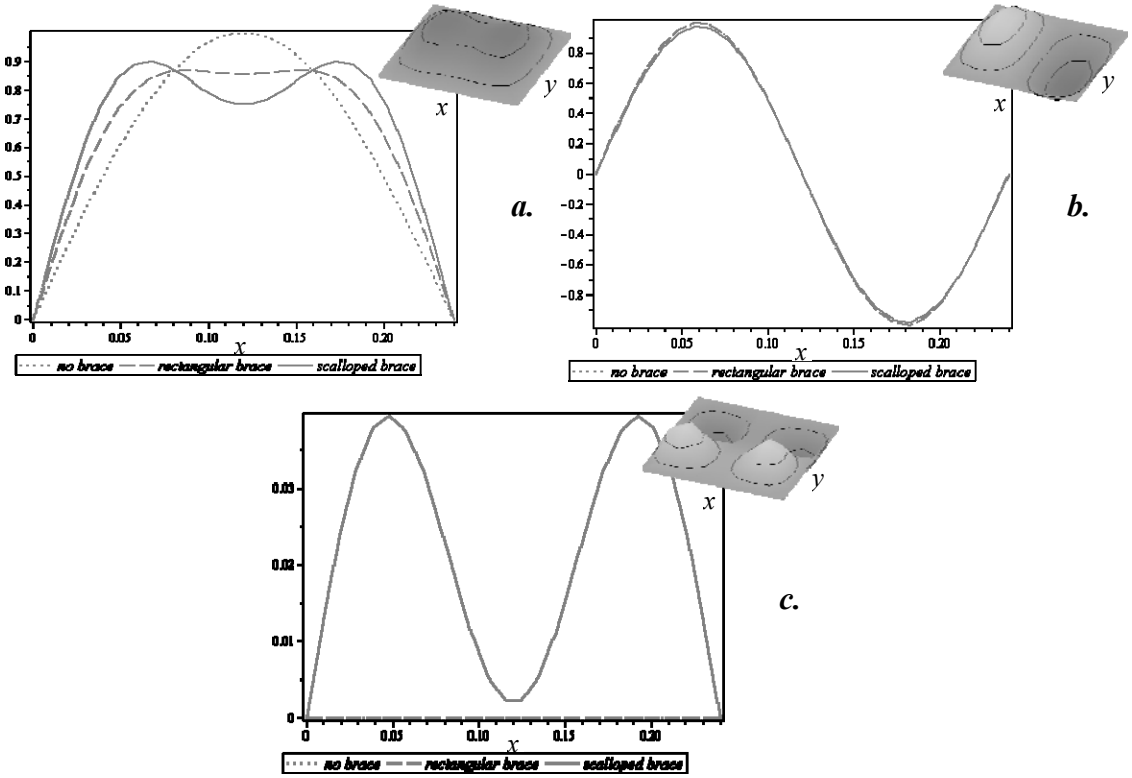

Figure 14. Section "A-A" comparison of modeshapes: a. 1×1, b. 2×1, c. 1×2.

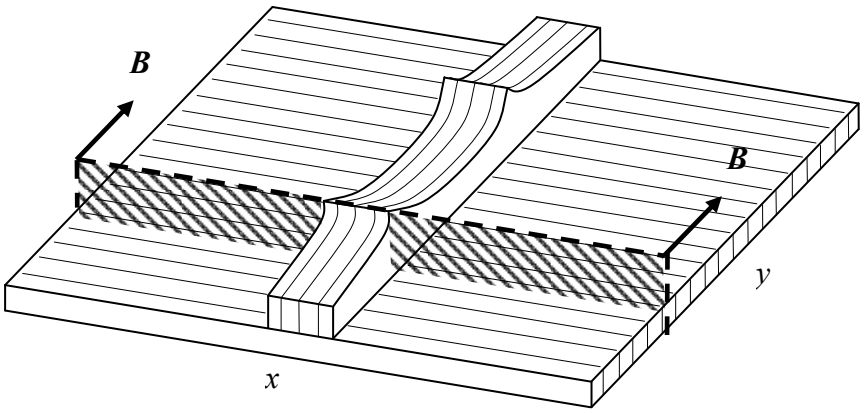

Figure 15. Location of cross-section for modeshape comparison.

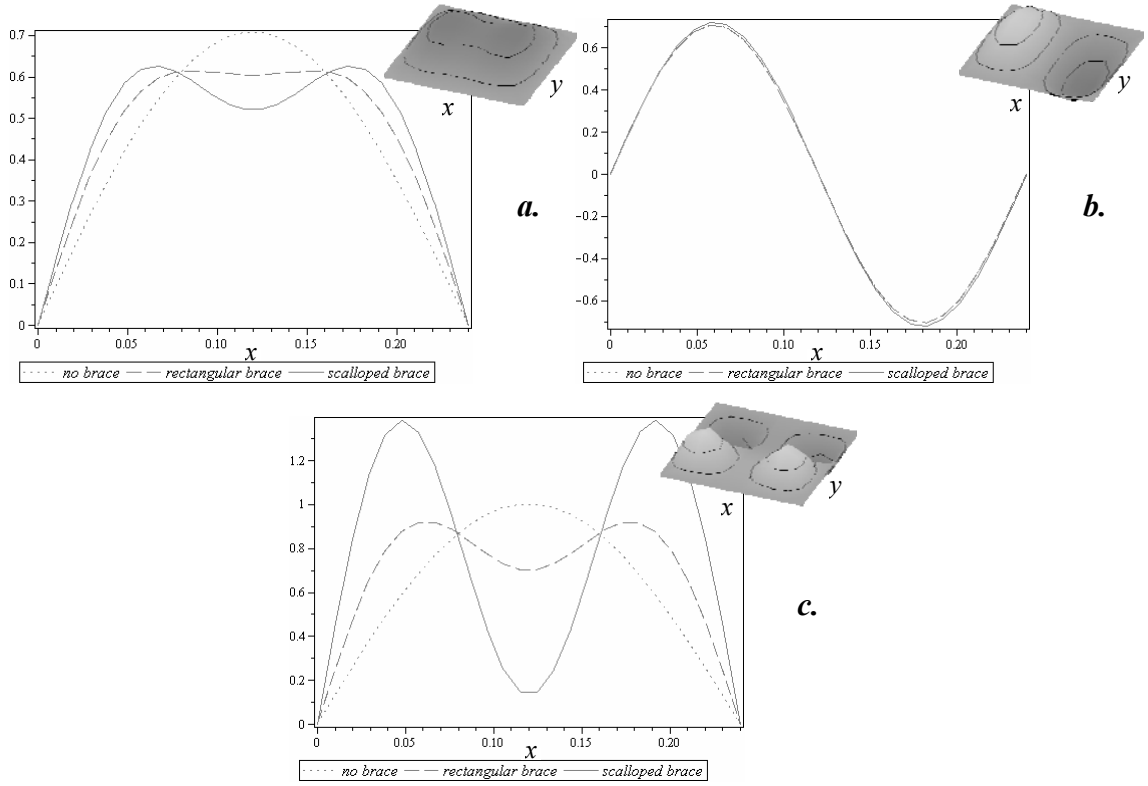

Figure 16. Section "B-B" comparison of modeshapes: a. 1×1, b. 2×1, c. 1×2.

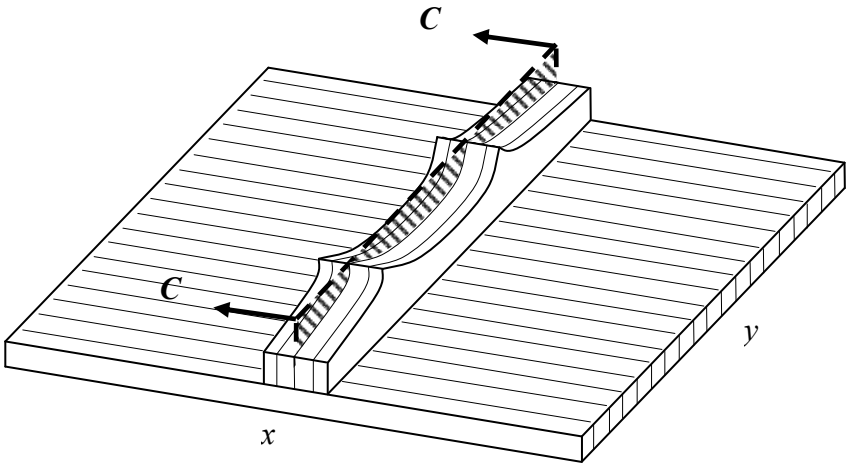

Figure 17. Location of cross-section for modeshape comparison.

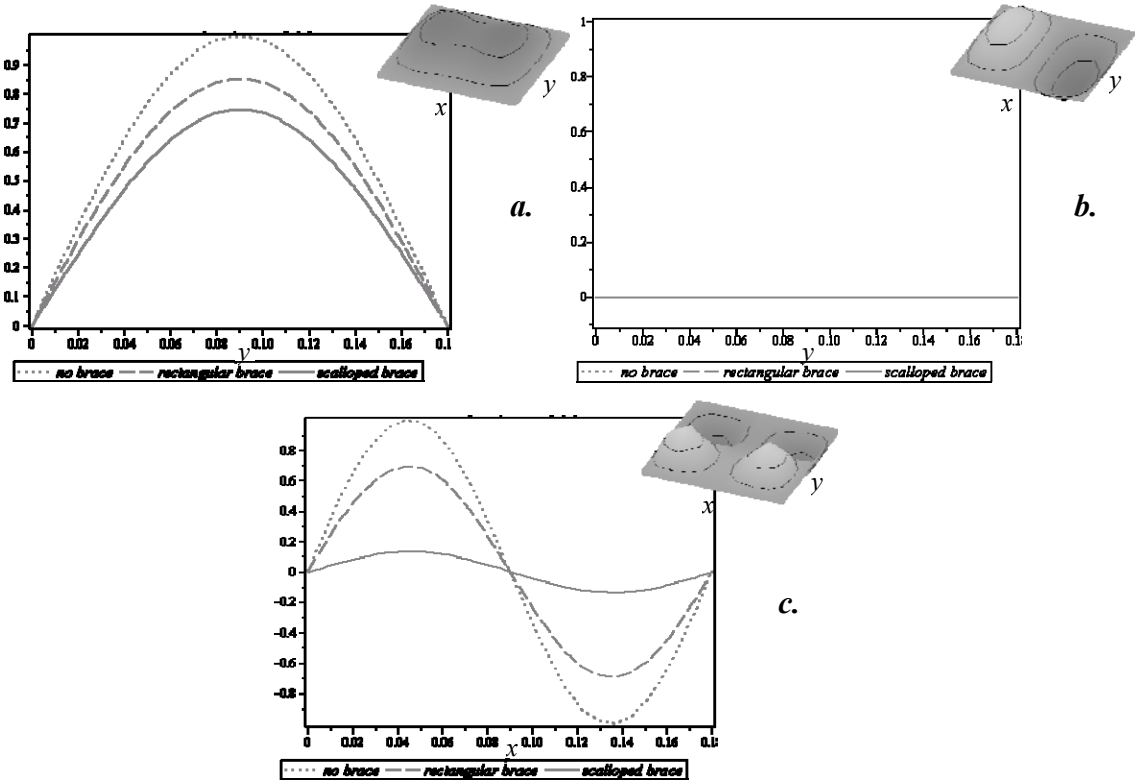

Figure 18. Section "C-C" comparison of modeshapes: a. 1×1, b. 2×1, c. 1×2.

Previous studies have shown that locally stiffening a plate increases certain frequencies while having very little effect on others. The reasons for this can be directly observed from the modeshapes.

3.4.4 Discussion

From Figures 14a and 16a and c, it is clear that locally stiffening the plate with a brace reduces the maximum amplitude possible for its vibration. This implies that frequencies associated with these modeshapes will increase. However, from Figures 14a and 16a, it can be observed that scalloping the brace has very little impact compared to the simple rectangular brace on the average modeshape amplitude. This follows since the base thickness of the scalloped brace is very similar to that of the rectangular brace and since the maximum amplitude of the first modeshape occurs at the centre of the brace, the effect of both braces is similar.

Effects of a Scalloped and Rectangular Brace on the Modeshapes of a Brace-Plate System

The flattening of the modshape visible in Figure 14a and Figure 16a is to be expected and occurs because the brace is finite in width and is located at the centre of this fundamental modeshape. It is interesting to note that although the scalloped brace flattens out the centre portion of the modeshape more than it does for the rectangular brace, the amplitude of the modeshape seems to be compensated in the portions of the modeshape lying outside of the braced region. This helps explains why the fundamental frequency is less affected by the scalloped peaks than higher frequencies [20].

Conversely, observing the third modeshape in Figure 16c, it can be seen that scalloping the brace has a significant effect on the maximum possible amplitude. This is because the peaks of the scalloped brace were designed to occur directly in the location of the maximum amplitude of this modeshape. Therefore this region is locally significantly stiffer with the scalloped brace versus the rectangular brace.

Furthermore, it can be observed from Figure 14b and Figure 16b that there is very little effect from either brace since the braces are positioned along the nodal line of the second modeshape.

Finally, Figures 17 and 18 show the first three modeshapes along the brace in the *y*-direction, and it can be seen that the scalloped-shaped brace has the same effects as discussed previously. Once again, the scalloped shape has a much larger effect on the third modeshape, as seen in Figure 18c, than it does on the first modeshape of Figure 18a when compared to the rectangular brace.

Clearly this particular brace was designed to have the most significant effect on the third modeshape since the scalloped peaks occur exactly at the point of maximum amplitude for this modeshape. Looking at other modehsapes, it could easily be seen that if a maximum amplitude occurred near the region of the scalloped peak, the peak would have a larger effect on this modeshape than if it had a node at the same location. If the goal, then, is to significantly affect one particular frequency, the potential solution is to locally change the stiffness and mass using a scalloped peak of extra material at the location of maximum amplitude of the frequency associated with that modeshape.

3.5 Conclusion

It thus becomes clear that by properly designing the shape of the braces on a soundboard and placing them in specific positions, an instrument maker has great control over the shape of modeshapes. By selecting some positions over others, it also allows some modeshapes to be modified without significantly affecting others.

Reducing the maximum amplitude of a modeshape increases the associated frequency. Reducing the maximum amplitude of a modeshape can be achieved by physically stiffening the system globally or locally. In this case, locally stiffening the system with a brace becomes much more interesting due to the requirement for the system to remain flexible overall. It also allows the modification of certain modeshapes (and therefore their associated frequencies) without significantly affecting others. This is extremely important when trying to control multiple frequencies associated with a set of modeshapes.

In the end, it may not be the modeshapes that control the sound produced by a musical instrument. However, by being able to locally control the stiffness and mass of various regions of a soundboard and hence the maximum possible amplitudes for a given modeshape, it is possible to control the frequencies associated with these modeshapes. A desired increase in a certain natural frequency requires a simple stiffening of the areas associated with the maximum amplitudes of the related modeshape.

3.6 References

[1] A. H. Benade, “Fundamentals of Musical Acoustics,” New York, NY: Dover Publications, 1990, pp. 254–280.

[2] M. Brooke and B. E. Richardson, “Mechanical vibrations and radiation fields of guitars,” *J. Acoust. Soc. Am.*, vol. 94, no. 3, p. 1806, 1993.

[3] N. H. Fletcher and T. D. Rossing, *The Physics of Musical Instruments*, 2nd ed. Springer, 1998.

[4] A. Chaigne, “Recent advances in vibration and radiation of musical instruments,” *Flow Turbul. Combust.*, vol. 61, pp. 31–34, 1999.

[5] B. E. Richardson, "Experimental and theoretical studies of the modes of stringed instruments and their relevance for quality control of instrument manufacture," *J. Acoust. Soc. Am.*, vol. 105, no. 2, p. 1124, Feb. 1999.

[6] G. A. Knott, Y. S. Shin, and M. Chargin, "A modal analysis of the violin," *Finite Elem. Anal. Des.*, vol. 5, no. 3, pp. 269–279, Oct. 1989.

[7] J. Bretos, C. Santamaría, and J. A. Moral, "Vibrational patterns and frequency responses of the free plates and box of a violin obtained by finite element analysis," *J. Acoust. Soc. Am.*, vol. 105, no. 3, p. 1942, 1999.

[8] M. J. Elejabarrieta, A. Ezcurra, and C. Santamaría, "Vibrational behaviour of the guitar soundboard analysed by the finite element method," *Acta Acust. United Acust.*, vol. 87, no. 1, pp. 128–136, 2001.

[9] E. Bécache, A. Chaigne, G. Derveaux, and P. Joly, "Numerical simulation of a guitar," *Comput. Struct.*, vol. 83, no. 2–3, pp. 107–126, Jan. 2005.

[10] M. J. Elejabarrieta, A. Ezcurra, and C. Santamaría, "Evolution of the vibrational behavior of a guitar soundboard along successive construction phases by means of the modal analysis technique," *J. Acoust. Soc. Am.*, vol. 108, no. 1, p. 369, 2000.

[11] A. Okuda and T. Ono, "Bracing effect in a guitar top board by vibration experiment and modal analysis," *Acoust. Sci. Technol.*, vol. 29, no. 1, pp. 103–105, 2008.

[12] R. M. French, *Engineering the Guitar: Theory and Practice*, 1st ed. New York: Springer, 2008.

[13] R. H. Siminoff, *The Luthier's Handbook: A Guide to Building Great Tone in Acoustic Stringed Instruments*. Milwaukee, WI: Hal Leonard, 2002.

[14] J. Natelson and W. Cumpiano, "Guitarmaking: Tradition and Technology: A Complete Reference for the Design & Construction of the Steel-String Folk Guitar & the Classical Guitar," San Francisco, CA: Chronicle Books, 1994, pp. 93–113.

[15] H. Turnbull, *The Guitar from the Renaissance to the Present Day*. Bold Strummer, 1992.

[16] E. Somogyi, "Principles of Guitar Dynamics and Design from the 1992 convention lecture," *Am. Luth.*, vol. 36, 1993.

[17] I. Curtu, M. D. Stanciu, N. C. Cretu, and C. I. Rosca, "Modal analysis of different types of classical guitar bodies," in *Proceedings of the 10th WSEAS international*

conference on Acoustics & music: theory & applications, Stevens Point, Wisconsin, USA, 2009, pp. 30–35.

[18] T. Sumi and T. Ono, "Classical guitar top board design by finite element method modal analysis based on acoustic measurements of guitars of different quality," *Acoust. Sci. Technol.*, vol. 29, no. 6, pp. 381–383, 2008.

[19] R. Lawther, "Assessing how changes to a structure can create gaps in the natural frequency spectrum," *Int. J. Solids Struct.*, vol. 44, no. 2, pp. 614–635, Jan. 2007.

[20] P. Dumond and N. Baddour, "Effects of using scalloped shape braces on the natural frequencies of a brace-soundboard system," *Appl. Acoust.*, vol. 73, no. 11, pp. 1168–1173, Nov. 2012.

[21] L. Meirovitch, *Principles and Techniques of Vibrations*. Upper Saddle River, NJ: Prentice Hall, 1996.

[22] C. Hutchins and D. Voskuil, "Mode tuning for the violin maker," *CAS J.*, vol. 2, no. 4, pp. 5–9, 1993.

[23] S. P. Timoshenko and S. W.- Kreiger, "Theory of Plates and Shells," 2nd ed., New York: McGraw-Hill Higher Education, 1964, pp. 364–377.

[24] Forest Products Labratory (US), *Wood Handbook: Wood as an Engineering Material*. U.S. Department of Agriculture, Forest Service, Madison, WI, 1999.

Chapter 4

A Structured Approach to Design-for-Frequency Problems Using the Cayley-Hamilton Theorem

SpringerPlus
DOI: 10.1186/2193-1801-3-272
Volume 3, May 2014, article 272

4.1 Abstract

An inverse eigenvalue problem approach to system design is considered. The Cayley-Hamilton theorem is developed for the general case involving the generalized eigenvalue vibration problem. Since many solutions exist for a desired frequency spectrum, a discussion of the required design information and suggestions for including structural constraints are given. An algorithm for solving the inverse eigenvalue design problem using the generalized Cayley-Hamilton theorem is proposed. A method for solving partially described systems is also specified. The Cayley-Hamilton theorem algorithm is shown to be a good design tool for solving inverse eigenvalue problems of mechanical and structural systems.

4.2 Introduction

In mechanical and structural system design, engineers are often faced with the task of designing systems which either have natural frequencies which must fall outside a specific range or operate at exactly certain frequencies. These design problems can be considered as eigenvalue problems, since the eigenvalues are used to determine the natural frequencies (frequency spectrum) of the system. Generally, the problem begins by defining the system's physical parameters and then calculating the natural frequencies using eigenvalue theory. If specific natural frequencies are sought, empirical or iterative methods are used to modify the system's physical parameters until the desired eigenvalues are obtained. This approach is both time consuming and indirect. A better approach would be to design the system directly from the natural frequencies.

From a mathematical point of view, this problem is ill-posed. This is because a single set of natural frequencies can be produced by multiple systems and thus multiple solutions are possible. One area that seeks to solve these difficulties and which potentially holds great promise for addressing the problem of design for frequency spectrum is that of inverse eigenvalue problems. Although not currently used for such purpose, the theory could potentially be applied to such design problems. A rather broad field covering many subjects, such as control systems, structural analysis, particle physics and vibrations, inverse eigenvalue problems have an interesting and large field of

application. While continuous inverse theories have been studied, such as the classical Sturm-Liouville problem [1]–[3], a more interesting approach for the purpose of design is to use discrete theory. For the application of inverse eigenvalue theory to the field of vibrations, this would involve the use of discrete matrix representations of real systems. This approach presents greater value since many numerical and analytical tools already exist for the solution of discrete problems and many engineering systems are often modeled as discrete systems.

Much focus has been applied to the study of discrete inverse eigenvalue problems. This has been made clear by a thorough review of the topic by Chu and Golub [4], [5]. Gladwell takes a more direct route in which he considers specific inverse problems and matrix structures related to mechanical vibrations [6]. Particularly, it appears that most of the literature focuses on system identification. One of the most common techniques in inverse eigenvalue problems is to use/measure the system's spectrum and then constrain the system in some fashion in order to obtain a second spectrum [7]–[11]. This clearly indicates that a system usually exists and that it can be tested to obtain data required for the inverse problem of mathematically reconstructing the system. Although interesting, this approach cannot be used for novel engineering design to construct a system having a specific spectrum without another system on which to base the design.

In most cases, the solution to the inverse problem begins by placing the given desired eigenvalues along the main diagonal entries of a diagonal matrix $\mathbf{\Lambda}$. Additionally, any arbitrary invertible matrix $\mathbf{P}$ can be used to obtain another solution (matrix) with the same spectrum, namely $\mathbf{P\Lambda P}^{-1}$. Since $\mathbf{P\Lambda P}^{-1}$ is the trivial solution, pre-conditioning of the $\mathbf{P}$ matrix is required so that any given structural requirements of the system can be satisfied. Various methods can be used to impose such structure. According to Chu, these methods can be distinguished by the types of procedures used in imposing structure to the matrix [4]. Structuring matrices by prescribing specific entries has been studied in [12] and [13]. Modifying the matrix through the addition of another matrix has also been considered in [14]–[16]. Dias de Silva, de Oliveira, and others have studied how multiplying the discrete system by another matrix can affect its structure [17]–[19]. The use of the well-developed matrix theory for certain structured matrices, such as Jacobi or band matrices, as applied to inverse problems has also been investigated [20]–[23].

Finally, applying least squares methods have shown to be an effective method for finding an approximate solution to inverse eigenvalue problems [24], [25].

In most cases, the research on inverse eigenvalue problems has focused on the existence, uniqueness and computability of a solution. Other studies are typically variations on those described above, including partially-described problems, where not all spectral information is known. These types of problems have been considered in [26] and [27], and are of interest for problems requiring only certain frequencies to be specifically determined.

Once an inverse eigenvalue problem has been set up and the type of solution has been chosen, various algorithms can be used to numerically solve the problem. These include orthogonal polynomial methods, the block Lanczos algorithm, the Newton method and the divide and conquer method, as well as several others [20], [28]–[32]. A great deal of research has advanced the field of optimization and has improved our ability to find feasible solutions to various problems. A comprehensive work on the subject is the Encyclopedia of Optimization [33]. Although broad in scope, very little has been done to apply inverse eigenvalue theory to actual engineering design problems. In the case of mechanical or structural design, the potential advantage of using such theory when designing a frequency spectrum into a system appears to be immense.

Interestingly, Dias de Silva and de Oliveira have shown that an $n \times n$ matrix always exists when a minimum of $n-1$ prescribed matrix entries and a prescribed characteristic polynomial are given as design information [34], [35]. Dias de Silva and de Oliveira's results guarantee existence but not uniqueness of the matrix.

One of the main shortcomings of current inverse eigenvalue theory is the lack of a solution for general matrices having predefined forms but which do not fit within current known solutions. In this paper, a novel approach is considered using the Cayley-Hamilton theorem. The Cayley-Hamilton theorem relates a square matrix over a commutative ring to its characteristic polynomial [36], [37]. To the authors' knowledge, the Cayley-Hamilton theorem has not been used as a design tool for inverse eigenvalue problems.

4.3 Problem Definition

In this paper, we consider the following problems:

PROBLEM A: *Given a specified frequency spectrum or equivalently a set of eigenvalues,* $\lambda_1,...,\lambda_n$*, construct an* n^{th} *order system, described by an* $n \times n$ *matrix* $\mathbf{A}$*, which has* $\lambda_1,...,\lambda_n$ *as its eigenvalues.*

Although this problem has been considered for specific forms of matrices (i.e. Jacobi, band or other matrix forms as described above), a general solution approach does not currently exist. Problem A leads into the vibration problem of interest which is also presented here:

PROBLEM B: *Given a specified frequency spectrum or equivalently a set of eigenvalues,* $\lambda_1,...,\lambda_n$*, construct an* n^{th} *order system, described by two* $n \times n$ *matrices (the mass matrix* $\mathbf{M}$ *and the stiffness matrix* $\mathbf{K}$*), which has* $\lambda_1,...,\lambda_n$ *as its generalized eigenvalues:* $\det(\mathbf{K} - \lambda\mathbf{M}) = 0$ *for the given* $\lambda_1,...,\lambda_n$*.*

For an engineer, Problem B relates directly to the design problem stated earlier, where a conservative vibrating system having specific natural frequencies is sought. Finally, a partially described system is considered:

PROBLEM C: *Given a certain number of specified natural frequencies or equivalently eigenvalues, as well as a number of matrix entries, where together there is no less than* n *pieces of given information, construct an* n^{th} *order system, described by an* $n \times n$ *matrix* $\mathbf{A}$*, which has* $\lambda_1,...,\lambda_n$ *as its eigenvalues.*

Problem C can be extended to a two matrix problem in the same manner as described for problem B. However, this has not been specifically considered herein.

4.4 Cayley-Hamilton Theorem

4.4.1 Basic Theory

In order to solve Problem A, a discussion of the Cayley-Hamilton theorem is required. The Cayley-Hamilton theorem states that if $p(\lambda)$ is the characteristic polynomial of a square matrix $\mathbf{A}$, obtained from $p(\lambda) = \det(\lambda\mathbf{I} - \mathbf{A})$, then substituting $\mathbf{A}$ for λ in the polynomial gives the zero matrix. Thus, by applying the theorem, matrix $\mathbf{A}$ satisfies its own characteristic polynomial, $p(\mathbf{A}) = 0$ [38].

The Cayley-Hamilton theorem can be useful in inverse eigenvalue problems beyond the typical statement that a square matrix satisfies its own characteristic equation. Once the characteristic polynomial of a system is found from desired spectral data, the Cayley-Hamilton theorem can be used to find an unknown matrix $\mathbf{A}$, which represents the system. A set of unknown entries of the matrix $\mathbf{A}$ can be solved from the set of equations that arise from the Cayley-Hamilton theorem. For example, suppose that a 2×2 matrix $\mathbf{A}$ has the form

$$\mathbf{A} = \begin{bmatrix} a_{11} & a_{12} \\ a_{21} & a_{22} \end{bmatrix} \tag{15}$$

In order to solve the inverse eigenvalue problem we must populate the entries of matrix $\mathbf{A}$ by using the Cayley-Hamilton theorem and the set of desired eigenvalues. In order to visualize the process, suppose that the desired eigenvalues are -2 and -3. The characteristic polynomial is then constructed as

$$p(\lambda) = (\lambda + 2)(\lambda + 3) = \lambda^2 + 5\lambda + 6 \tag{16}$$

Using the Cayley-Hamilton theorem, λ is replaced by $\mathbf{A}$ of Equation (15) in Equation (16), such that

$$p(\mathbf{A}) = \mathbf{A}^2 + 5\mathbf{A} + 6\mathbf{I} = 0 \tag{17}$$

where $\mathbf{I}$ is the identity matrix. Expanding Equation (17) gives us four equations with four unknowns:

$$\begin{bmatrix} a_{11}^2 + a_{12}a_{21} + 5a_{11} + 6 & a_{11}a_{12} + a_{12}a_{22} + 5a_{12} \\ a_{11}a_{21} + a_{21}a_{22} + 5a_{21} & a_{22}^2 + a_{12}a_{21} + 5a_{22} + 6 \end{bmatrix} = \begin{bmatrix} 0 & 0 \\ 0 & 0 \end{bmatrix} \tag{18}$$

However, equation independence is unclear. A discussion is found in Section 4.5.1. Solving Equation (18) leads to two dependent solutions:

$$\left[a_{11} = -a_{22} - 5, \;\; a_{12} = -\frac{a_{22}^2 + 5a_{22} + 6}{a_{21}}, a_{21} = a_{21}, a_{22} = a_{22} \right] \tag{19}$$

At this point, any values can be assigned to a_{21} and a_{22} and the matrix $\mathbf{A}$ will have the desired eigenvalues given in Equation (16). Consequently, Problem A has been solved, although it is clear that many solutions exist. This solution is particularly useful in solving inverse eigenvalue problems as it gives a range of $\mathbf{A}$ matrix values for which a system produces the same eigenvalues. The limiting factors are then based on the physical limits and fixed parameters of the system.

4.4.2 Generalized Cayley-Hamilton Theorem for Mass and Stiffness Matrices

Problem B is related to Problem A, but takes on a more general form which is conducive to real physical systems. When considering a conservative vibrating system, the factors that control its frequency spectrum are the system's mass and stiffness. Typically, continuous systems are discretized in order to simplify the analysis. By doing so, the system is described using mass ($\mathbf{M}$) and stiffness ($\mathbf{K}$) matrices. The forward generalized eigenvalue problem involves solving the equation $\det(\mathbf{K} - \lambda\mathbf{M}) = 0$ for the system's generalized eigenvalues, λ. Although the characteristic polynomial is similar to the single matrix case, it now involves two matrices rather than one. Therefore, the lesser-known generalized Cayley-Hamilton theorem must be used [39].

The generalized Cayley-Hamilton theorem is modified to include a second square matrix $\mathbf{B}$. The characteristic polynomial takes the form $p(\lambda) = \det(\mathbf{A} - \lambda\mathbf{B})$. By substituting $\mathbf{A}$ and $\mathbf{B}$ for λ into the characteristic polynomial a similar relationship is satisfied,

$$p(\mathbf{A}, \mathbf{B}) = c_n(\mathbf{B}^{-1}\mathbf{A})^n + c_{n-1}(\mathbf{B}^{-1}\mathbf{A})^{n-1} \ldots + c_1(\mathbf{B}^{-1}\mathbf{A}) + c_0\mathbf{I} = 0 \tag{20}$$

where c_n is the coefficient of λ^n in $p(\lambda)$. Equation (20) is valid as long as $\mathbf{B}$ is non-singular.

If matrices $\mathbf{A}$ and $\mathbf{B}$ commute (i.e. $\mathbf{AB} = \mathbf{BA}$), then the generalized Cayley-Hamilton theorem can be written as

$$p(\mathbf{A},\mathbf{B}) = c_n\mathbf{A}^n + c_{n-1}\mathbf{A}^{n-1}\mathbf{B}... + c_1\mathbf{A}\mathbf{B}^{n-1} + c_0\mathbf{B}^n = 0 \tag{21}$$

where no other restrictions are placed on matrix $\mathbf{B}$.

For the generalized eigenvalue problem of a vibrating system, the characteristic equation of the system is obtained by calculating the determinant of $(\mathbf{K} - \lambda\mathbf{M})$. Thus, the Cayley-Hamilton theorem for a conservative vibrating system is obtained by replacing the matrix $\mathbf{B}$ with the mass matrix $\mathbf{M}$ and the $\mathbf{A}$ matrix by the stiffness matrix $\mathbf{K}$ in Equations (20) and Equation (21). Solving these equations leads to the solution of Problem B.

4.4.3 Numerical Example

Once again, a numerical example is used to demonstrate concepts. Using the same eigenvalues as for the previous example gives the characteristic polynomial of Equation (16). This time, the modified generalized Cayley-Hamilton theorem is used to form an equation for unknown matrices $\mathbf{K}$ and $\mathbf{M}$ such that

$$p(\mathbf{K},\mathbf{M}) = \left(\mathbf{M}^{-1}\mathbf{K}\right)^2 + 5\left(\mathbf{M}^{-1}\mathbf{K}\right) + 6\mathbf{I} = 0 \tag{22}$$

Assuming the $\mathbf{K}$ and $\mathbf{M}$ matrices have a similar form to that of $\mathbf{A}$ in Equation (15), then Equation (22) can be expanded to give four equations with eight unknowns. Solving these equations produces several results, one of which can be written as

$$\left[\begin{array}{l} k_{11} = \dfrac{k_{12}k_{21}k_{22} + 5k_{12}k_{21}m_{22} + 6k_{12}m_{21}m_{22} + 6k_{21}m_{12}m_{22} - 6k_{22}m_{12}m_{21}}{(k_{22} + 2m_{22})(k_{22} + 3m_{22})}, \\ m_{11} = \dfrac{k_{21}k_{22}m_{12} + k_{12}k_{22}m_{21} - k_{12}k_{21}m_{22} + 5k_{22}m_{12}m_{21} + 6m_{12}m_{21}m_{22}}{(k_{22} + 2m_{22})(k_{22} + 3m_{22})}, \\ k_{12} = k_{12},\ m_{12} = m_{12},\ k_{21} = k_{21},\ m_{21} = m_{21},\ k_{22} = k_{22},\ m_{22} = m_{22} \end{array}\right] \tag{23}$$

Once again it becomes clear that only 2 solutions are dependent, and selecting any values for $k_{12}, m_{12}, k_{21}, m_{21}, k_{22}, m_{22},$ will result in **K** and **M** matrices that produce a solution with the desired eigenvalues.

Increasing the size of the square matrices increases the number of independent variables quicker than it does the dependent variables. In other words, for an n^{th} order system with n specified eigenvalues (natural frequencies), $2n^2$ unknown variables are required to find **K** and **M**, but as will be shown later in this paper, the generalized Cayley-Hamilton theorem only produces n independent equations.

4.4.4 Spring-Mass System Example

Using a typical 2 degree-of-freedom (2DOF) spring-mass system, as seen in Figure 19, many properties of the method can be explored. Although simple, this problem allows us to see the basics of how the method works. A more complicated problem is included as an appendix for further reading.

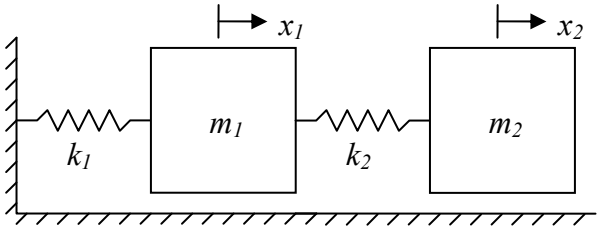

Figure 19. 2DOF spring-mass system.

In order to use the Cayley-Hamilton inverse method, the structure of the system must first be explored in the forward sense. In essence we must pre-condition the mass and stiffness matrices to account for the system's physical constraints. The equation of motion of the system can be written as

$$\underbrace{\begin{bmatrix} m_1 & 0 \\ 0 & m_2 \end{bmatrix}}_{\mathbf{M}} \begin{bmatrix} \ddot{x}_1 \\ \ddot{x}_2 \end{bmatrix} + \underbrace{\begin{bmatrix} k_1 + k_2 & -k_2 \\ -k_2 & k_2 \end{bmatrix}}_{\mathbf{K}} \begin{bmatrix} x_1 \\ x_2 \end{bmatrix} = \begin{bmatrix} 0 \\ 0 \end{bmatrix} \tag{24}$$

where $\vec{x} = \left[x_1, x_2\right]^T$ is the displacement vector and **M** and **K** are the mass and stiffness matrices respectively. The goal of the approach is: given the system eigenvalues, λ_1 and

λ_2, determine the **M** and **K** matrices that give rise to these eigenvalues. Determining the matrices **M** and **K** in accordance with relevant system constraints would be the engineering design problem.

Once the structure of the system has been set, the inverse solution can begin. First, from the set of desired eigenvalues, λ_1 and λ_2, a characteristic polynomial is formed such that

$$\lambda^2 - (\lambda_1 + \lambda_2)\lambda + (\lambda_1\lambda_2) = 0 \tag{25}$$

Using the Cayley-Hamilton theorem with **M** and **K** as given in Equation (24), along with the desired characteristic Equation (25), a set of four equations and four unknowns is found:

$$\begin{bmatrix} \dfrac{(k_1+k_2)^2}{m_1^2} + \dfrac{k_2^2}{m_1 m_2} + \dfrac{(k_1+k_2)(\lambda_1+\lambda_2)}{m_1} + \lambda_1\lambda_2 = 0, \\ -\dfrac{k_2(k_1+k_2)}{m_1^2} - \dfrac{k_2^2}{m_1 m_2} - \dfrac{k_2(\lambda_1+\lambda_2)}{m_1} = 0, \\ -\dfrac{k_2^2}{m_2^2} - \dfrac{k_2(k_1+k_2)}{m_1 m_2} - \dfrac{k_2(\lambda_1+\lambda_2)}{m_2} = 0, \\ \dfrac{k_2^2}{m_2^2} + \dfrac{k_2^2}{m_1 m_2} + \dfrac{k_2(\lambda_1+\lambda_2)}{m_2} + \lambda_1\lambda_2 = 0 \end{bmatrix} \tag{26}$$

A solution is obtained as

$$\begin{bmatrix} k_1 = \dfrac{m_2^2 k_2 \lambda_1 \lambda_2}{(k_2 + m_2\lambda_1)(k_2 + m_2\lambda_2)}, \\ m_1 = \dfrac{m_2 k_2^2}{(k_2 + m_2\lambda_1)(k_2 + m_2\lambda_2)}, \\ k_2 = k_2,\ m_2 = m_2 \end{bmatrix} \tag{27}$$

In this case, choosing any value for two of the four variables will lead to a solution which satisfies the characteristic polynomial and thus has the given natural frequencies/eigenvalues. This solution is the same as that presented by Gladwell in [6], although the method of obtaining this solution is different.

4.5 Analysis

4.5.1 Information Produced by the Cayley-Hamilton Theorem

We show here that given n distinct eigenvalues for an n^{th} order system, the Cayley-Hamilton theorem can produce at most n independent equations, even though n^2 equations are produced. Let $p(t) = c_n t^n + c_{n-1} t^{n-1} + ...c_1 t + c_0$ be the characteristic polynomial of an $n \times n$ matrix $\mathbf{A}$. The Cayley-Hamilton theorem states that $p(\mathbf{A}) = c_n \mathbf{A}^n + c_{n-1} \mathbf{A}^{n-1} + ...c_1 \mathbf{A} + c_0$ is the zero matrix. Suppose that the matrix $\mathbf{A}$ is diagonal and let the diagonal entries be $\lambda_1, \lambda_2, ..., \lambda_n$. The characteristic polynomial is

$$p(t) = (t - \lambda_1)(t - \lambda_2)...(t - \lambda_n) \tag{28}$$

In this case, $p(\mathbf{A})$ is also a diagonal matrix with exactly n equations. In fact, the i$^{\text{th}}$ diagonal entry is $p(\lambda_i)$.

Now consider the case that $\mathbf{A}$ is not diagonal. Given n distinct eigenvalues for $\mathbf{A}$, then $\mathbf{A}$ is diagonalizable, so that $\mathbf{A}' = \mathbf{P}^{-1}\mathbf{A}\mathbf{P}$ is diagonal for some invertible matrix $\mathbf{P}$. The characteristic polynomial of $\mathbf{A}'$ is the same as the characteristic polynomial $p(t)$ of $\mathbf{A}$. In fact, the diagonal matrix $\mathbf{A}'$ is the trivial solution to our design problem and the 'structure' of the design problem is housed in the matrix $\mathbf{P}$. It is known that [37]

$$p(\mathbf{A}) = \mathbf{P}\, p(\mathbf{A}')\mathbf{P}^{-1} \tag{29}$$

Equation (29) states that $p(\mathbf{A})$ can be obtained by combining the equations contained in $p(\mathbf{A}')$. At the same time, since $\mathbf{A}'$ is itself diagonal, then matrix $p(\mathbf{A}')$ contains exactly n equations. Thus, this states that $p(\mathbf{A})$ is a combination of exactly n independent equations and we can expect that although $p(\mathbf{A})$ has n^2 equations, only n of them are independent.

It is also important to point out that the n independent equations obtained from the Cayley-Hamilton theorem are each n^{th} order polynomials. For a polynomial system with

n unknowns and also n equations, then Bézout's theorem states that our problem has n^n complex solutions [40].

4.5.2 Required Design Information

It is clear that the spectral information (eigenvalues) alone is not enough information to complete a design. The method presented, along with all other methods, is limited by the fact that an n^{th} order system can produce at most n independent equations, even though n^2 equations are obtained via applying the generalized Cayley-Hamilton theorem, as discussed above. If the matrices are completely unknown then there may be as many as $2n^2$ unknown entries in the mass and stiffness matrices. The Cayley-Hamilton method can produce at most n independent variables and the remaining equations must be specified in other ways. For creating physically realistic systems, this generally entails pre-conditioning or constraining the structure of the matrices.

For solving discrete conservative vibration problems, Equation (20) can be used as long as the $\mathbf{M}$ matrix is non-singular and Equation (21) can be used if $\mathbf{M}$ and $\mathbf{K}$ commute. It becomes very clear by considering Equation (23) that more information is required in order to build a suitable vibrating system based on mass and stiffness. From an engineer's point of view, any system which can produce similar eigenvalues has the potential of being suitable, as long as it fits within the physical criteria set at the outset of the project. It is obvious that Equation (23) can produce an infinite number of possible solutions. Equation (23) represents only one of several solutions to the equation presented in (22). As the system's order increases, so does the number of potential solutions (Bézout's theorem). Thus, engineers have many solutions at their disposal for creating suitable and optimized designs.

It is then evident why many engineers develop and adopt their own unique methods for creating and optimizing designs. These represent but one of many possible solutions. Evidence tends to contradict arguments that there is only one approach to design or only one solution to the problem.

The inverse problem is then not limited by the eigenvalues, and in fact the eigenvalues alone do not contain enough information from which to build a physical system. Therefore, other information is required in order to complete the design.

4.5.3 Structural Constraints

One of the easiest ways to limit the number of matrix entries and include structural constraints is by including zero entries or by incorporating symmetry into the matrices. These constraints are interesting because they follow directly from real systems. Taking as an example the 2DOF spring-mass system developed in Section 4.4.4, it can be seen that only diagonal entries are present in the mass matrix and the stiffness matrix is made symmetric by forcing off-diagonal terms to be the same. Physically, the structure of these matrices reflects the fact that the two degrees of freedom of the system are coupled via a stiffness element coupling. It can be seen in Figure 19 that the masses are connected via springs (stiffness elements) only. Furthermore, the symmetry of the stiffness matrix is a consequence of Newton's third law. The system is further constrained by the fact that the off-diagonal terms in the stiffness matrix are not independent, but are related to the diagonal terms, once again reducing the number of unknowns. In this case, incorporating physical constraints into the mathematical structure of the problem has reduced the number of unknowns from $2n^2$ to just n^2.

In this case, the engineer still has the freedom to choose from several systems which would satisfy the requirements. Further constraints may come in the form of available components such as stiffeners which must fit within specified physical dimensions or the financial budget.

From this stems the importance of the forward problem. Continuous systems are typically discretized using various methods which produce a model of the system in matrix form. The form of the matrix is heavily dependent on the choice of discretization method. The inverse problem is consequently affected since it seeks to create a matrix that matches the form as stipulated at the outset. Although the Cayley-Hamilton theorem does not discriminate in its ability to solve these various matrix forms, it is possible that certain discretization methods lead to simpler forms or matrices containing fewer variables. In this sense, the design may be easier to fully define.

4.5.4 Partially Described Systems

Another aspect that affects the amount of design information required is the information available for the design. Thus far, the entire spectral set has been used as design information, as well as specification of matrix entries when necessary. However, as stated in [4], often only portions of the entire spectrum are available. This is termed a partially-described inverse eigenvalue problem. This is true whether it is the information stipulated via the design requirements or whether it is the experimental data available for system identification. Regardless of the information available, the Cayley-Hamilton theorem can be used to produce n pieces of information for an n^{th} order system stemming from n degrees of freedom. If certain eigenvalues are missing, the Cayley-Hamilton theorem can still be used.

Typically, in order to completely solve an n^{th} order inverse problem using the Cayley-Hamilton theorem, only n unknown values should be present in the problem, regardless of their appearance along the solution path. Problem C makes full use of this detail during its solution by pre-conditioning the matrix being solved to account for this. For a 3DOF system then, only three unknowns should be present. Consider for example the following system which has three known eigenvalues $\lambda_1 = 0.47,\ \lambda_2 = 4.66,\ \lambda_3 = 10.87$ and three unknown entries in the matrix

$$\mathbf{A} = \begin{bmatrix} a_1 + a_2 & -a_2 & 0 \\ -a_2 & a_2 + a_3 & -a_3 \\ 0 & -a_3 & a_3 \end{bmatrix} \tag{30}$$

Using the Cayley-Hamilton theorem as described in Section 4.4, the matrix $\mathbf{A}$ can be determined such that $a_1 = 9.43,\ a_2 = 1.23,\ a_3 = 2.06$ which gives a matrix solution for the system of

$$\mathbf{A} = \begin{bmatrix} 10.66 & -1.23 & 0 \\ -1.23 & 3.28 & -2.06 \\ 0 & -2.06 & 2.06 \end{bmatrix} \tag{31}$$

As in Problem C, it is often the case that only partial spectral information is available. Therefore, the Cayley-Hamilton theorem can be used if the amount of missing spectral information is replaced by the same amount of matrix entry information. So, if only

$\lambda_3 = 10.87$ is known then two of the three a matrix entries must be known. If $a_2 = 1.23$ and $a_3 = 2.06$ are known in the example above, then solving the Cayley-Hamilton equations gives $a_1 = 9.43,\ \lambda_1 = 0.47,\ \lambda_2 = 4.66$. Consequently, solving Problem C is not much different from solving Problem A.

The same is true if the system is made up of a mass matrix $\mathbf{M}$ and a stiffness matrix $\mathbf{K}$, except in this case, the generalized Cayley-Hamilton theorem must be used.

The question then becomes what is the better strategy for design? Is it better to specify the entire spectrum even though only a select few eigenvalues are critical? In this case, the analysis would lead to a full solution of the matrix if any real solutions are possible based on the prescribed matrix form. Or is it better to only specify the critical eigenvalues and solve for the remainder by specifying more information in the matrix? In this case, an alternate method for determining this extra matrix information would be required. From experience, it would appear that the latter method is generally easier given the need to produce a real system, especially since not all spectra produce real systems. The main difficulty appears to be in setting up the matrix form. This is achieved by looking at the forward solution method. In most cases, the forward solution will utilize some form of discretization, be it finite elements, global elements, finite difference or other methods. The method chosen has a large impact on the structure of the matrix, making the solution easier or more difficult depending on the situation. Also, in discretizing, the method chosen to relate material parameters has a large effect on the number of independent variables. Therefore it is extremely important to ensure that simplification methods are properly considered.

4.6 Discussion

4.6.1 Implementation

The implementation of the Cayley-Hamilton theorem is particularly suited to symbolic computer algebra systems such as Maple, Mathematica or Mathcad since the problem can be efficiently set up within the software. Firstly, the characteristic polynomial can be directly created from the eigenvalues. Subsequently, the Cayley-

Hamilton theorem equation can be constructed in order to produce the set of governing equations. Finally, the equations can be solved (in some cases analytically) in order to populate the given matrices. If the system is 5^{th} order or higher, it may be easier to use a minimization procedure such as the DirectSearch package available in Maple to simplify computation. The DirectSearch package provides universal derivative-free direct searching methods which do not require the objective function and constraints to be differentiable and continuous.

On the other hand, if a solution to the set of governing equations is all that is sought, then numerical solvers such as MATLAB are particularly well-suited for obtaining numerical solutions.

4.6.2 Non-Physical Solutions

Like most design tools, the Cayley-Hamilton theorem is not without drawbacks. Certain aspects of the theorem must be diligently considered by the engineer in order to ensure proper solution compliance.

It is of utmost importance that the system matrices be constructed from physical knowledge. Although a solution is possible with the Cayley-Hamilton theorem, it may not always produce real entries in the matrices. Since the goal is to reproduce a real system, complex matrix entries do not satisfy the design goal.

It is well known, that the roots of the polynomials are sensitive to perturbations of the coefficients [4], therefore polynomials constructed this way are usually easily subject to errors. This is especially true for system identification, where experimental data is quite often inexact. However, since frequencies specified in design (that is, the desired frequencies of vibration) are generally obtained from extensive experimentation or through other means altogether, the effect of perturbations is significantly lessened.

4.6.3 Algorithm

In order to use the Cayley-Hamilton theorem as a tool for the design of an n-dimensional vibrating system based on knowledge of desired natural frequencies and/or physical parameters, $2n^2 - n$ additional pieces of design information are required

in addition to the n desired natural frequencies. An algorithm for solving Problem B is as follows:

ALGORITHM. *Given the* n *desired eigenvalues* $\lambda_1,...,\lambda_n$ *of an* n^{th} *order vibrating system*

1. *Generate the characteristic polynomial:*

$$p(\lambda)=(\lambda-\lambda_1)...(\lambda-\lambda_{n-1})(\lambda-\lambda_n)=c_n\lambda^n+c_{n-1}\lambda^{n-1}+...+c_1\lambda+c_0$$

2. *Generate the* $\mathbf{M}$ *and* $\mathbf{K}$ *matrices from physical parameters and by using the* $2n^2-n$ *pieces of design information, applying symmetry and any other techniques based on the discretized forward problem and leaving an* n *number of unknowns;*

3. *Generate the Cayley-Hamilton theorem equation:*

$$p(\mathbf{K},\mathbf{M})=c_n(\mathbf{M}^{-1}\mathbf{K})^n+c_{n-1}(\mathbf{M}^{-1}\mathbf{K})^{n-1}...+c_1(\mathbf{M}^{-1}\mathbf{K})+c_0\mathbf{I}=0$$

or for commuting $\mathbf{M}$ *and* $\mathbf{K}$ *matrices:*

$$p(\mathbf{K},\mathbf{M})=c_n\mathbf{K}^n+c_{n-1}\mathbf{K}^{n-1}\mathbf{M}...+c_1\mathbf{K}\mathbf{M}^{n-1}+c_0\mathbf{M}=0$$

4. *Extract* n^2 *equations from the Cayley-Hamilton equation in 3;*

5. *Select* n *non-zero independent equations (the Cayley-Hamilton matrix diagonal entries work well);*

6. *Compute the* n *unknowns by solving the* n *independent equations;*

7. *Insert the* n *computed values into their appropriate places in the* $\mathbf{M}$ *and* $\mathbf{K}$ *matrices;*

8. *Verify that a valid solution is obtained by calculating* $\det(\mathbf{K}-\lambda\mathbf{M})=0$ *and ensuring that the initially given eigenvalues are obtained.*

The output consists of n *matrix entries of the* $\mathbf{M}$ *and* $\mathbf{K}$ *matrices.*

A similar algorithm can be applied to Problems A and C. In the case of Problem C, $n-m$ eigenvalues are given, as well as m matrix entries, where m is the number of unknown or unspecified eigenvalues. The output consists of m eigenvalues and the remainder of the unknown matrix entries.

4.7 Conclusion

In this paper, we considered a tool that can be used for discrete design-for-frequency engineering problems. An engineer would generally prefer a direct approach to design-for-frequency when designing a mechanical or structural system, rather than a heuristic trial-by-error approach. In this paper, we showed that the Cayley-Hamilton theorem can be a good design tool for achieving this. Unlike other methods, this approach is not limited in application to any specific type of matrix structure. Although many mathematical solutions usually exist, only a finite number of solutions are actually physically valid. This does not, however, depend on the eigenvalues, but rather on the dimensions, the physical requirements and the structure of the system, which dictate many of its parameters. The Cayley-Hamilton theorem allows the easy inclusion of these extra parameters in order to get a physically-realistic design without iteration.

Regardless of the specified design information for an n^{th} order system, $n^2 - n$ (or $2n^2 - n$ for the general case) additional pieces of information are required as input in addition to the n desired eigenvalues, in order to completely solve the inverse eigenvalue problem and hence design the system. This follows since the Cayley-Hamilton theorem can supply at most n pieces of information to the design, as shown in this paper. The source of the information, whether eigenvalues or matrix entries, is of little significance. Hence, establishing the forward equations of motion in order to pre-condition the discrete matrix system structure based on the physical system of interest is emphasized.

4.8 Appendix - Example of using the Cayley-Hamilton inverse method for brace design

4.8.1 Problem Statement

Given a desired fundamental frequency, construct a brace-plate system as described by a mass matrix **M** and a stiffness matrix **K**. All dimensional (geometric) properties of the brace-plate system are assumed to be specified and fixed except for the thickness of the brace h_c, the design variable for which we must solve.

4.8.2 Forward Model

The model is based on an orthotropic plate structurally reinforced by a brace in the weaker plate direction. The model is shown in Figure 20.

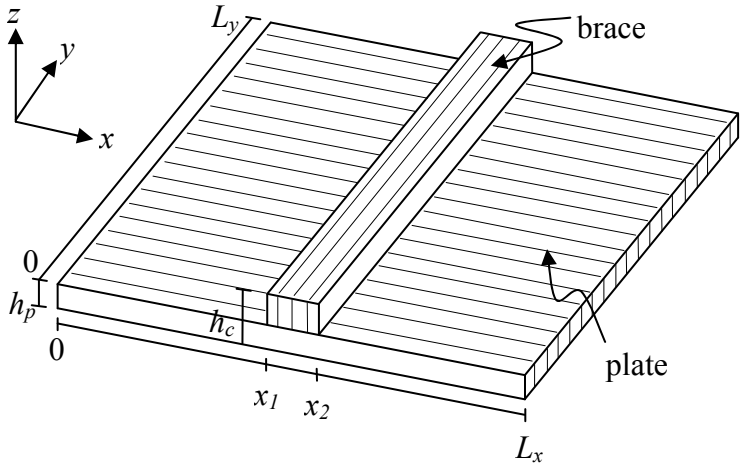

Figure 20. Orthotropic plate reinforced with a rectangular brace.

The forward model is discretized using the assumed shape method. The assumed shape method is an energy method which uses global plate elements within the kinetic and strain energy plate equations in order to determine the system's equations of motion, from which the mass and stiffness matrices are extracted [41]. For the details of the development of the large mass and stiffness matrices, the reader is referred to [42]. The system is assumed simply supported, conservative and the material properties are assumed orthotropic. The forward model is created assuming the mechanical properties are all related to Young's Moduli in the *y*-direction.

4.8.3 Inverse Model

The goal is to reconstruct the brace-plate system from a desired fundamental frequency. The generalized Cayley-Hamilton theorem inverse eigenvalue method is used as explained in Section 4.4.2.

A cross section of the fundamental modeshape is shown in Figure 21. It is clear that the brace affects the maximum amplitude of this modeshape, thus also affecting the associated frequency. In order to adjust the fundamental frequency of the brace-plate system to a desired value, it is necessary to adjust the thickness of the brace [43].

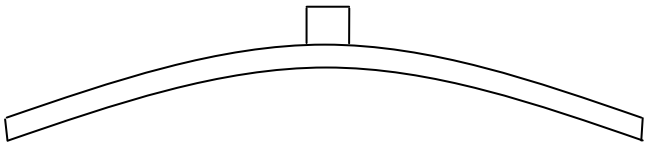

Figure 21. Cross section of the brace-plate system's fundamental modeshape.

4.8.4 Modeling Considerations

Since the mechanical properties vary based on E_y, and that the brace thickness controls the brace-plate system's fundamental frequency, the forward model is created using the assumed shape method while leaving these two parameters as variables. Thus, the mass matrix **M** is a function of h_c, the height of the brace-plate system at the (assumed fixed) location of the brace, and the stiffness matrix **K** is a function of h_c and also E_y. Here, we use 2 × 2 trial functions in the assumed shape method. Hence, 4^{th} order square matrices are created. The trial functions used are those of the simply supported rectangular plate such that

$$w(x,y,t)=\sum_{n_x=1}^{m_x}\sum_{n_y=2}^{m_y}\sin\left(\frac{n_x\pi x}{L_x}\right)\sin\left(\frac{n_y\pi y}{L_y}\right)q_{n_xn_y}(t) \tag{32}$$

where m are the modal numbers, q the time function and w is the displacement variable normal to the plate. The displacement variable w is then used directly in creating the kinetic and strain energy equations of the simply supported rectangular plate. These equations are broken into three sections as shown in Figure 20 in order to take into account the brace. This procedure is well described in [42]. It is assumed that the E_y is known and used as input information into the stiffness matrix. This leaves h_c as the only unknown parameter, appearing in both the mass and stiffness matrices.

In order to solve these matrices from the desired fundamental frequency, we must first create the characteristic polynomial using the desired frequency,

$$p(\lambda) = (\lambda - a) \cdot (\lambda - b_1) \cdot (\lambda - b_2) \cdot (\lambda - b_3) \tag{33}$$

where a is the desired frequency in $(\text{rad/s})^2$ and b_1-b_3 are unknown frequencies which need to be found. Since we have assumed 2 × 2 trial functions so that the mass and stiffness matrices are both 4 × 4, the characteristic polynomial must be fourth order, as shown in Equation (33). Subsequently, $p(\lambda)$ is expanded so that the polynomial's coefficients can be found. Once the polynomial is created, the Cayley-Hamilton equation can be written by substituting $(\mathbf{M}^{-1}\mathbf{K})$ for λ into Equation (33):

$$p(\mathbf{K}, \mathbf{M}) = c_4(\mathbf{M}^{-1}\mathbf{K})^4 + c_3(\mathbf{M}^{-1}\mathbf{K})^3 + c_3(\mathbf{M}^{-1}\mathbf{K})^2 + c_1(\mathbf{M}^{-1}\mathbf{K}) + c_0\mathbf{I} = 0 \tag{34}$$

where c_n are the coefficients of λ in $p(\lambda)$ determined via Equation (33). Equation (34) produces sixteen equations, of which only four are independent. Solving the equations on the main diagonal for the four unknowns (h_b, b_1, b_2, b_3) produces $4^4 = 256$ possible solutions, according to Bézout's theorem. From the set of all possible solutions, complex solutions can be immediately eliminated as not being physically meaningful. Clearly, further constraints must be added to the solution in order to get a solution which fits within the desired physical limits. These physical limits are based on the maximum and minimum brace dimensions which are required to compensate for the range of plate stiffnesses used during the analysis, as well as the range of natural frequencies which can be obtained using these system dimensions. Thus, the following constraints are implemented into the solution:

$$\begin{aligned} &0.013 \le h_b \le 0.016 \quad \text{m} \\ &1\times10^7 \le b_1 \le 9\times10^8 \quad (\text{rad/s})^2 \\ &1\times10^7 \le b_2 \le 9\times10^8 \quad (\text{rad/s})^2 \\ &1\times10^7 \le b_3 \le 9\times10^8 \quad (\text{rad/s})^2 \end{aligned} \tag{35}$$

Solving the four equations obtained from Equation (34) within the constraints provided by (35) yields a physically-realistic solution which satisfies the desired fundamental frequency, as well as the system's parameters.

4.8.5 Results

The material properties used during the analysis are given in Table 9.

Table 9. Material properties.

Material properties	Values
Density – μ (kg/m^3)	403.2
Young's modulus – E_y (MPa)	850
Young's modulus – E_x (MPa)	E_y / 0.078
Shear modulus – G_{xy} (MPa)	E_x × 0.064
Poisson's ratio – v_{xy}	0.372
Poisson's ratio – v_{yx}	$v_{LR} \times E_y / E_x$

The dimensions used for the model throughout the analysis of the brace-plate system are shown in Table 10.

Table 10. Dimensions of brace-plate model.

Dimensions	Values
Length – L_x (m)	0.24
Length – L_y (m)	0.18
Brace width – L_b (m)	0.012
Reference – x_1 (m)	$L_x / 2 - L_b / 2$
Reference – x_2 (m)	$x_1 + L_b$
Thickness – h_p (m)	0.003
Thickness – h_b (m)	0.012
Thickness – h_c (m)	$h_p + h_b$

These dimensions refer to those shown in Figure 20, where 'p' refers to the plate's dimensions, 'b' refers to the brace's dimensions and 'c' refers to the dimensions of the combined system.

As a basis for comparison, a plate having a Youngs' modulus of E_y = 850 MPa to which a brace is attached with a combined brace-plate thickness of h_c = 0.015 m is found to have a fundamental natural frequency of 687 Hz, calculated using the forward model. The analysis is then performed using the inverse method described in the previous section. As E_y of the plate is varied, the thickness of the brace-plate section is calculated such that the fundamental frequency of the brace-plate system is kept consistent at 687 Hz. The results of the computations can be found in Table 11.

Table 11. Results of the inverse model analysis.

Young's modulus E_R (MPa)	Brace thickness h_c (m)	Fundamental Frequency a (Hz)
750	0.01576	687
800	0.01536	687
813	0.01527	687
850	0.01500	687
900	0.01466	687
950	0.01435	687

Clearly, adjusting the thickness of the brace also has an effect on the other natural frequencies. These can be seen in Table 12.

Table 12. Calculated frequencies of the inverse model analysis.

Young's modulus E_R (MPa)	Brace thickness h_c (m)	b_1 (Hz)	b_2 (Hz)	b_3 (Hz)
750	0.01576	774	1360	2653
800	0.01536	782	1363	2650
813	0.01527	784	1364	2650
850	0.01500	790	1366	2648
900	0.01466	798	1370	2645
950	0.01435	806	1374	2642

Interestingly, the constraints indicated in Equation (35), although physically strict, allow for more than one solution in certain cases. An example is shown in Table 13.

Table 13. Alternate brace thickness solution satisfying the physical constraints.

Young's modulus E_R (MPa)	Brace thickness h_c (m)	a (Hz)	b_1 (Hz)	b_2 (Hz)	b_3 (Hz)
750	0.01359	687	570	1149	2185

4.8.6 Discussion

From these results, it is evident that designing a brace-plate system starting with a desired fundamental frequency, and using the proposed Cayley-Hamilton method, is possible. Table 11 clearly shows that by adjusting the thickness of the brace by small

increments (10^{-5} m, machine limit), it is possible to compensate for the variation in the cross-fibre stiffness (E_y) of the plate so that the fundamental frequency of the combined system is equal to that of the benchmark value of 687 Hz. The results obtained using the Cayley-Hamilton theorem algorithm match those values obtained using the forward model exactly. However, since no account has been taken of the other frequencies during the analysis, Table 12 shows that frequencies b_1 to b_3 vary considerably from those values obtained for E_y = 850 MPa. Therefore, it is important to ensure that there is a good understanding of what your model can control. Moreover, it is interesting to note that within the strict physical constraints of (35), there is more than one brace-plate system (solution) that satisfies the Cayley-Hamilton theorem of Equation (34). From Table 13 it can be seen that an alternate solution to the system exists, different from the one presented in Table 11, for a plate having an E_y of 750 MPa. In this case, by reducing the thickness of the brace, it is still possible to achieve a system having the desired frequency of 687 Hz. However, the desired frequency is no longer the fundamental frequency but rather becomes the second frequency and the fundamental has been replaced with a fundamental frequency of 570 Hz. It is important to keep this phenomenon in mind while designing a system. This is especially true if the order in the spectrum of a certain frequency associated with a certain modeshape is absolutely critical.

4.9 Acknowledgments

A special thank you goes to Dr. Moody T. Chu for his valuable insight and knowledge of inverse eigenvalue problems.

4.10 References

[1] K. Chadan, *An Introduction to Inverse Scattering and Inverse Spectral Problems*. SIAM, 1997.

[2] I. M. Gel'fand and B. M. Levitan, "On the determination of a differential equation from its spectral function," *Izv. Akad. Nauk SSSR Ser. Mat.*, vol. 15, no. 4, pp. 309–360, 1951.

[3] F. R. Gantmakher and M. G. Kreĭn, *Oscillation Matrices and Kernels and Small Vibrations of Mechanical Systems*. Providence, RI: American Mathematical Soc., 2002.

[4] M. T. Chu, "Inverse eigenvalue problems," *SIAM Rev*, vol. 40, pp. 1–39, 1998.

[5] M. T. Chu and G. H. Golub, *Inverse Eigenvalue Problems: Theory, Algorithms, and Applications*. Oxford University Press, USA, 2005.

[6] G. M. L. Gladwell, *Inverse problems in vibration*. Kluwer Academic Publishers, 2004.

[7] H. Hochstadt, "On some inverse problems in matrix theory," *Archiv der Mathematik*, vol. 18, no. 2, pp. 201–207, 1967.

[8] O. H. Hald, "Inverse eigenvalue problems for Jacobi matrices," *Linear Algebra and its Applications*, vol. 14, no. 1, pp. 63–85, 1976.

[9] D. Boley and G. Golub, "Inverse eigenvalue problems for band matrices," in *Numerical Analysis*, vol. 630, G. Watson, Ed. Springer Berlin / Heidelberg, 1978, pp. 23–31.

[10] C. de Boor and E. B. Saff, "Finite sequences of orthogonal polynomials connected by a Jacobi matrix," *Linear Algebra and its Applications*, vol. 75, no. 0, pp. 43–55, Mar. 1986.

[11] G. M. L. Gladwell, "The Inverse Problem for the Vibrating Beam," *Proc. R. Soc. Lond. A*, vol. 393, no. 1805, pp. 277–295, Jun. 1984.

[12] M. T. Chu, "Numerical Methods for Inverse Singular Value Problems," *SIAM Journal on Numerical Analysis*, vol. 29, no. 3, pp. 885–903, Jun. 1992.

[13] S. Friedland, J. Nocedal, and M. L. Overton, "The Formulation and Analysis of Numerical Methods for Inverse Eigenvalue Problems," *SIAM Journal on Numerical Analysis*, vol. 24, no. 3, pp. pp. 634–667, 1987.

[14] P. Morel, "Des algorithmes pour le problème inverse des valeurs propres," *Linear Algebra and its Applications*, vol. 13, no. 3, pp. 251–273, 1976.

[15] Z. Bohte, "Numerical Solution of the Inverse Algebraic Eigenvalue Problem," *The Computer Journal*, vol. 10, no. 4, pp. 385–388, Feb. 1968.

[16] V. Pereyra, A. Reinoza, J. Nocedal, and M. Overton, "Numerical methods for solving inverse eigenvalue problems," in *Numerical Methods*, vol. 1005, Springer Berlin / Heidelberg, 1983, pp. 212–226.

[17] A. C. Downing,Jr. and A. S. Householder, "Some Inverse Characteristic Value Problems," *J. ACM*, vol. 3, no. 3, pp. 203–207, Jul. 1956.

[18] J. A. Dias da Silva, "On the multiplicative inverse eigenvalue problem," *Linear Algebra and its Applications*, vol. 78, no. 0, pp. 133–145, Jun. 1986.

[19] G. N. de Oliveira, "On the multiplicative inverse eigenvalue problem," in *Canadian Mathematical Bulletin*, Montreal, QC: Canadian Mathematical Society, 1972.

[20] C. de Boor and G. H. Golub, "The numerically stable reconstruction of a Jacobi matrix from spectral data," *Linear Algebra and its Applications*, vol. 21, no. 3, pp. 245–260, Sep. 1978.

[21] R. Erra and B. Philippe, "On some structured inverse eigenvalue problems," *Numerical Algorithms*, vol. 15, no. 1, pp. 15–35, 1997.

[22] F. W. Biegler-König, "Construction of band matrices from spectral data," *Linear Algebra and its Applications*, vol. 40, no. 0, pp. 79–87, Oct. 1981.

[23] D. Boley and G. H. Golub, "A survey of matrix inverse eigenvalue problems," *Inverse Problems*, vol. 3, no. 4, p. 595, 1987.

[24] M. T. Chu and J. L. Watterson, "On a Multivariate Eigenvalue Problem: I. Algebraic Theory and a Power Method," *SIAM J. Sci. Comput.*, vol. 14, pp. 1089–1106, 1993.

[25] X. Chen and M. T. Chu, "On the Least Squares Solution of Inverse Eigenvalue Problems," *SIAM Journal on Numerical Analysis*, vol. 33, no. 6, pp. 2417–2430, Dec. 1996.

[26] G. M. L. Gladwell and N. B. Willms, "A discrete Gel'fand-Levitan method for band-matrix inverse eigenvalue problems," *Inverse Problems*, vol. 5, no. 2, pp. 165–179, Apr. 1989.

[27] Y. M. Ram and S. Elhay, "An Inverse Eigenvalue Problem for the Symmetric Tridiagonal Quadratic Pencil with Application to Damped Oscillatory Systems," *SIAM Journal on Applied Mathematics*, vol. 56, no. 1, pp. 232–244, Feb. 1996.

[28] G. H. Golub and R. R. Underwood, "The block Lanczos method for computing eigenvalues," in *Mathematical Software III*, J.R. Rice., New York: Springer, 1977.

[29] F. W. Biegler-König, "A Newton iteration process for inverse eigenvalue problems," *Numerische Mathematik*, vol. 37, no. 3, pp. 349–354, 1981.

[30] W. B. Gragg and W. J. Harrod, "The numerically stable reconstruction of Jacobi matrices from spectral data," *Numerische Mathematik*, vol. 44, no. 3, pp. 317–335, 1984.

[31] G. M. L. Gladwell, "The application of Schur's algorithm to an inverse eigenvalue problem," *Inverse Problems*, vol. 7, no. 4, pp. 557–565, Aug. 1991.

[32] M. T. Chu, "A Fast Recursive Algorithm for Constructing Matrices with Prescribed Eigenvalues and Singular Values," *SIAM Journal on Numerical Analysis*, vol. 37, no. 3, pp. 1004–1020, Jan. 2000.

[33] C. A. Floudas and P. Pardalos, *Encyclopedia of Optimization*, 2nd ed. 2009.

[34] G. N. de Oliveira, "Matrices with prescribed entries and eigenvalues. I," *Proc. Amer. Math. Soc.*, vol. 37, pp. 380–386, 1973.

[35] J. A. Dias da Silva, "Matrices with Prescribed Entries and Characteristic Polynomial," *Proceedings of the American Mathematical Society*, vol. 45, no. 1, pp. 31–37, Jul. 1974.

[36] M. F. Atiyah and I. G. Macdonald, "Introduction to commutative algebra," in *Introduction to commutative algebra*, Reading, Mass: Addison-Wesley pub Co, 1969, p. 21.

[37] M. Artin, "Algebra," in *Algebra*, 2nd ed., Boston: Pearson Prentice Hall, 2011, p. 140.

[38] A. W. Knapp, "Basic Algebra," in *Basic Algebra*, Boston: Birkhäuser, 2006, p. 219.

[39] F. R. Chang and H. C. Chen, "The generalized Cayley-Hamilton theorem for standard pencils," *Systems & Control Letters*, vol. 18, pp. 179–182, 1992.

[40] J. L. Coolidge, *Treatise on Algebraic Plane Curves*. Mineola, New York: Dover Publications, 1959.

[41] L. Meirovitch, "Principles and Techniques of Vibrations," Upper Saddle River, NJ: Prentice Hall, 1996, pp. 542–543.

[42] P. Dumond and N. Baddour, "Can a brace be used to control the frequencies of a plate?," *SpringerPlus*, vol. 2, no. 1, p. 558, Oct. 2013.

[43] P. Dumond and N. Baddour, "Effects of a Scalloped and Rectangular Brace on the Modeshapes of a Brace-Plate System," *International Journal of Mechanical Engineering and Mechatronics*, vol. 1, no. 1, pp. 1–8, 2012.

Chapter 5

A Structured Method for the Design-for-Frequency of a Brace-Soundboard System Using a Scalloped Brace

Applied Acoustics
DOI: 10.1016/j.apacoust.2014.08.004
Volume 88, Issue 1, February 2015, Pages 96-103

5.1 Abstract

Design-for-frequency of mechanical systems has long been a practice of iterative procedures in order to construct systems having desired natural frequencies. Especially problematic is achieving acoustic consistency in systems using natural materials such as wood. Inverse eigenvalue problem theory seeks to rectify these shortfalls by creating system matrices of the mechanical systems directly from the desired natural frequencies. In this paper, the Cayley-Hamilton and determinant methods for solving inverse eigenvalue problems are applied to the problem of the scalloped braced plate. Both methods are shown to be effective tools in calculating the dimensions of the brace necessary for achieving a desired fundamental natural frequency and one of its higher partials. These methods use the physical parameters and mechanical properties of the material in order to frame the discrete problem in contrast to standard approaches that specify the structure of the matrix itself. They also demonstrate the ability to find multiple solutions to the same problem. The determinant method is found to be computationally more efficient for partially described inverse problems due to the reduced number of equations and parameters that need to be solved. The two methods show great promise for techniques which could lead to the design of complex mechanical systems, including musical instrument soundboards, directly from knowledge of the desired natural frequencies.

5.2 Introduction

Designing mechanical systems to achieve desired natural frequencies has long been a trial-and-error exercise. The approach generally involves forward model design and iteration of design parameters until desired frequencies are achieved. This approach, while effective, is inefficient. A better approach would be to design the system directly from the desired frequencies, thus a structured method is desirable. Furthermore, iterative forward model design only works well for typical engineered materials such as metals and plastic, which demonstrate dependable mechanical properties. For systems using materials with highly variable mechanical properties, such as wood, this iterative design approach proves to be unpractical. In essence, in order to design-for-frequency using

material specimens that demonstrate large variations in mechanical properties, it is much easier to design the system directly from those desired frequencies.

A particular field of study, known as inverse eigenvalue problems, attempts to address such problems. A discrete inverse eigenvalue problem attempts to construct matrices, representative of physical systems, directly from a set of given eigenvalues (natural frequencies) [1]. Discrete inverse eigenvalue theory uses knowledge of matrix algebra and numerical methods in order to create matrices which yield the desired frequency spectrum (sets of eigenvalues). Thus, using these methods, it should be possible to design a system (represented by a set of mass and stiffness matrices) from a set of desired frequencies.

It is well known that inverse eigenvalue problems are ill-posed, meaning that many matrices exist which satisfy a single set of eigenvalues [2]. In engineering, the existence of multiple solutions could potentially be beneficial, giving the designer many design options. However, it is important to keep in mind that in order to ensure that a design is physically realizable, physical constraints must be included. Most methods developed for inverse eigenvalue problems stem from the field of structured matrix theory (e.g. Jacobi, band matrices and other matrix forms) using proven numerical algorithms to reconstruct unknown matrices from a full or partial set of desired eigenvalues [3]–[10]. Thus the typical approach is to limit the number of solutions by framing the inverse problem within a pre-determined matrix structure. Although structured matrices generally imply various physical constraints, very few methods exist for matrices which have a more general form. One of the goals of this paper is to demonstrate the use of the recently-proposed inverse eigenvalue technique using the Cayley-Hamilton theorem [11]. This approach is particularly interesting because it enables the solution of *any* matrix structure. Thus, the solution of any matrix can be obtained from a set of eigenvalues and applying the physical constraints to the matrix structure becomes an exercise in the forward modeling process. The system can then be limited by the material of choice rather than a certain matrix structure.

From the Cayley-Hamilton theorem method, we derive a second method, which we refer to as the determinant method and which will be explained herein. In certain situations, including the problem presented in this paper, only a select few frequencies, as

opposed to the full spectrum, are required to be specified. These problems are known as partially-described problems. The determinant method approach has the benefit of solving partially described systems using fewer equations.

In this paper, we apply the Cayley-Hamilton theorem method, as well as the determinant method to the problem of designing a scalloped-shaped brace on a simple rectangular plate in order to achieve desired system frequencies. This brace-plate model is chosen to demonstrate the validity of the methods because it has been previously analyzed to examine the effects of the scalloped brace on the natural frequencies of a brace-soundboard system [12] and thus the forward problem is well understood. In this prior paper, the dimensions of the brace were adjusted by trial and error. In this paper, structured methods will be used to calculate the requisite dimensions of the scalloped brace required in order to achieve the desired system frequencies. Results are then validated by comparison to those previously presented.

5.3 Model

5.3.1 The Mechanical System

The model used during the analysis is based on a typical section of a guitar soundboard structurally reinforced by a single brace along the weaker grain direction and first developed in [12] to explore the effects that a scalloped-shaped brace has on the frequencies of a system. The layout of the model is shown in Figure 22.

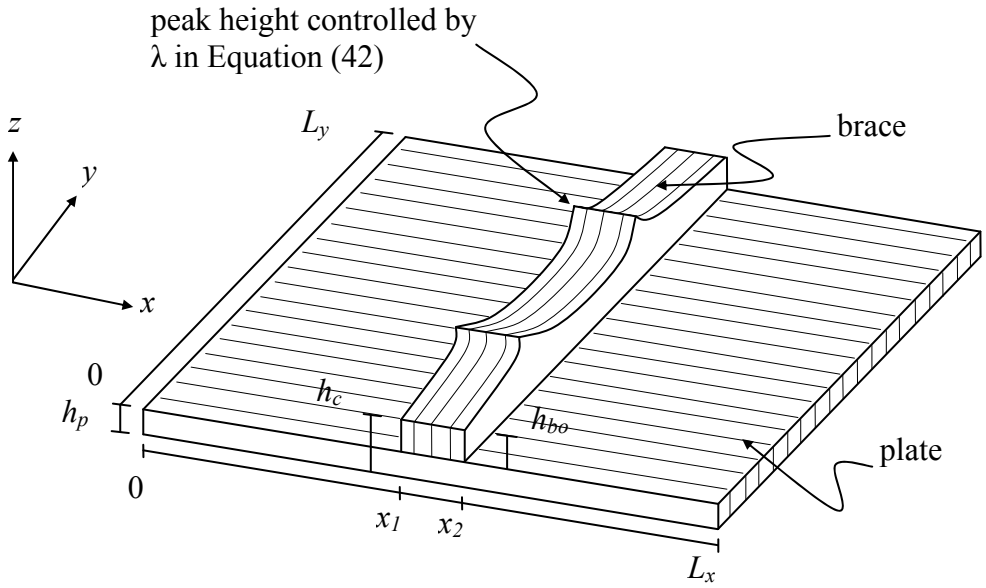

Figure 22. Orthotropic plate reinforced with a scalloped brace.

Since this prior paper demonstrated that scalloped-shaped braces typically used by musical instrument makers can be used to control two natural frequencies of the combined brace-plate system simultaneously, the same brace shape will be used herein. A scalloped-shaped brace can be seen in Figure 23.

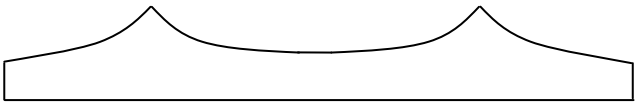

Figure 23. Shape of a scalloped brace.

5.3.2 Problem Statement

The problem we seek to solve can be stated as follows: calculate the dimensions of the scalloped brace so that the brace-plate system, described by a mass matrix **M** and a stiffness matrix **K**, has a specified given fundamental frequency and a specified higher partial (two frequencies specified) as the radial stiffness of the plate (E_R) varies. The variation of the radial stiffness of the plate is the means by which we model the natural occurring specimen-to-specimen variations in the material properties of wood. Although the methods presented herein work when any number of mechanical properties are

varied. Thus, for a plate specimen with a given radial stiffness, we demonstrate how to calculate the corresponding requisite brace dimensions that will ensure two frequencies in the plate's spectrum are at specified values.

Since the model presented in [12] is made of wood, all mechanical properties of the system are assumed to be a function of the material radial stiffness E_R, which is assumed known and given but which tends to vary from specimen to specimen. This inter-specimen variation of the radial stiffness is the cause of acoustic inconsistencies in the manufacture of musical instruments in spite of tight dimensional manufacturing tolerances [13]. All dimensional (geometric) properties of the brace-plate system are assumed to be specified and fixed except for the base thickness of the brace h_{bo} and the scallop peak height adjustment factor λ, the design variables to be calculated.

5.3.3 Forward Model

Rather than choosing a pre-determined matrix structure, the shape of the matrix is defined through the process of constructing a forward system model, taking into account the fixed geometric and mechanical properties of the physical system, but leaving as variables to be solved the parameters that remain under the control of the designer.

Although any discretization method could be used, following on our prior paper, the assumed shape method is used to discretize the forward model. The assumed shape method is intended as a theoretical model for generating the **M** and **K** matrices in order to demonstrate the inverse methods presented in Section 5.3.4.1 and Section 5.3.4.2. The assumed shape method is an energy method which applies global elements to the kinetic and strain energy equations in order to determine the mass and stiffness matrices representative of the system [14]. The kinetic energy of a conservative, simply supported orthotropic Kirchhoff plate is used. Although this is an accurate assumption for the plate, it may imply a certain error at the location of the brace where thicker plate theories may be more appropriate. The kinetic energy is separated into three sections in order to take into account the presence of the brace, as shown in Figure 22, and is given by

$$T = \frac{1}{2}\int_0^{x_1}\int_0^{L_y} \dot{w}^2 \rho_p \, \mathrm{d}y\mathrm{d}x + \frac{1}{2}\int_{x_1}^{x_2}\int_0^{L_y} \dot{w}^2 \rho_c \, \mathrm{d}y\mathrm{d}x + \frac{1}{2}\int_{x_2}^{L_x}\int_0^{L_y} \dot{w}^2 \rho_p \, \mathrm{d}y\mathrm{d}x \tag{36}$$

where L_x and L_y are the dimensions of the plate in the x and y directions respectively. The dot above the transverse displacement variable w represents the time derivative, ρ is the mass per unit area of the plate such that

$$\rho_p = \mu \cdot h_p \text{ and } \rho_c = \mu \cdot h_c, \tag{37}$$

μ is the material density and h_p and h_c are the thickness of the plate and combined brace-plate sections, respectively.

Similar assumptions are made for the strain energy, which after modification to model the addition of the brace, becomes

$$\begin{aligned} U = &\frac{1}{2}\int_0^{x_1}\int_0^{L_y}\left[D_{xp}w_{xx}^2 + 2D_{xyp}w_{xx}w_{yy} + D_{yp}w_{yy}^2 + 4D_{kp}w_{xy}^2\right]\mathrm{d}y\mathrm{d}x \\ &+\frac{1}{2}\int_{x_1}^{x_2}\int_0^{L_y}\left[D_{xc}w_{xx}^2 + 2D_{xyc}w_{xx}w_{yy} + D_{yc}w_{yy}^2 + 4D_{kc}w_{xy}^2\right]\mathrm{d}y\mathrm{d}x \\ &+\frac{1}{2}\int_{x_2}^{L_x}\int_0^{L_y}\left[D_{xp}w_{xx}^2 + 2D_{xyp}w_{xx}w_{yy} + D_{yp}w_{yy}^2 + 4D_{kp}w_{xy}^2\right]\mathrm{d}y\mathrm{d}x \end{aligned} \tag{38}$$

Here, the subscripts on w refer to partial derivatives in the given direction, as per standard notation. The stiffnesses, D, are section-specific because of the change in thickness h from x_1 to x_2 and are given by

$$D_{xp} = \frac{S_{xx}h_p^3}{12}, \quad D_{yp} = \frac{S_{yy}h_p^3}{12}, \quad D_{xyp} = \frac{S_{xy}h_p^3}{12}, \quad D_{kp} = \frac{G_{xy}h_p^3}{12}, \tag{39}$$

and

$$D_{xc} = \frac{S_{xx}h_c^3}{12}, \quad D_{yc} = \frac{S_{yy}h_c^3}{12}, \quad D_{xyc} = \frac{S_{xy}h_c^3}{12}, \quad D_{kc} = \frac{G_{xy}h_c^3}{12}, \tag{40}$$

where G is the shear modulus and the S parameters are stiffness components that are defined as

$$S_{xx} = \frac{E_x}{1-\nu_{xy}\nu_{yx}}, \qquad S_{yy} = \frac{E_y}{1-\nu_{xy}\nu_{yx}}, \qquad S_{xy} = S_{yx} = \frac{\nu_{yx}E_x}{1-\nu_{xy}\nu_{yx}} = \frac{\nu_{xy}E_y}{1-\nu_{xy}\nu_{yx}}. \tag{41}$$

The subscripts represent the direction of the plane in which the material properties act. Therefore, E_x is Young's modulus along the *x*-axis, E_y along the *y*-axis and ν_{xy} and ν_{yx} are the major Poisson's ratios along the *x*-axis and *y*-axis, respectively.

In order to take into account the scallop shape of the brace shown in Figure 23, a second-order piece-wise polynomial is used to describe the thickness of the brace, h_b, along its length so that

$$h_b = \begin{cases} \lambda \cdot y^2 + h_{bo} & \text{for} \quad y < \dfrac{L_y}{4} \\ \lambda \cdot \left(y - \dfrac{L_y}{2} \right)^2 + h_{bo} & \text{for} \quad \dfrac{L_y}{4} \le y \le \dfrac{3L_y}{4} \\ \lambda \cdot \left(y - L_y \right)^2 + h_{bo} & \text{for} \quad y > \dfrac{3L_y}{4} \end{cases} \tag{42}$$

where h_{bo} is the height of the brace at its ends and centre and λ is the scallop peak height adjustment factor (a non-dimensional real value whose range is given in Section 5.3.4.1). The thickness of the brace is then added to the thickness of the plate to give the combined thickness of the brace-plate system such that $h_c = h_b + h_p$.

Furthermore, in order to account for the brace, which has mechanical properties that run perpendicular to those of the plate, the kinetic and strain energy equations are modified in order accommodate for the mechanical properties of the brace between x_1 and x_2. In doing so, the mechanical properties of the plate must also change direction. This is considered to be a reasonable assumption since the properties of the brace dominate this region of the combined system. This is due to the fact that the brace has a much thicker section when compared to that of the plate.

5.3.4 Inverse Model

Once the forward model is determined, the brace dimensions are calculated via the inverse models as outlined below. The problem is to calculate the base thickness of the brace h_{bo} and the scallop peak height adjustment factor λ, (which appear in both mass and stiffness matrices) given a desired fundamental system frequency, as well as one of the higher partials. Two methods are proposed and demonstrated for solving this problem. The first method, first described in [11], consists of using the generalized Cayley-Hamilton theorem as an algorithm for solving the inverse eigenvalue problem. The second method is referred to as the determinant method and is described below.

5.3.4.1 Cayley-Hamilton Algorithm

As described in [11], the Cayley-Hamilton theorem can be used to solve general structured inverse eigenvalue problems. The generalized Cayley-Hamilton theorem states that if $p(t)$ is the characteristic polynomial of the generalized eigenvalue problem (**K**,**M**), where **K** and **M** are square matrices obtained from $p(t) = \det(\mathbf{K} - t\mathbf{M})$, then substituting ($\mathbf{M}^{-1}\mathbf{K}$) for t in the polynomial gives the zero matrix [15], [16]. Thus, if the structure of the mass and stiffness matrices is determined via the forward modeling procedure, and leaving as unknown variables the parameters that affect the frequencies which need to be controlled, then it is possible to solve for these parameters and consequently design the brace-plate system for these desired frequencies.

Using the assumed shape method, the mass and stiffness matrices are constructed using 3 × 3 trial functions leading to ninth order, square matrices. The trial functions used are those of the simply supported rectangular plate given by

$$w(x,y,t) = \sum_{n_x=1}^{m_x}\sum_{n_y=2}^{m_y} \sin\left(n_x \cdot \pi \cdot \frac{x}{L_x}\right) \cdot \sin\left(n_y \cdot \pi \cdot \frac{y}{L_y}\right) \cdot q_{n_x n_y}(t) \tag{43}$$

where m_x and m_y are the mode numbers in the x and y directions respectively and $q(t)$ is the time function.

To solve the design problem, the stiffness of the wooden plate being used (E_R) is measured and input into the analysis, leaving the two brace parameters (ie. h_{bo} and λ) as the design variables for which we must solve in order to obtain the two desired natural frequencies from the system.

In order to solve these unknown parameters using the Cayley-Hamilton theorem, it is necessary to first construct the characteristic equation of the system using the given desired natural frequencies

$$p(t) = \prod_{i=1}^{2}(t - a_i) \cdot \prod_{j=1}^{7}(t - b_j) \tag{44}$$

where a_1 and a_2 are numerical values associated with the desired eigenvalues and calculated from the desired natural frequencies, and b_1 to b_7 are the remaining unknown eigenvalues, which must also be found. Since the **M** and **K** matrices are ninth order (in

h_{bo}, λ, and b_1-b_7), then Equation (44) must be as well. Substituting ($\mathbf{M}^{-1}\mathbf{K}$) for t in Equation (44), based on the Cayley-Hamilton theorem, gives

$$p(\mathbf{K},\mathbf{M}) = c_0\mathbf{I} + \sum_{i=1}^{9} c_i(\mathbf{M}^{-1}\mathbf{K})^i = 0 \tag{45}$$

where the c_i coefficients are obtained by expanding Equation (44). Equation (45) is a matrix containing eighty one ninth order equations, of which only nine are independent, as shown in [11]. If we solve these nine independent equations for the two unknown geometric/structural parameters and seven unknown eigenvalue parameters, solutions to the system are obtained. Since each of the scalar equations being solved is a ninth order polynomial and there are nine unknown parameters, Bézout's theorem states that there exists 9^9 possible solutions (over three hundred million solutions) [17]. Complex-valued solutions can be immediately discarded as having no physical meaning. However, an enormous amount of possibilities still remain. Therefore, further constraints must be implemented. These typically take the form of dimensions which are physically required for the type of instrument being created. Specifically, the dimensions of the braces themselves must be within a specific range in order to meet the design requirements. Thus, the following constraints are included in the analysis:

$$\begin{aligned}
0.011 \le h_{bo} \le 0.013 \quad &\text{m} \\
-0.4 \le \lambda \le 2.2 \quad & \\
2.5\times10^7 \le b_1 \le 2.8\times10^7 \quad &(\text{rad/s})^2 \\
6.6\times10^7 \le b_2 \le 7.7\times10^7 \quad &(\text{rad/s})^2 \\
7.4\times10^7 \le b_3 \le 8.3\times10^7 \quad &(\text{rad/s})^2 \\
9.3\times10^7 \le b_4 \le 9.9\times10^7 \quad &(\text{rad/s})^2 \\
1.8\times10^8 \le b_5 \le 2.0\times10^8 \quad &(\text{rad/s})^2 \\
5.0\times10^8 \le b_6 \le 6.2\times10^8 \quad &(\text{rad/s})^2 \\
2.3\times10^9 \le b_7 \le 2.6\times10^9 \quad &(\text{rad/s})^2
\end{aligned} \tag{46}$$

The ranges on the structural constraints given in Equation (46) are obtained directly from the physical/aesthetic constraints demanded by such a guitar soundboard. The constraints on the eigenvalues are more difficult to obtain and require complete forward modeling of the system using the minimum and maximum possible values of plate stiffness (E_R).

Solving the nine equations obtained from (45) within the constraints indicated in (46), yields a physically-realistic system which satisfies all physical constraints, while delivering the desired natural frequencies sought of the system.

5.3.4.2 The Determinant Method for Partially-described Systems

Although effective, the Cayley-Hamilton method for solving inverse eigenvalue problems described in the previous section may not be the most computationally efficient method when solving partially described systems. Partially described systems are those for which only a select few eigenvalues are specified, as opposed to the entire spectrum being given. Therefore, the second method, proposed for the first time in this paper and which we refer to as the determinant method, involves solving a variation of the generalized eigenvalue problem equation itself. If the roots of the characteristic equation are calculated from $p(t) = \det(\mathbf{K} - t\mathbf{M})$, then knowing the desired eigenvalues (t_1,t_2), (where $t = \omega^2$ and ω are the natural frequencies), a new set of equations to be solved are obtained via $\det(\mathbf{K} - (t_1, t_2)\mathbf{M}) = 0$, where once again the variables needing to be solved are the unknown parameters affecting the desired frequencies. In the problem being considered, two of the possible nine roots (in this case the eigenvalues a_1 and a_2) are required to be of a certain value, as described in Section 5.3.4.1. Replacing t with the specified a_1 and a_2 in turn, leads to two scalar equations and two unknowns such that

$$\begin{aligned} p(a_1) &= \det(\mathbf{K} - a_1\mathbf{M}) = 0 \\ p(a_2) &= \det(\mathbf{K} - a_2\mathbf{M}) = 0 \end{aligned} \tag{47}$$

Again, the unknown design parameters are the base height of the brace h_{bo} and the peak height adjustment factor λ. Although the equations obtained from (47) are still ninth order (but only in h_{bo} and λ), only two equations are being simultaneously solved, therefore Bézout's theorem specifies that the number of solutions is given by $9^2 = 81$ system possibilities. This greatly reduces the computational effort involved. Once again, constraints similar to those provided by (46) can be used to create a physically-realistic system.

5.4 Results

5.4.1 Material Properties

The material used in the system for analysis is Sitka spruce. The statistical average properties of Sitka spruce are obtained from the US Forest Products Laboratory in [18] and are shown in Table 14 below.

Table 14. Material properties for Sitka spruce as an orthotropic material.

Material properties	Values
Density – μ (kg/m^3)	403.2
Young's modulus – E_L (MPa)	E_R / 0.078
Shear modulus – G_{LR} (MPa)	E_L × 0.064
Poisson's ratio – v_{LR}	0.372
Poisson's ratio – v_{RL}	$v_{LR} \times E_R / E_L$

Although wood is typically treated as an orthotropic material having three directions of material properties, it is here treated as having only two coordinate directions of importance. The tangential axis is ignored because the wood used for making soundboards is quartersawn. Therefore, the '*R*' and '*L*' used in Table 14 refer to the radial and longitudinal directions respectively. Quartersawn wood refers to wood which has been cut perpendicular to its annular growth rings. When looking at a cross section of a flat quartersawn plate, these growth rings appear to be directed normal to the plate's surface, as shown in Figure 24.

Figure 24. Quartersawn Sitka spruce plate.

These values are used as benchmarks only, since the goal of this paper is to demonstrate methods which calculate the brace dimensions which will compensate for variations in E_R in order to obtain consistent system natural frequencies.

5.4.2 System Dimensions

The dimensions used in the construction of the model are listed in Table 15 and are based on the model of Figure 22.

Table 15. Model geometric dimensions.

Dimensions	Values
Length – L_x (m)	0.24
Length – L_y (m)	0.18
Length – L_b (m)	0.012
Reference – x_1 (m)	$L_x / 2 - L_b / 2$
Reference – x_2 (m)	$x_1 + L_b$
Thickness – h_p (m)	0.003
Thickness – h_c (m)	$h_p + h_b$

In Table 15, subscript '*p*' stands for plate, '*b*' for brace and '*c*' for combined plate and brace.

5.4.3 Forward Modeling Results for Benchmark Model

The system's natural frequencies are calculated using the forward modeling process as outlined above, using the material properties of Table 14 and the geometric dimensions of Table 15. As a benchmark, a radial stiffness of E_R = 850 MPa, a brace height of h_{bo} = 0.012 m and scalloped peak height adjustment factor of λ = 1 are also used. The first five natural frequencies and their modeshapes are shown in Table 16, where m_x and m_y represent the mode number in the *x* and *y* directions respectively.

Table 16. First five natural frequencies of the benchmark system.

m_x	m_y	Natural frequency (Hz)	Modeshape
1	1	$\omega_1 = 619$	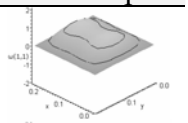
2	1	$\omega_2 = 820$	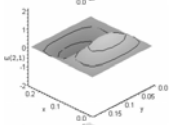
1	2	$\omega_3 = 1131$	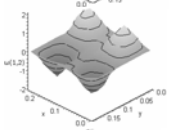
1	3	$\omega_4 = 1346$	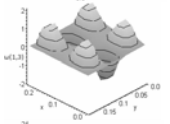
2	2	$\omega_5 = 1400$	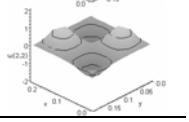

The fundamental frequency value of 619 Hz and the second partial of 1131 Hz obtained from our benchmark system are used throughout the remainder of the analysis as the desired values which we want to keep constant despite changes in the material properties of the wood.

5.4.4 Procedure for the Inverse Problem

In order to use the Cayley-Hamilton theorem method or the determinant method to solve the problem at hand, a desired fundamental frequency, as well as its second partial must be chosen as input design information. Here, these are obtained from the benchmark model used in the forward modeling process of the previous section. The radial stiffness (E_R) of the plate is assumed to have been measured experimentally and used as input material information. Here, we will vary the value of the radial stiffness (material property) to demonstrate that for a given measured value of radial stiffness, the method can be used to calculate the corresponding geometric properties of the brace so that desired spectral system properties are achieved. The general procedures for solving the problem stipulated above are as follows:

A Structured Method for the Design-for-Frequency of a Brace-Soundboard System Using a Scalloped Brace

i. CAYLEY-HAMILTON PROCEDURE. *A desired fundamental and second partial natural frequency, as well as the Young's modulus in the radial direction of a quartersawn wooden plate are given as input information.*

1. *Generate the* **M** *and* **K** *matrices from the chosen forward modeling technique leaving as variables h_{bo}, λ and E_R;*
2. *Input the (assumed measured) wooden plate's E_R value;*
3. *Generate the characteristic polynomial:*

   $$p(t) = (t-a_1)(t-a_2)(t-b_1)(t-b_2)(t-b_3)(t-b_4)(t-b_5)(t-b_6)(t-b_7)$$

   where a_1 and a_2 are numerical values calculated from the desired natural frequencies; and the b's are the remaining natural frequencies in $(rad/s)^2$ to be found.
4. *Generate the generalized Cayley-Hamilton theorem equation:*

   $$p(\mathbf{K},\mathbf{M}) = c_9(\mathbf{M}^{-1}\mathbf{K})^9 + c_8(\mathbf{M}^{-1}\mathbf{K})^8 \ldots + c_1(\mathbf{M}^{-1}\mathbf{K}) + c_0\mathbf{I} = 0$$

   where c_1-c_9 are the coefficients obtained from the characteristic polynomial in 3;
5. *Extract the nine diagonal equations from the Cayley-Hamilton matrix polynomial equation in 4;*
6. *Solve the nine equations for h_{bo}, λ, and b_1-b_7 within the stipulated constraints;*
7. *Insert h_{bo} and λ into the* **M** *and* **K** *matrices and calculate the system's natural frequencies using the forward modeling process in order to verify that the solution is consistent with the input values.*

ii. DETERMINANT PROCEDURE. *A desired fundamental and second partial natural frequency, as well as the Young's modulus in the radial direction of a quartersawn wooden plate are given as input information.*

1. *Generate the* **M** *and* **K** *matrices from the chosen forward modeling technique leaving as variables h_{bo}, λ and E_R;*
2. *Input the wooden plate's (assumed measured) E_R value;*
3. *Generate determinant equations for each desired frequency:*

   $$p(a_1) = \det(\mathbf{K} - a_1\mathbf{M}) \text{ and } p(a_2) = \det(\mathbf{K} - a_2\mathbf{M})$$

where a_1 and a_2 are numerical values calculated from the desired natural frequencies;

4. *Solve the two equations for h_{bo} and λ within the stipulated constraints;*
5. *Insert h_{bo} and λ into the* **M** *and* **K** *matrices and calculate the system's natural frequencies using the forward modeling process in order to verify that the solution is consistent with the input values.*

5.4.5 Cayley-Hamilton Method Results

Using the Cayley-Hamilton method to solve the inverse eigenvalue problem described, the values for the base height of the scalloped brace, h_{bo}, and the peak height adjustment factor, λ, are calculated so that the brace-plate system produces the desired natural frequencies. The remaining eigenvalues b_1-b_7, are also produced as outputs of the method. Using the benchmark values of Section 5.4.3, the fundamental frequency and the second partial are chosen to be 619 Hz and 1131 Hz respectively. These frequencies are the ones which will be held constant by solving for the base height and peak height of the brace as the radial stiffness of the plate is varied in order to simulate the natural material property variations that occur in wood. A reminder is given that $a_1 = (\omega_1 \times 2\pi \text{ rad/cycle})^2$ and $a_2 = (\omega_3 \times 2\pi \text{ rad/cycle})^2$, which are used directly in the Cayley-Hamilton method. The results of these computations are shown in Table 17.

Table 17. Results of the Cayley-Hamilton method.

Young's modulus E_R (MPa)	Brace base thickness h_{bo} (m)	Peak height adjustment factor λ	1st natural frequency ω_1 (Hz)	3rd natural frequency ω_3 (Hz)
750	0.01221	2.1761	619	1133
800	0.01211	1.5470	619	1130
850	0.01206	0.9049	619	1129
900	0.01200	0.3663	619	1131
950	0.01207	-0.3234	619	1132

In Table 17, E_R is assumed measured and given, h_{bo} and λ are calculated using the inverse Cayley-Hamilton method, while ω_1 and ω_3 are calculated by substituting h_{bo} and λ (found

via solving the inverse problem) back into the **K** and **M** matrices and solving the *forward* eigenvalue problem with the now completely known **K** and **M** matrices in order to verify the solution that was obtained using the inverse method. The reader is reminded that the benchmark (desired) values, the fundamental frequency and the second partial, were chosen to be 619 Hz and 1131 Hz respectively. Thus, although the benchmark frequencies are within a reasonable 0.2% error margin, the values aren't completely recovered due to numerical errors during the computation. These errors appear due to solver sensitivity based on rounding required in order to make the calculations numerically reasonable. Error sensitivity also increases with increasing frequency partials.

Since the procedure solves for the dimensions of the brace which keep the fundamental and second partial frequency constant, the other frequencies are also affected. This is clearly seen in Table 18.

Table 18. Other calculated partial frequencies.

Young's modulus E_R (MPa)	Brace base thickness h_{bo} (m)	Peak height adjustment factor λ	ω_2 (Hz)	ω_4 (Hz)	ω_5 (Hz)
750	0.01221	2.1761	815	1305	1377
800	0.01211	1.5470	817	1325	1389
850	0.01206	0.9049	820	1346	1403
900	0.01200	0.3663	824	1367	1418
950	0.01207	-0.3234	828	1389	1441

5.4.6 Determinant Method Results

Since this particular problem represents a partially described problem, as indicated in [1], it is beneficial to solve the problem without needing to find the entire system spectrum. This is where the determinant method demonstrates a clear advantage. In this case, only h_{bo} and λ are unknown parameters and only two equations are solved. Once again the desired benchmark values for frequency are input into the problem and the radial stiffness of the plate is varied. The results are shown in Table 19.

Table 19. Results of the determinant method.

Young's modulus E_R (MPa)	Brace base thickness h_{bo} (m)	Peak height adjustment factor λ	1st natural frequency ω_1 (Hz)	3rd natural frequency ω_3 (Hz)
750	0.01224	2.1073	619	1131
800	0.01209	1.5707	619	1131
850	0.01195	1.0683	619	1132
900	0.01203	0.3161	619	1130
950	0.01211	-0.3846	619	1131

In Table 19, h_{bo} and λ are calculated using the inverse determinant method, while ω_1 and ω_3 are then calculated by substituting the found h_{bo} and λ back into the **K** and **M** matrices and solving the forward generalized eigenvalue problem in order to verify the solution obtained using the inverse method.

5.4.7 Comparison of Results

Since the forward model used was previously developed in [12] and results were obtained by adjusting the dimensions of the brace through trial and error, a direct comparison of these results to those calculated in Table 17 and Table 19 using inverse methods is possible. In a manner similar to this paper, ω_1 and ω_3 were held as close to the benchmark values as possible. Some of the results of [12] are restated in Table 20.

Table 20. Results of a previous study using trial and error.

Young's modulus E_R (MPa)	Brace base thickness h_{bo} (m)	Peak height adjustment factor λ	1st natural frequency ω_1 (Hz)	3rd natural frequency ω_3 (Hz)
750	0.0123	2.0	619	1128
800	0.0121	1.6	620	1133
850	0.0120	1.0	619	1131
900	0.0118	0.6	618	1134
950	0.0120	-0.2	620	1134

As can be seen in Table 20, values for h_{bo} and λ found by trial error are less successful at obtaining the desired system frequencies than those same variables calculated using the the Cayley-Hamilton and determinant methods shown in Table 17

and Table 19. Much more time and effort were also spent using trial and error to adjust the values obtained in Table 20 until desired values of ω_1 and ω_3 were obtained.

5.4.8 Alternative Solutions

As mentioned previously, one of the benefits of using the Cayley-Hamilton or determinant methods is that multiple solutions are possible. This gives the designer options in choosing a design, or exploring solutions which may not be intuitive. The use of physical constraints, such as those of Equation (46), are necessary in order to limit the number of solutions and to ensure a physically realistic system. Although many other solutions may be buildable, constraining the system in this sense should prevent a designer from being overwhelmed and ensure that the system meets more restrictive physical and aesthetic criteria. However, for these reasons, the constraints need to be carefully studied. Generally this involves studying the limits of the desired system in the forward modeling sense.

In this study, the constraints were carefully studied and designed to find solutions which were similar to those of the previous study [12]. Interestingly, using the determinant method within the constraints of Equation (46), a unique solution to the problem was found in each case when varying E_R. Slightly expanding the limits of these constraints (which represent the maximum allowable based on physical space requirements) to

$$\begin{aligned} 0.001 \le h_{bo} \le 0.023 \quad \text{m} \\ -3 \le \lambda \le 4.8 \end{aligned} \tag{48}$$

where the allowable range of h_{bo} has been increased by 0.01m in both directions (so that the allowable range of h_{bo} is 0.022m wide whereas it was 0.002m wide in the prior simulations) and λ has been increased by 2.6 in both directions, allowed us to find alternate "non-intuitive" solutions, which are shown in Table 21.

Table 21. Alternate solutions found by expanding the constraints.

Young's modulus E_R (MPa)	Brace base thickness h_{bo} (m)	Peak height adjustment factor λ	Natural frequency ω (Hz)	Natural frequency ω (Hz)
750	0.01020	-2.6534	618	1130
900	0.00414	-2.3055	619	1131
950	0.00417	-2.5871	619	1131

Solutions shown in Table 21 are "non-intuitive" because they have a negative peak height adjustment factor. This leads to braces which are created by scalloping into the wood such as in Figure 25, rather than the typical shape of Figure 23.

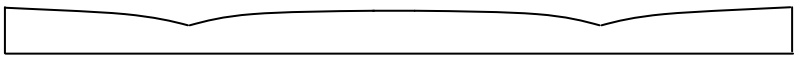

Figure 25. The effect of a negative peak height adjustment factor.

It should be pointed out that although the solution for E_R = 750 MPa is a physically realistic solution, the ones obtained for 900 and 950 MPa are not. This is because the peak height adjustment factor in both cases is too large for the base thickness of the brace and would require cutting out a section of brace thicker than the base thickness. Furthermore, the order of natural frequencies within the spectrum has changed with regards to the desired order. For the case of E_R = 750 MPa, 619 Hz no longer represents the fundamental, but rather the 2nd frequency. The 1131 Hz frequency has also shifted up from 3rd to 5th position in the spectrum. Similar reordering has occurred for the 900 and 950 MPa cases. It is important to keep this phenomenon in mind while designing a system. This is especially true if the order in the spectrum of a certain frequency associated with a certain modeshape is absolutely critical.

The results presented herein, along with their importance, are discussed below.

5.5 Discussion

Based on these results, it is evident that using a structured method, such as the Cayley-Hamilton or determinant method, makes it possible to calculate the dimensions of a scalloped brace so that two of the natural frequencies of a wooden brace-plate system remain constant even though there are variations in the radial stiffness of the wooden

plate. This study clearly shows that the fundamental frequency and one of its higher partials can be used to calculate the dimensions of the brace in order to ensure that the combined system achieves desired frequencies. By calculating changes to both the base height of the brace (h_{bo}) and the peak height adjustment factor (λ) by small increments (held to 10^{-5} m, machine limit), it is possible to compensate for variations in the radial stiffness (E_R) of the wooden plate. This is clearly seen in Table 17 and Table 19 where the benchmark values of ω_1 = 619 Hz and ω_2 = 1131 Hz are held to within a 0.2% threshold, well within the 1% threshold of auditory perception [19], [20]. Although the Cayley-Hamilton method and the determinant method offer similar results, there are significant gains in time and computational efficiency when using the determinant method, since the determinant method seeks to solve two equations and two unknowns rather than the nine equations and nine unknowns of the Cayley-Hamilton method. This observation remains true as long as the problem remains partially described. If all discrete frequencies must be specified, then no computational gains are obtained from the determinant method.

In modifying the two brace parameters, the other frequencies are also affected. Table 18 shows three additional frequencies ω_2, ω_4 and ω_5. These too change when modifying the brace dimensions. In this case the ω_2, ω_4 and ω_5 frequencies vary by up to 1.0%, 3.2% and 2.7 % respectively. The impact on ω_2 is minimal due to the fact that the brace runs along its associated modeshape's nodal line. Consequently, it is primordial that there is a good understanding of what can be controlled with the brace and its shape. This understanding comes directly from knowledge of the system's modal properties, usually obtained from a careful study of the forward problem. Evidently, if more freedom were given to the number of braces and their position, more frequencies could be controlled simultaneously.

These methods are not without difficulties. These difficulties present themselves within the sheer number of possible solutions which follow from the fact that a discrete frequency spectrum has a large number of matrices which produce them. Therefore, the most important aspects in ensuring results which satisfy the physical and aesthetic needs of the problem are the selection of constraints applied to the solution process, as well as the parameters that remain as variables to solve in order to control the desired

frequencies. Generally speaking, in order to obtain the constraints, it is necessary to do a forward analysis using the minimum and maximum values for the varying parameters in order to frame the output values that we are trying to calculate. Modeling assumptions are left to the forward modeling process. It should be noted that forward models which reduce the discrete system's matrix order are preferred, because they reduce the computational effort involved by reducing the order of the equations being solved. A good equation solver is also required. This study used the DirectSearch package available for Maple [21]. DirectSearch uses universal derivative-free direct searching methods which do not require the objective function and constraints to be differentiable and continuous. This solver gave many options for constraints and step sizes. Maple is a symbolic computer algebra package, developed and sold by Maplesoft, which works particularly well for solving equations symbolically rather than numerically. This allows us to gain insight into the problems we are trying to solve.

In the particular situation of the musical instrument soundboard, where the lower natural frequencies associated with body modes of vibration have the largest impact on its acoustic properties [22], it has become clear that the dimensions of the brace play a fundamental role in compensating for variations in the material properties of the wooden plate. The methods presented in this paper indicate a precise way in which the dimensions of the brace can be calculated in order to design the fundamental and second partial frequencies into the braced plate system from the outset.

When comparing the results of the Cayley-Hamilton and determinant methods (Table 17 and Table 19) to those obtained previously by trial and error (Table 20), it is clear that better precision is obtained for the values of h_{bo} and λ when calculating via a structured inverse method, in addition to better accuracy for the desired frequencies. Although increased accuracy in the trial-and-error method could likely be achieved, it is limited by the fact that small, manual adjustments to the repetitive solution of the forward problem are extremely labour intensive and time consuming. A significant time savings could likely be obtained if an optimization algorithm were implemented in order to make the adjustments to the trial-and-error approach.

Multiple solutions are possible using the Cayley-Hamilton and determinant methods, as shown in Table 21. However, they depend heavily on the chosen constraints. Multiple

solutions represent both a benefit and a curse to the designer. With little insight into the limits of a system, the number of solutions can be overwhelming. Moreover, systems which may seem plausible at first may contain parameters which exceed what is physically realistic after further investigation. Nonetheless, the availability of multiple solutions may lead to a system design which outperforms that which is considered normal or intuitive.

5.6 Conclusion

This paper gives two direct methods, the Cayley-Hamilton and the determinant method, for calculating the dimensions of a scalloped brace required in order to satisfy the desired fundamental and second partial frequency by using these frequencies as inputs along with information on the cross-grain stiffness of the wooden plate. While these methods can be used for many types of systems, they have been demonstrated and validated herein against the problem developed in [12]. These methods demonstrate a significant improvement over empirical methods because they are able to calculate physical parameters and design systems directly from chosen desired natural frequencies without iteration. They also frame the inverse eigenvalue problem based on the physical parameters of the system and the mechanical properties of the material being used rather than the structure of the matrix itself. In the case of the partially-described problem presented, the determinant method was found to be computationally more efficient than the Cayley-Hamilton method because it solved fewer equations with fewer parameters. While a simple model was used herein in order to get a fundamental understanding of the structured methods, it is clear that there are unlimited possibilities in the design-for frequency of brace-soundboard systems using multiple braces and brace positions. Therefore the Cayley-Hamilton and determinant methods were demonstrated as proofs of concept for future work in the field of inverse eigenvalue problems. These techniques hold great potential in creating system matrices of complex systems from a desired frequency spectrum by calculating the parameters within these system matrices using the set of desired natural frequencies as input to the design.

5.7 Acknowledgments

The authors would like to acknowledge the generous support provided by the Natural Sciences and Engineering Research Council of Canada.

5.8 References

[1] M. T. Chu and G. H. Golub, *Inverse Eigenvalue Problems: Theory, Algorithms, and Applications*. Oxford University Press, USA, 2005.

[2] G. M. L. Gladwell, *Inverse problems in vibration*. Kluwer Academic Publishers, 2004.

[3] D. Boley and G. H. Golub, "A survey of matrix inverse eigenvalue problems," *Inverse Problems*, vol. 3, no. 4, p. 595, 1987.

[4] M. T. Chu and J. L. Watterson, "On a Multivariate Eigenvalue Problem: I. Algebraic Theory and a Power Method," *SIAM J. Sci. Comput.*, vol. 14, pp. 1089–1106, 1993.

[5] R. Erra and B. Philippe, "On some structured inverse eigenvalue problems," *Numerical Algorithms*, vol. 15, no. 1, pp. 15–35, 1997.

[6] M. T. Chu, "Inverse eigenvalue problems," *SIAM Rev*, vol. 40, pp. 1–39, 1998.

[7] F. W. Biegler-König, "Construction of band matrices from spectral data," *Linear Algebra and its Applications*, vol. 40, no. 0, pp. 79–87, Oct. 1981.

[8] G. H. Golub and R. R. Underwood, "The block Lanczos method for computing eigenvalues," in *Mathematical Software III*, J.R. Rice., New York: Springer, 1977.

[9] F. W. Biegler-König, "A Newton iteration process for inverse eigenvalue problems," *Numerische Mathematik*, vol. 37, no. 3, pp. 349–354, 1981.

[10] M. T. Chu, "A Fast Recursive Algorithm for Constructing Matrices with Prescribed Eigenvalues and Singular Values," *SIAM Journal on Numerical Analysis*, vol. 37, no. 3, pp. 1004–1020, Jan. 2000.

[11] P. Dumond and N. Baddour, "A structured approach to design-for-frequency problems using the Cayley-Hamilton theorem," *SpringerPlus*, vol. 3, no. 1, p. 272, May 2014.

[12] P. Dumond and N. Baddour, "Effects of using scalloped shape braces on the natural frequencies of a brace-soundboard system," *Applied Acoustics*, vol. 73, no. 11, pp. 1168–1173, Nov. 2012.

[13] R. M. French, "Engineering the Guitar: Theory and Practice," 1st ed., New York: Springer, 2008, pp. 159–208.

[14] L. Meirovitch, "Principles and Techniques of Vibrations," Upper Saddle River, NJ: Prentice Hall, 1996, pp. 542–543.

[15] A. W. Knapp, "Basic Algebra," in *Basic Algebra*, Boston: Birkhäuser, 2006, p. 219.

[16] F. R. Chang and H. C. Chen, "The generalized Cayley-Hamilton theorem for standard pencils," *Systems & Control Letters*, vol. 18, no. 3, pp. 179–182, Mar. 1992.

[17] J. L. Coolidge, *Treatise on Algebraic Plane Curves*. Mineola, New York: Dover Publications, 1959.

[18] Forest Products Laboratory (US), "Wood Handbook, Wood as an Engineering Material," Madison, WI: U.S. Department of Agriculture, Forest Service, 1999, pp. 4.1–13.

[19] A. Chaigne, "Recent advances in vibration and radiation of musical instruments," *Flow, Turbulence and Combustion*, vol. 61, pp. 31–34, 1999.

[20] J. Woodhouse, E. K. Y. Manuel, L. A. Smith, A. J. C. Wheble, and C. Fritz, "Perceptual Thresholds for Acoustical Guitar Models," *Acta Acustica united with Acustica*, vol. 98, no. 3, pp. 475–486, 2012.

[21] S. Moiseev, "Universal derivative-free optimization method with quadratic convergence," arXiv e-print 1102.1347, Feb. 2011.

[22] C. Hutchins and D. Voskuil, "Mode tuning for the violin maker," *CAS Journal*, vol. 2, no. 4, pp. 5–9, 1993.

Chapter 6

Experimental Investigation of the Mechanical Properties and Natural Frequencies of Simply Supported Sitka Spruce Plates

6.1 Abstract

Abundant and easy to work, wood has historically been the material of choice for stringed musical instruments. However, due to large variations in growth, wood also presents a challenge to implementing acoustic consistency into a production line. As the manufacture of musical instruments continues to increase while supplies of suitable wood decrease, a need to maximize and optimize the use of available timber also arises. In the past, mechanical properties of wood have been compiled using distinctive samples of the same species. Since such large variations exist within a species, the emphasis has been placed on describing average properties of the species, rather than determining exact values for one specimen. Nonetheless, manufacturing processes require direct measurements of the mechanical properties of a given specimen in order to construct acoustically consistent musical instruments.

In this paper, non-destructive mechanical property tests have been developed so that they can all be performed on a single wooden specimen. In this way, relationships between mechanical properties of clear, straight-grained, quartersawn timber can be investigated. Measured properties include density, moisture content, Young's modulus in the longitudinal and radial directions using a three point bending test, shear modulus using a two point square plate twist test and Poisson's ratios using a tension test, both in the longitudinal-radial plane. Furthermore, the natural frequencies of the same specimens have been measured for the rectangular plate having simply supported boundary conditions, in order to verify the accuracy of the mechanical properties.

Sitka spruce of three different grades, commonly used for North American soundboards, is studied. Relationships between various mechanical properties are found and suggestions for using Poisson's ratio are proposed. These relationships are shown to reduce the number of measurements required by musical instrument builders wishing to construct acoustically-consistent instruments. Great correlation is found between the theoretical model and experimental results for the simply supported rectangular plate.

6.2 Introduction

From an engineering perspective, wood has always been a challenging material. The large variability of its mechanical properties is due to the tree's growth which is at the mercy of its climatic and environmental conditions [1]. Structural engineers have overcome these challenges by choosing values for the mechanical properties of various species of wood to be the 5th percentile of the statistical bell curve associated with the given species' mechanical properties [2]. By doing so they ensure that most pieces of lumber are stronger than the assumed properties. Although generally over-designed, this method works well when coupled with redundant structural design. However, when using wood for its acoustic abilities, the 5th percentile cannot be used because acoustic properties are directly related to mechanical properties. Thus, an exact knowledge of any given specimen's mechanical properties is an asset. Although, these can be measured, it is typically not economically feasible or convenient to do so on a per-specimen basis, during manufacturing [3].

In certain instances, it has been observed in the guitar manufacturing industry that the soundboard's radial stiffness (Young's modulus, E_R) can be used as a measure of acoustic quality [4]. However, no scientific backing currently exists for this approach. Many studies have given the average range for a number of mechanical properties of wood, where each measurement was made on a separate piece of wood of the same species and then averaged [1], [5]–[7]. McIntyre and Woodhouse discussed the measurement of the elastic and damping constants by interpreting the frequencies and Q-factors of the lowest modes of vibration of a wooden plate [8], [9]. Some studies have even taken a microstructure approach to mechanical properties [10], [11]. Nonetheless, very little is known with regards to the relationship between mechanical properties within the same wooden specimen.

Furthermore, a recent study has demonstrated the possibility of compensating for different mechanical properties of a wooden brace-plate system by adjusting the dimensions of the brace [12]. In doing so, it is possible to render the brace-plate system's acoustic properties consistent. Therefore, a need exists for gathering mechanical property

information during manufacturing. Any possible simplification to this procedure would be an asset.

In this study, a series of non-destructive tests are used to verify the mechanical properties of a number of wooden specimens. These tests measure Young's modulus in both the radial and longitudinal directions (E_L and E_R), as well as the shear modulus in the *L-R* plane (G_{LR}), the major and minor Poisson's ratio (ν_{LR} and ν_{RL}), the moisture content (*MC*) and finally the density (μ), based on the specimen mass at the given moisture content, rather than the typically-measured specific gravity determined from oven dry wood. The natural frequencies of the given wooden specimens are then measured using a simply supported plate setup as described in [13], [14], based on the plate dimensions of [12]. These measured values are then compared to those calculated analytically.

In all cases, measurements are made on clear, straight-grained and quartersawn Sitka spruce. This wood is chosen due to its common use in North American industry. Quartersawn wood (wood with grain as perpendicular to the surface of the plate as possible), was chosen in order to limit grain angle as a variable during the analysis. The Sitka spruce soundboards were obtained from Stewart-Macdonald (www.stewmac.com). Three book-matched specimens of each grade (AA, AAA, and AAAA, based on their own grading system) were measured, for a total of nine samples. The soundboards were prepared using standard luthier techniques by gluing two book-matched boards together and ensuring a perfect joint. This simplifies the analysis by creating symmetry in the mechanical properties of the soundboards.

6.3 Specimen Samples

Non-destructive testing is preferred so that the specimens can be used for future investigations after mechanical property measurements have been made. In many tests for mechanical properties, damage can easily occur. Therefore, the tests, as well as the dimensions of the wooden plate were carefully considered. Dimensions of the plates were chosen so that their natural frequencies could be measured and compared to those of a

previous study [12]. Since this plate is rectangular and the square plate twist test [15] requires a square plate, the test plate was divided into sections as shown in Figure 26.

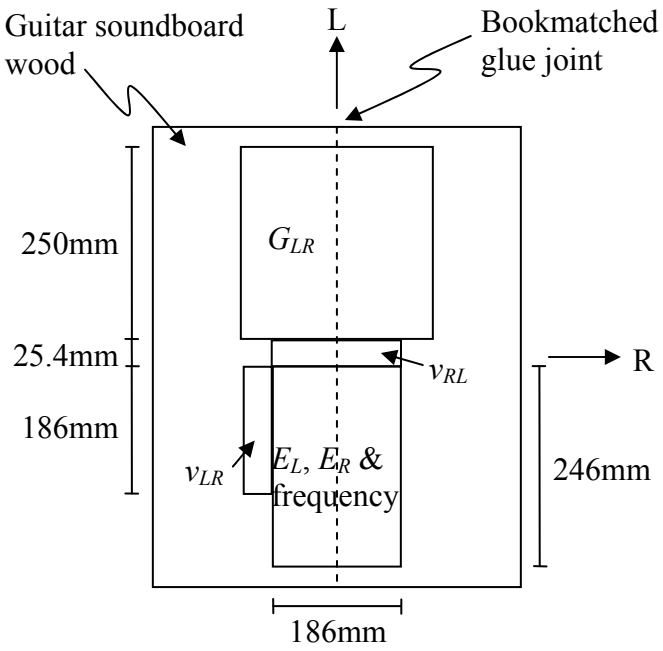

Figure 26. Sectioned soundboard.

The square plate section marked with G_{LR} was used for the two point square plate twist test. Strips marked with v_{LR} and v_{RL} were used for tension tests, and were the only samples that were destroyed. The rectangular plate section marked with E_L and E_R was used for the three point bending test, as well as the frequency test. However, the edges of the plate were tapered to a point for the frequency test. Finally the remaining sections were used to measure moisture content and volumetric mass density.

6.4 Methods

6.4.1 Mechanical Properties

All mechanical properties were measured using non-destructive testing based partially on ASTM standard test methods for wood-based materials, ISO standards for fibre-reinforced composite materials and on the book Static Test Methods for Composites

[15]. Other references will be addressed in sequence. Great pain was taken to ensure that the best approach was chosen in each case.

6.4.1.1 Young's Modulus

Young's moduli in both the longitudinal and radial directions were measured using a three point bending test. A modified version of ASTM D3043-2011 for wooden structural panels, method A, was used [16]. Dimensions of the test rig were modified to account for those of the plate specified in Section 6.3. Tarnopol'skii and Kincis [15] recommend that $s/h > 40$ for accurate measurements of Young's modulus, where s is the span between supports and h the thickness of the plate. Furthermore, although s and h values as given in the results section satisfy the recommended value, greater span length also increases the stringency with which the supports must be designed. The three point bending test rig setup is shown in Figure 27.

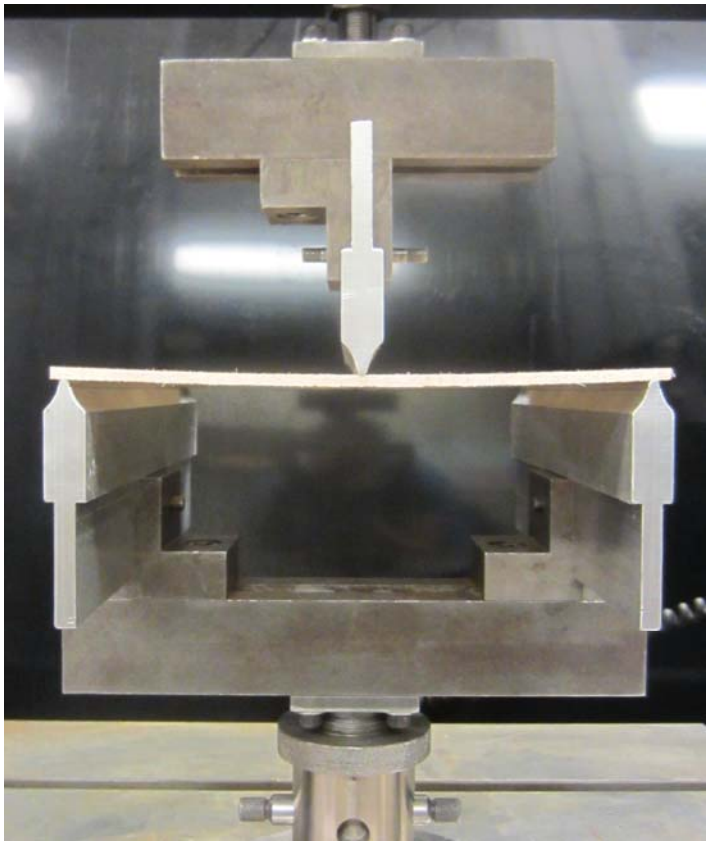

Figure 27. Three point bending test rig.

Based on an applied force of P and a flexural displacement of w, the Young's modulus, E_x, can be calculated from Equation (49):

$$E_x = \frac{Ps^3}{48Iw_{\max}} \tag{49}$$

where I is the second moment of area of the cross section of the plate such that $I = bh^3/12$ and b is the depth of the plate.

Supports were designed in accordance with the study conducted by Ogorkiewicz and Mucci [17], which tested six different support types on fibre-plastic composite plates. Their conclusion was that supports having a supporting edge diameter of less than 3.5 mm but no smaller than 2.4 mm prevented specimen indentation of soft material and had a negligible effect on elastic moduli values due to span shortening while bending. Thus, supports of 3.2mm (1/8in) diameter were used. Their tests were conducted using a span of 176 mm, which is the same as that used in this study. Roller supports were not considered because of the negligible friction effect at the supports.

6.4.1.2 Shear Modulus

Shear modulus, for the purpose of this study, was only measured in the *L*-*R* plane. Since non-destructive testing is sought, the two point square plate twist method was used. A modified version of ISO 15310-1999 for fibre-reinforced composites was used [18]. Although ASTM D3044-2011 for wooden structural panels [19] was also considered, it has been reported that the ISO method is easier to use and produces better results [20]–[22]. Dimensions of the test rig were modified to account for those of the plate specified in Section 6.3. Tarnopol'skii and Kincis [15] recommend that $25 \le l/h \le 100$ and ISO recommends measurements be taken between $0.1h \le w_{load} \le 0.3h$, where h is the thickness of the plate and l the length of the plate's edges, both of which were satisfied in this study. The span at the points of application (S) measured 328.34 mm. The two point square plate twist rig is shown in Figure 28.

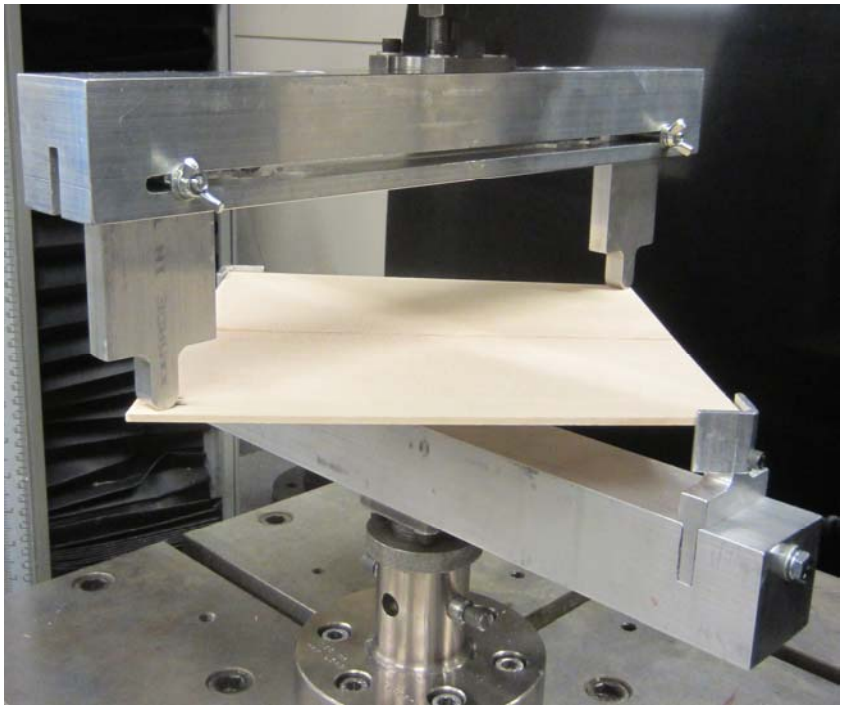

Figure 28. Two point plate twist test rig.

Under the applied load, the shear modulus can be calculated from

$$G_{xy} = \frac{3Pl^2}{2wh^3}K \tag{50}$$

where K is a correction factor to account for the application of the load at a position other than the corners. K can be calculated from the point of application span S and the diagonal dimension of the plate D using Equation (51):

$$K = 3\left(\frac{S}{D}\right)^2 - 2\left(\frac{S}{D}\right) - 2\left(1-\frac{S}{D}\right)^2 \ln\left(1-\frac{S}{D}\right) \tag{51}$$

6.4.1.3 Poisson's ratios

Both the major and minor Poisson's ratios were measured in the *L-R* plane. To do so, two tension tests were used. The first applied the load in the grain's longitudinal directions (parallel to the grain), while the second applied the load in the radial direction (perpendicular to the grain). The tension tests were based on those proposed in [23]. Since ultimate strength was not measured, test specimens with constant cross-section could be used. The test rig setup is shown in Figure 29.

Figure 29. Tension test rig.

Micro-Measurements foil strain gauges (model CEA-06-250UW-120) with a gauge factor of $GF = 2.1$ were used to measure strain in the axial and transverse directions. Two strain gauges per direction were placed at at 0° and 90° to the load direction. Their layup can also be seen in Figure 29. Thus, strain in both the axial and transverse directions were calculated from

$$\varepsilon = \frac{\Delta R / R_G}{GF} \tag{52}$$

where R_G is the value of the strain gauge's undeformed resistance and ΔR, the change in resistance. Having found the strains, Poisson's ratios were calculated using the standard formula:

$$\nu_{xy} = -\frac{\varepsilon_y}{\varepsilon_x} = -\frac{\varepsilon_{tranverse}}{\varepsilon_{axial}} \tag{53}$$

6.4.1.4 Moisture Content

All wood used during mechanical testing was kiln-dried by the supplier to a moisture content of 6% and then air-dried for a year before it was received for testing. However, since wood's moisture content has such a large impact on its mechanical properties, a measure must be taken. An Electrophysics model MT808 pin type moisture meter with a stipulated accuracy of 0.1% between the ranges of 4-10% and 1% above 10% was used. Moisture measurements were made throughout the various property measurements in order to ensure consistent values and were found to range between 8-11%.

6.4.1.5 Density

Volumetric mass density was measured at the given moisture content in order to ensure accurate subsequent frequency calculations. The density measurements were partially based on ASTM D2395-07 for wood-based materials [24], but without using the mass of the wooden specimen when oven dry. The specimen's volume was calculated from

$$V = L_L L_R h \tag{54}$$

and the density was then calculated as

$$\mu = \frac{m_{MC}}{V} \tag{55}$$

where m_{MC} is the mass of the specimen at the given moisture content.

6.4.2 Natural Frequencies

The natural frequencies of the simply supported plate were calculated in a number of ways using the measured mechanical properties, as well as with mechanical property

relationships developed in Section 6.5.1. The theoretical natural frequencies can be calculated analytically using the typical orthotropic plate equation [25]:

$$\omega_{m_x,m_y} = \frac{\pi^2}{\sqrt{\mu h}}\sqrt{\frac{m_x^4 D_x}{L_x^4} + \frac{2m_x^2 m_y^2\left(D_{xy}+2D_k\right)}{L_x^2 L_y^2} + \frac{m_y^4 D_y}{L_y^4}} \tag{56}$$

where

$$D_x = \frac{E_x h^3}{12\left(1-\nu_{xy}\nu_{yx}\right)}, D_y = \frac{E_y h^3}{12\left(1-\nu_{xy}\nu_{yx}\right)}, D_{xy} = \frac{\nu_{yx} E_x h^3}{12\left(1-\nu_{xy}\nu_{yx}\right)}, D_k = \frac{G_{xy} h^3}{12} \tag{57}$$

In order to experimentally measure the natural frequencies of the simply supported plate described in Section 6.3, the simply supported experimental setup proposed by Amabili [13], [14] is used. To achieve the required simply supported boundary conditions, a 90° v-groove was cut into the edge supports as shown in Figure 30.

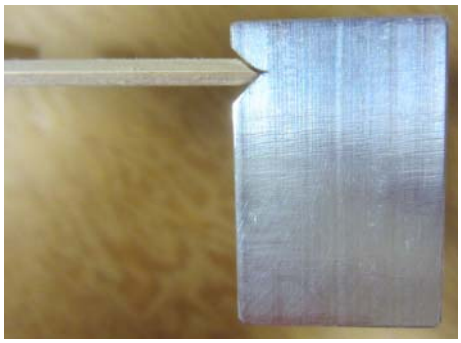

Figure 30. Experimental simply supported boundary conditions.

The plate has its edges tapered to an angle of 45°, allowing it to rotate freely about the contact line within the edge support v-grooves. A bead of caulking was applied to the edge support v-groove before inserting the plate, to ensure proper contact of the plate at all times. Seal 'N Peel caulking was chosen for its ease of removal between specimen tests. It has been found that caulking has a negligible effect on the motion of the plate and thus, on its natural frequencies [13]. The edge supports are connected at one end by a bolt through an elongated slot at the opposite end of each support, as shown in Figure 31. This ensures an accurate, adjustable and tight fit for every plate specimen.

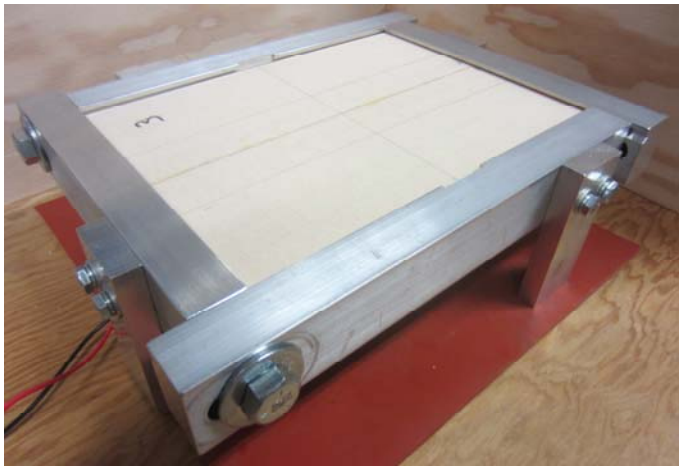

Figure 31. Experimental frequency test frame.

For natural frequency measurements, a speaker was placed directly beneath the plate. Cake sprinkles were added to the top of the plate in order to form Chladni patterns. A tone generator connected to an amplifier varied the frequencies supplied to the plate by the speaker until a distinct Chladni pattern formed. A sound level meter was also placed above the plate to help determine the natural frequencies. The frequency and modeshape were recorded and the procedure repeated until the desired number of frequencies was obtained. The experimental frequencies were then compared to the theoretical frequencies calculated using Equation (56). Figure 32 shows the entire experimental frequency setup.

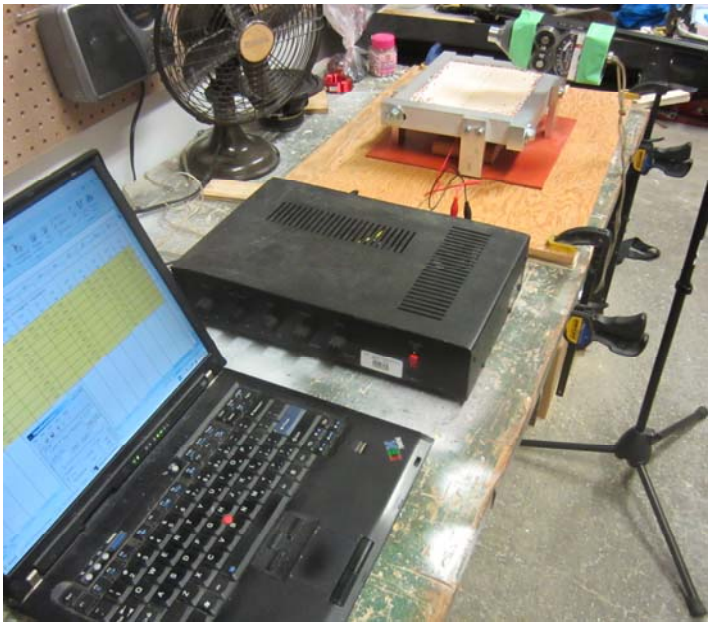

Figure 32. Frequency tests experimental setup.

6.5 Results

The mechanical property tests were conducted using an Instron machine model 4482. Frequency measurements were conducted last. All tests were conducted on each specimen in sequence before moving on to the next test. Moisture content was verified on a regular basis in order to ensure consistent results.

6.5.1 Mechanical Properties

Actual dimensions of the specimens are presented in Table 22 and results of the mechanical property tests are presented in Table 23 below.

Table 22. Measured dimensions of the test specimens.

Specimens	l_L (mm)	l_R (mm)	h (mm)
1	245.64	185.70	3.27
2	245.92	186.51	3.26
3	245.87	186.41	3.30
4	245.85	186.36	3.27
5	245.92	186.41	3.40
6	245.92	186.46	3.20
7	245.80	186.31	3.23
8	245.85	186.49	3.34
9	245.82	186.44	3.22
Average	245.84	186.34	3.28

Table 23. Experimentally measured mechanical properties of Sitka spruce.

Specimens	Moisture MC (%)	Grains ψ (grains/in)	Density μ (kg/m^3)	Shear G_{LR} (MPa)	Young's Modulus E_R (MPa)	E_L (MPa)	Poisson's Ratio ν_{RL}	ν_{LR}
Standard [1]	12	N/A	403.2	697.0	849.4	10890.0	0.04	0.372
1	9.1	17.6	404.9	954.3	1149.2	9875.5	0.077	0.533
2	8.5	16.8	387.3	653.6	962.8	12727.5	0.036	0.352
3	8.2	22.2	401.0	661.3	856.6	11984.1	0.052	0.411
4	8.4	14.5	400.5	734.9	849.7	11908.8	0.050	0.394
5	8.9	17.4	512.7	1028.0	1085.8	11393.3	0.056	0.491
6	8.3	19.2	396.2	711.7	717.9	13406.8	0.014	0.343
7	7.9	14.5	395.7	737.4	923.3	12412.6	0.063	0.383
8	8.3	24.0	433.1	823.8	796.8	12490.8	0.043	0.478
9	8.3	15.0	414.7	687.8	721.8	13069.4	0.040	0.396
Average	8.4	17.9	416.2	777.0	896.0	12141.0	0.048	0.420
σ (SD)	0.4	3.4	38.5	132.6	150.4	1047.3	0.018	0.066
Average (without 1, 5)	8.3	18.0	404.1	715.8	832.7	12571.4	0.042	0.394
σ (SD, no 1, 5)	0.2	3.9	15.2	57.9	93.8	545.6	0.015	0.044

Specimens marked as standard possess the average values as given by the US Forest Products Laboratory [1]. Specimens 1-9 are those that were specially prepared for this study and their average values are calculated in the second last row of Table 23, marked as "Average". It is interesting to note that all the experimentally-calculated values, including their average are found to be close to those standard values. The one exception is the Young's moduli in the longitudinal direction (E_L) which is rather low compared to our experimentally obtained values. However, the Forest Products Laboratory also tabulates the average value of E_L for Canadian Sitka Spruce imported into the US as 12320 MPa, much closer to our values.

Specimens 1, 4 and 7 are grade AA, specimens 2, 5 and 8 are grade AAA and specimens 3, 6 and 9 are grade AAAA. From the experimentally-obtained mechanical properties presented in Table 23, it is clear that there exists no direct relationship between the grading scheme offered by Stewart-Macdonald and the actual mechanical properties of the wooden specimens. This is immediately obvious from the very wide scatter of results. Any relationship between any of these properties is also not immediately obvious. However, further analysis in this paper reveals certain possible simplifications.

The first observation that can be made is that specimens 1 and 5 vary considerably from their peers as seen by the significant reduction in the standard deviation (σ) when these specimens are removed. Thus, these specimens were discarded. No obvious visual differences were observed in these two specimens except for the rather coarse grain of specimen 5 (thick latewood lines) compared to the rest. Further investigation is required to determine possible causes. With specimens 1 and 5 discarded, the average mechanical properties of the experimental specimens were recalculated. It becomes clear that minimal variations exist in both the major and minor Poisson's ratios. Thus, it is postulated that the average values can be used as a simplification. However, the average values obtained from the Forest Products Laboratory appear to be low for such instrument-grade wood. Therefore, we propose to use $\nu_{LR} = 0.394$ and $\nu_{RL} = 0.042$. This simplification will be verified by calculating the natural frequencies of a wooden plate having these properties. Furthermore, a simple relationship can be found between μ, G_{LR}, E_R and E_L, where the former properties are divided by the latter. These ratios are found in Table 24, where specimens are presented in their grading order rather than their numerical order.

Table 24. Mechanical property ratios with regards to E_L.

Specimens	μ / E_L	G_{LR} / E_L	E_R / E_L
Standard [1]	0.037	0.064	0.078
4	0.034	0.062	0.071
7	0.032	0.059	0.074
2	0.030	0.051	0.076
8	0.035	0.066	0.064
3	0.033	0.055	0.071
6	0.030	0.053	0.054
9	0.032	0.053	0.055
Average	0.032	0.057	0.066
σ (SD)	0.002	0.005	0.009

Although the ratios in Table 24 are not exactly the same, the standard deviations (σ) demonstrate that there is less variation in the ratios than what was expected based on current knowledge. Consequently, by using the average ratios of Table 24 calculated in this study for each material property and measuring only E_L, it would be possible to calculate μ, G_{LR} and E_R from $\mu = 0.032E_L$, $G_{LR} = 0.057E_L$ and $E_R = 0.066E_L$ for each specimen with a maximum error of 9%, 14% and 24% respectively. Although the errors are not negligible, of more interest to an instrument maker would be the effects of these calculated values on the natural frequencies. Thus, a theoretical frequency analysis was performed.

6.5.2 Theoretical Natural Frequencies

Results of the fundamental natural frequency calculations are presented in Table 25 below. Values were calculated using direction L as x and R as y in Equations (56) and Equation (57).

Table 25. Calculated fundamental frequencies of the simply supported spruce plates.

Specimens	Frequencies (actual) Eq. (56) Hz	Frequencies (with ratios) Hz	Err. %	Frequency (with ν(avg) and ratios) Hz	Error %	Frequency (with ν(avg) & actual E_R) Hz	Err. %
4	181.9	183.5	-0.9	181.8	0.1	182.5	-0.4
7	186.8	183.9	1.6	179.6	3.8	180.9	3.2
2	184.2	179.6	2.5	181.1	1.7	182.5	0.9
8	181.9	186.0	-2.2	185.6	-2.0	185.2	-1.8
3	182.1	185.5	-1.9	183.4	-0.7	184.2	-1.2
6	175.8	171.9	2.2	177.8	-1.1	175.7	0.0
9	176.4	178.5	-1.2	179.0	-1.4	177.2	-0.4

In Table 25, the first frequency column represents the fundamental natural frequencies calculated using all the actual measured properties of Table 23 and the plate dimensions of Table 22. The second frequency column uses the mechanical properties calculated using the ratios of Table 24 and the actual Poisson's ratios. The third frequency column is similarly calculated using the ratios of Table 24 and the average Poisson's ratios of $\nu_{LR} = 0.394$ and $\nu_{RL} = 0.042$. Finally, the last frequency column is the same as the previous column, but uses the actual values of E_R. It is clear that using the simplifications does not have a large effect on the calculation of the natural frequencies, with the largest error of 3.8% obtained with specimen 7. Using the average values of Poisson's ratio only increases the error slightly in certain cases. The advantages of using these values far out-weigh the disadvantages, especially since Poisson's ratios are the most time consuming to measure experimentally. Finally, using the actual values of E_R improves the natural frequency calculations and since these values are not more difficult to obtain than E_L, it is a recommended procedure.

A consideration of the lowest three partial frequencies above the fundamental reveals a similar trend regarding error in the frequency estimations. These are tabulated in Table 26 for frequencies calculated using ratios of μ / E_L, G_{LR} / E_L, average values of $\nu_{LR} = 0.394$ and $\nu_{RL} = 0.042$ and actual values of E_R.

Table 26. Partial frequencies calculated using mechanical property simplifications (Hz).

Specimens	Approx. *m_L=1, m_R=2	Actual	Error %	Approx. *m_L=2, m_R=1	Actual	Error %	Approx. *m_L=2, m_R=2	Actual	Error %
4	354.3	353.4	-0.3	590.8	582.8	-1.4	730.2	727.6	-0.4
7	354.1	366.0	3.3	584.0	594.5	1.8	723.5	747.2	3.2
2	358.3	361.3	0.8	588.8	600.5	1.9	730.0	736.6	0.9
8	351.4	345.9	-1.6	603.1	586.1	-2.9	740.7	727.6	-1.8
3	357.6	353.6	-1.1	596.1	587.3	-1.5	736.7	728.3	-1.2
6	323.0	320.8	-0.7	577.0	590.7	2.3	702.9	703.1	0.0
9	327.5	325.4	-0.6	581.1	582.6	0.3	708.9	705.7	-0.4

*where m_L is the modal number in the longitudinal direction and m_R in the radial direction

6.5.3 Experimental Natural Frequencies

The experimentally-measured natural frequencies of the simply supported rectangular Sitka spruce plate are presented in Table 27 and Table 28 and are compared to those calculated using the theoretical model of Equation (56). In both tables, m_L represents the modal number in the longitudinal direction and m_R the modal number in the radial direction.

Table 27. Theoretical and experimental frequencies for the 1x1, 1x2 and 2x1 modes (Hz).

Specimens	*MC* %	Theo. m_L=1, m_R=1	Exp.	Error %	Theo. m_L=1, m_R=2	Exp.	Error %	Theo. m_L=2, m_R=1	Exp.	Error %
1	11	187	185	1.0	399	405	-1.5	554	537	3.2
2	10	184	184	0.4	361	366	-1.3	601	586	2.4
3	10	182	180	1.1	354	357	-1.0	587	582	1.0
4	10	182	178	2.1	353	368	-4.1	583	585	-0.4
5	10	176	188	-6.6	362	398	-9.8	538	596	-10.7
6	10	176	182	-3.3	321	346	-7.9	591	585	1.0
7	10	187	178	4.7	366	368	-0.5	595	581	2.3
8	10	182	182	-0.1	346	353	-1.9	586	593	-1.1
9	11	176	175	1.1	325	342	-5.1	583	570	2.3

Table 28. Theoretical and experimental frequencies for the 1x3 and 2x2 modes (Hz).

Specimens	*MC* %	Theo. m_L=1, m_R=3	Exp.	Error %	Theo. m_L=2, m_R=2	Exp.	Error %
1	11	765	764	0.1	747	723	3.2
2	10	688	695	-1.0	737	731	0.8
3	10	663	671	-1.1	728	718	1.4
4	10	660	673	-1.9	728	726	0.2
5	10	685	734	-7.1	706	768	-8.9
6	10	591	615	-4.0	703	717	-1.9
7	10	685	694	-1.3	747	723	3.2
8	10	637	672	-5.4	728	731	-0.5
9	11	596	613	-2.8	706	700	0.8

It is clear from both Table 27 and Table 28 that experimental results for the plate's natural frequencies show great agreement with those calculated theoretically from Equation (56). The average error is around 1-3%, with a few outliers. The only specimen that demonstrates a significant departure from the theoretical model is specimen 5, which has already been discarded earlier for lack of conformity.

6.5.4 Discussion

Frequency calculations were performed using D_{LR} rather than D_{RL} of Equation (57) since it was found that errors were reduced by using this approach. This is likely due in part to the fact that ν_{RL} is a much smaller value than ν_{LR}, thus any errors stemming from slight variations in the measurements are diminished. Furthermore, an additional frequency analysis was performed by varying individual mechanical properties within the range of those experimentally obtained. In doing so, it was found that the values at the limit of the range for all properties significantly affected the natural frequencies, with the exception of Poisson's ratio. The maximum variation in frequency by varying Poisson's ratio was 1.5%. Thus, the use of constant average values for Poisson's ratio as a simplification is justified. Finally, grain density (ie. number of grain line per inch) was not a good indication of any mechanical property.

Experimental measurements of the natural frequencies of the wooden plates using the mechanical properties of Table 23 were obtained using simply supported boundary conditions. While simply supported boundary conditions are the easiest to model

theoretically, they present quite a significant challenge experimentally. Few studies have attempted to measure natural frequencies using these boundary conditions. Based on the results obtained in this study, using an adjustable frame with a v-notch filled with silicon presents a good experimental representation of the simply supported boundary conditions and should be explored further.

6.6 Conclusion

The goal of this study was to investigate the existence of relationships between mechanical properties of clear straight-grained and quartersawn Sitka spruce, verify their effect on the natural frequencies and validate those properties and frequencies experimentally. It was shown that using average values for the major and minor Poisson's ratios of $\nu_{LR} = 0.394$ and $\nu_{RL} = 0.042$ as well as using the relationships $\mu = 0.032E_L$, $G_{LR} = 0.057E_L$ and $E_R = 0.066E_L$ is a good approximation for calculating natural frequencies, with an error not exceeding 3.8%. Results can be improved by using actual values of E_R.

Experimental results for the natural frequencies of the simply supported rectangular plates have shown good correlation with those calculated analytically, their average error falling between 1% and 3%, with only a few outliers.

If wooden musical instrument manufacturers are to improve the acoustical consistency of their instruments, then knowledge of the mechanical properties of the wood is required. A reduction in the number of mechanical properties that require direct measurement is desired. It is suggested that a measure of E_L and E_R be taken. A simple three point bending rig could easily accommodate both measurements.

6.7 Acknowledgements

The authors would like to acknowledge the generous support provided by the Natural Science and Engineering Research Council of Canada.

6.8 References

[1] Forest Products Laboratory (US), "Wood Handbook, Wood as an Engineering Material," Madison, WI: U.S. Department of Agriculture, Forest Service, 1999, pp. 4.1–13.

[2] Canadian Wood Council, *Wood Design Manual 2010*. Ottawa, ON: Canadian Wood Council, 2010.

[3] R. M. French, "Engineering the Guitar: Theory and Practice," 1st ed., New York: Springer, 2008, pp. 159–208.

[4] R. Godin, "Godin Guitars Factory Visit, Princeville, QC, Canada," 22-Oct-2007.

[5] H. Carrington, "CV. The elastic constants of spruce," *Philosophical Magazine Series 6*, vol. 45, no. 269, pp. 1055–1057, 1923.

[6] M. E. Haines, "On Musical Instrument Wood," *J. Catgut Acoustical Society*, vol. 31, pp. 23–32, 1979.

[7] M. E. McIntyre and J. Woodhouse, "On measuring wood properties, Part 3," *J. Catgut Acoustical Society*, vol. 45, pp. 14–23, 1986.

[8] M. E. McIntyre and J. Woodhouse, "On measuring wood properties, Part 2," *J. Catgut Acoustical Society*, vol. 43, pp. 18–24, 1985.

[9] M. E. McIntyre and J. Woodhouse, "On measuring the elastic and damping constants of orthotropic sheet materials," *Acta Metallurgica*, vol. 36, no. 6, pp. 1397–1416, Jun. 1988.

[10] E. Kahle and J. Woodhouse, "The influence of cell geometry on the elasticity of softwood," *J Mater Sci*, vol. 29, no. 5, pp. 1250–1259, Mar. 1994.

[11] L. Mishnaevsky Jr. and H. Qing, "Micromechanical modelling of mechanical behaviour and strength of wood: State-of-the-art review," *Computational Materials Science*, vol. 44, no. 2, pp. 363–370, Dec. 2008.

[12] P. Dumond and N. Baddour, "Effects of using scalloped shape braces on the natural frequencies of a brace-soundboard system," *Applied Acoustics*, vol. 73, no. 11, pp. 1168–1173, Nov. 2012.

[13] M. Amabili, "Nonlinear vibrations of rectangular plates with different boundary conditions: theory and experiments," *Computers & Structures*, vol. 82, no. 31–32, pp. 2587–2605, Dec. 2004.

[14] M. Amabili, "Theory and experiments for large-amplitude vibrations of rectangular plates with geometric imperfections," *Journal of Sound and Vibration*, vol. 291, no. 3–5, pp. 539–565, Apr. 2006.

[15] Y. M. Tarnopol'skii and T. Kincis, *Static Test Methods for Composites*. Van Nostrand Reinhold Co., 1985.

[16] ASTM D3043-00, "Test Methods for Structural Panels in Flexure," ASTM International, 2011.

[17] R. M. Ogorkiewicz and P. E. R. Mucci, "Testing of fibre-plastics composites in three-point bending," *Composites*, vol. 2, no. 3, pp. 139–145, Sep. 1971.

[18] ISO 15310-1999, "Fibre-reinforced plastic composites - Determination of the in-plane shear modulus by the plate twist method," International Organization for Standardization, 1999.

[19] ASTM D3044-94, "Test Method for Shear Modulus of Wood-Based Structural Panels," ASTM International, 2011.

[20] G. D. Sims, W. Nimmo, A. F. Johnson, and D. H. Ferriss, "Analysis of plate-twist test for in-plane shear modulus of composite materials (revised)," *NASA STI/Recon Technical Report N*, vol. 95, p. 26749, Jan. 1994.

[21] B. Gommers, I. Verpoest, and P. Van Houtte, "Further developments in testing and analysis of the plate twist test for in-plane shear modulus measurements," *Composites Part A: Applied Science and Manufacturing*, vol. 27, no. 11, pp. 1085–1087, 1996.

[22] H. Yoshihara and Y. Sawamura, "Measurement of the shear modulus of wood by the square-plate twist method," *Holzforschung*, vol. 60, no. 5, pp. 543–548, 2006.

[23] A. Sliker, "Measuring Poisson's ratios in wood," *Experimental Mechanics*, vol. 12, no. 5, pp. 239–242, May 1972.

[24] ASTM D2395-07ae1, "Test Methods for Specific Gravity of Wood and Wood-Based Materials," ASTM International, 2007.

[25] Leissa, *Vibration of Plates. Nasa Sp-160*. NASA, 1969.

Chapter 7

Natural Frequencies and Modeshapes of Simply Supported Sitka Spruce Plates With and Without a Brace

Experimental measurements of the models and methods presented in previous chapters are important in order to validate the results. Experimental measurements were performed on rectangular Sitka Spruce plates with simply supported boundary conditions. The mechanical properties and natural frequencies of nine plates were measured. Subsequently, a scalloped brace, also made of Sitka spruce, was attached to plate number 2 and further measurements of the natural frequencies were performed. Chapter 6 gives details of the experimental setup.

7.1 Dimensions

The dimensions of the bookmatched and quartersawn plates are given in Table 29.

Table 29. Measured dimensions of the test plates.

Specimens	l_L (mm)	l_R (mm)	h (mm)
1	245.64	185.70	3.27
2	245.92	186.51	3.26
3	245.87	186.41	3.30
4	245.85	186.36	3.27
5	245.92	186.41	3.40
6	245.92	186.46	3.20
7	245.80	186.31	3.23
8	245.85	186.49	3.34
9	245.82	186.44	3.22

where l_L is the length of the plate in the longitudinal direction (parallel to the grain), l_R the length of the plate in the radial direction (perpendicular to the grain) and h is the plate's thickness.

Table 30 gives the dimensions of the scalloped brace which are based on those used in the theoretical modeling and analysis of Chapters 2, 3 and 5.

Table 30. Measured dimensions of the test brace.

Specimens	l_L (mm)	l_R (mm)	h_b (mm)	λ
Brace	186.51	11.9	12	1

In Table 30, l_L is the length of the brace, l_R the width of the brace, h_b is the base height of the brace and λ is the peak height adjustment factor. Although the theoretical models had a brace width of l_R of 12 mm, due to current manufacturing facilities, the experimental brace used a dimension of 11.9 mm.

7.2 Mechanical Properties

The mechanical properties of the plates were measured experimentally using the methods described in Chapter 6. Due to the dimensions of the brace wood, the density μ and Young's modulus in the longitudinal direction E_L were measured and subsequently the other mechanical properties were calculated from the relationships and simplifications developed in Section 6.5.1. The mechanical properties of the plates are shown in Table 23.

Table 31. Experimentally measured mechanical properties of the plates.

Specimens	Density μ (kg/m^3)	Young's Modulus E_L (MPa)	E_R (MPa)	Shear G_{LR} (MPa)	Poisson's Ratio ν_{RL}	ν_{LR}
1	404.9	9875.5	1149.2	954.3	0.077	0.533
2	387.3	12727.5	962.8	653.6	0.036	0.352
3	401.0	11984.1	856.6	661.3	0.052	0.411
4	400.5	11908.8	849.7	734.9	0.050	0.394
5	512.7	11393.3	1085.8	1028.0	0.056	0.491
6	396.2	13406.8	717.9	711.7	0.014	0.343
7	395.7	12412.6	923.3	737.4	0.063	0.383
8	433.1	12490.8	796.8	823.8	0.043	0.478
9	414.7	13069.4	721.8	687.8	0.040	0.396

The mechanical properties of the brace used during the analysis are shown in Table 32. Density was calculated by measuring the volume and mass of the specimen, E_L was measured experimentally using a three point bending test, Poisson's ratios were assumed to be ν_{LR} = 0.394 and ν_{RL} = 0.042 and the other properties used the relationships G_{LR} = 0.057E_L and E_R = 0.066E_L to approximate their value as explained in Section 6.5.1.

Table 32. Experimental and approximate values for the mechanical properties of the brace.

Specimens	Density μ (kg/m^3)	Young's Modulus E_L (MPa)	E_R (MPa)	Shear G_{LR} (MPa)	Poisson's Ratio ν_{RL}	ν_{LR}
Brace	467.4	5995.7	395.7	341.8	0.042	0.394

7.3 Natural Frequencies and Modeshapes

Theoretical natural frequencies of the wooden plates can be calculated using the orthotropic simply supported rectangular plate equation:

$$\omega_{m_L,m_R} = \frac{\pi^2}{\sqrt{\mu h}}\sqrt{\frac{m_L^4 D_L}{l_L^4} + \frac{2m_L^2 m_R^2 \left(D_{LR} + 2D_k\right)}{l_L^2 l_R^2} + \frac{m_R^4 D_R}{L_R^4}} \tag{58}$$

where

$$D_L = \frac{E_L h^3}{12\left(1-\nu_{LR}\nu_{RL}\right)},\quad D_R = \frac{E_R h^3}{12\left(1-\nu_{LR}\nu_{RL}\right)},\quad D_{LR} = \frac{\nu_{RL} E_L h^3}{12\left(1-\nu_{LR}\nu_{RL}\right)},\quad D_k = \frac{G_{LR} h^3}{12}, \tag{59}$$

and m_L, m_R are the mode numbers in the longitudinal and radial directions respectively. A comparison between the five lowest theoretical and experimental natural frequencies for the simply supported plates without a brace is shown in Table 27, along with their percentage error.

Table 33. Theoretical and experimental frequencies for the simply supported plates (Hz).

Spec.	Theo. m_L=1, m_R=1	Exp.	Err. %	Theo. m_L=1, m_R=2	Exp.	Err. %	Theo. m_L=2, m_R=1	Exp.	Err. %	Theo. m_L=1, m_R=3	Exp.	Err. %	Theo. m_L=2, m_R=2	Exp.	Err. %
1	187	185	1.0	399	405	-1.5	554	537	3.2	765	764	0.1	747	723	3.2
2	184	184	0.4	361	366	-1.3	601	586	2.4	688	695	-1.0	737	731	0.8
3	182	180	1.1	354	357	-1.0	587	582	1.0	663	671	-1.1	728	718	1.4
4	182	178	2.1	353	368	-4.1	583	585	-0.4	660	673	-1.9	728	726	0.2
5	176	188	-6.6	362	398	-9.8	538	596	-10.7	685	734	-7.1	706	768	-8.9
6	176	182	-3.3	321	346	-7.9	591	585	1.0	591	615	-4.0	703	717	-1.9
7	187	178	4.7	366	368	-0.5	595	581	2.3	685	694	-1.3	747	723	3.2
8	182	182	-0.1	346	353	-1.9	586	593	-1.1	637	672	-5.4	728	731	-0.5
9	176	175	1.1	325	342	-5.1	583	570	2.3	596	613	-2.8	706	700	0.8

The associated modeshapes, captured using Chladni patterns, are shown in Figure 33. The experimentally-produced modeshapes exactly match those obtained analytically.

m_L=1, m_R=1 m_L=1, m_R=2 m_L=2, m_R=1 m_L=1, m_R=3 m_L=2, m_R=2

Figure 33. Experimental modeshapes for the simply supported plates.

Table 34 gives the six lowest experimentally measured natural frequencies for the simply supported plate number two of Table 23, on which a scalloped brace was added using the dimensions of Table 30. Since no exact analytical solution exists for a braced plate, the experimental frequencies are compared to those calculated using the assumed shape method model developed in Chapter 2 with 6 × 6 trial functions. The experimental frequencies are also compared to those calculated using a finite element model. The finite element model is developed in ANSYS 10.0 using solid 8-node brick elements for a total of 21,401 nodes. The percentage error between the theoretical models and the experimental braced-plate are also given.

Table 34. Theoretical and experimental frequencies for the simply supported plates (Hz).

	Frequencies			
Braced-plate (2)	m_L=1, m_R=1	m_L=2, m_R=1	m_L=2, m_R=2	m_L=1, m_R=2
Experimental (Hz)	437	603	795	861
Assumed shape (Hz)	467	706	956	1051
Error (%)	6.4	14.6	16.9	18.1
FEA (Hz)	487	610	773	912
Error (%)	10.3	1.1	-2.9	5.5

The associated experimentally-obtained modeshapes of the braced plate are shown in Figure 34. Figure 35 shows those obtained using the finite element analysis. The experimentally-produced modeshapes exactly match those obtained analytically.

m_L=1, m_R=1 m_L=2, m_R=1 m_L=2, m_R=2 m_L=1, m_R=2

Figure 34. Experimental modeshapes for the simply supported plate with scalloped brace.

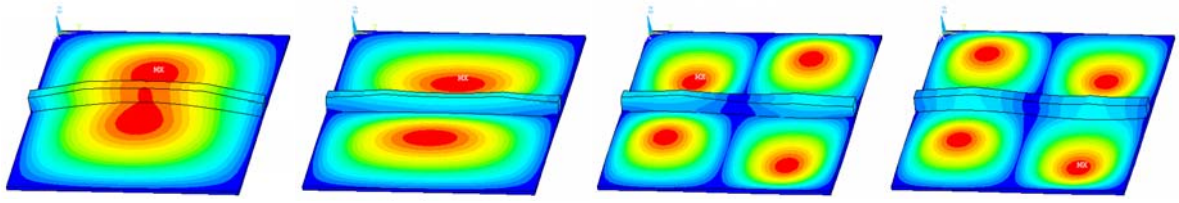

m_L=1, m_R=1 m_L=2, m_R=1 m_L=2, m_R=2 m_L=1, m_R=2

Figure 35. FEA modeshapes for the simply supported plate with scalloped brace.

7.4 Discussion

Natural frequencies for the simply supported Sitka spruce plates calculated from Equation (58) using the measured mechanical properties of Table 23 are found to correlate nicely with those measured experimentally in Table 27. Overlooking plate number 5, a distinct outlier, average errors for the simply supported plates are found to

fall well within the ranges of 1-3%, with only a few straying slightly outside. Since simply supported boundary conditions are generally known to be problematic for experimental analysis, such good correlation demonstrates the validity of the proposed experimental setup. Furthermore, the validity of the proposed non-destructive methods for experimentally measuring the mechanical properties of the plates is also demonstrated.

Comparing the experimentally-measured natural frequencies of the scalloped brace and plate system to those calculated using both the assumed shape method and the finite element method, it becomes evident that the brace introduces a certain amount of uncertainty into the problem. Although it would seem that the finite element method gives overall better results (having a maximum error of 10% compared to the maximum error of 18% provided by the assumed shaped method), it is important to remember that matrices produced by finite element methods are considerably larger than those produced by global element methods (such as the assumed shape method). Large matrices significantly increase the difficulty with which an inverse eigenvalue method, such as those presented in Chapters 4 and 5, can be applied. Furthermore, because of the limitations of each method, different approximations were made in both cases in order to build the models.

The assumed shape method assumed thin plate theory for the entire plate and brace system. The thin plate theory can be considered to be valid everywhere on the plate except at the location of the brace, were a thicker plate theory may be more appropriate. Additionally, because of the equation setup used for the analysis, the mechanical property directions of the plate had to match those of the brace at that location. Although the mechanical properties of the brace should dominate this region, this approximation may have a small impact on the results.

Since the finite element method uses three-dimensional brick elements in its solution, it was necessary to have knowledge of the material's tangential properties as well. However, these were not available. Thus, values provided by the US Forest Products Laboratory for Sitka spruce were used instead. Specifically, values added to the finite element model include: $E_T = E_L \times 0.043$, $G_{RT} = E_L \times 0.003$, $G_{LT} = E_L \times 0.061$, $\nu_{RT} = 0.435$ and

ν_{LT} = 0.467. As seen in Chapter 6, these values tend to be underestimates of the actual mechanical properties of instrument grade Sitka spruce.

Certain aspects of the actual experimental plate are unaccounted for in both theoretical models, such as small variations in the dimension of the plate or brace, grain angle variations and glue used for bonding the brace to the plate. Specifically, glue used to bond the brace increases the mass of the plate while hardly affecting its stiffness. This extra mass would exhibit itself as a decrease in the natural frequencies of the plate when compared to the theoretical models. This is the exact behaviour demonstrated by the assumed shape method. Further investigation of the effects of using glue as a bonding agent on the natural frequencies of a brace plate system would be an asset. Moreover, due to lack of precision manufacturing facilities for the brace, small variations in the scalloped-shaped brace dimensions may be present in the measured specimen. This would also have an effect on the expected results.

Finally, in all cases, the order of the modeshapes obtained experimentally exactly matched those solved using the numerical methods.

7.5 Measurement errors

Throughout the analysis, consideration was given to measurement error. Length dimensions were measured using a vernier caliper having a measurement error of ±0.02mm. Mass was measured using a scale having an error of ±0.0001g. Moisture content was measured using a pin type moisture meter having an error of ±0.1%. Force was measured using a load cell having an error of ±0.25N and displacement was measured to within ±0.02mm. Finally, the grid resistance and gauge factor of the strain gauges were stipulated to be within ±0.3% and ±0.5% respectively.

Chapter 8

Summary, Conclusions and Future Work

8.1 Summary

In this thesis, the problem of incorporating acoustical consistency into the design of manufactured wooden guitars has been considered. The problem was approached by investigating how the shape of a brace on a guitar soundboard can be modified in order to achieve a set of desired natural frequencies. Subsequently, new methods were developed in order to calculate the necessary brace dimensions based on those desired frequencies. In order to accomplish this, a vibrations approach was used. Chapter 2 developed the scalloped brace model based on the shape used by many luthiers when tuning a guitar's sound, and investigated the effect of the shape on the natural frequencies of the brace-plate system. Chapter 3 considered the effect of the scalloped-shaped brace on the modeshapes of the brace-plate system. Specifically, it demonstrated how the maximum amplitude of a modshape is affected by a localized change in mass or stiffness along the brace. Chapter 4 developed a novel inverse eigenvalue method for generalized matrices, based on the generalized Cayley-Hamilton theorem, which can be used to calculate the dimensions of a discrete system by using a set of desired eigenvalues (natural frequencies). Chapter 5 applied the proposed Cayley-Hamilton inverse eigenvalue method to the scalloped braced plate system in order to calculate the shape of the brace necessary in order to achieve the desired natural frequencies. A further method, based on the determinant of the generalized eigenvalue problem, was also developed and applied to the problem. Chapter 6 experimentally measured the mechanical properties of nine

Sitka spruce plates and then tested them under simply supported boundary conditions in order to measure their natural frequencies. Relationships between various mechanical properties were discussed and simplifications were suggested. Chapter 7 experimentally measured the natural frequencies of a plate with the addition of a scalloped brace and then compared the results to those predicted by the assumed shape method model, as well as a finite element model.

8.2 Conclusions

The analysis and experimental work set forth has laid the foundation for increasing the acoustical consistency of a guitar soundboard, generally considered the most acoustically active part of a wooden acoustic guitar. An explanation was given for the scalloped-shaped brace, which has been in use for over a century without any scientific explanation as to its purpose. Furthermore, novel inverse eigenvalue methods were developed in order to calculate the dimensions of the brace necessary in achieving the desired natural frequencies and experimental work was conducted in order to verify some assumptions and validate the results of the modeling analysis.

First, it was shown that a scalloped-shaped brace can control two natural frequencies of a brace-plate system simultaneously, giving the designer greater control of the soundboard's frequency output. During the analysis, it was also demonstrated that a local increase in mass or stiffness along the brace has the largest effect on the brace-plate system if it is located at an antinode (location of maximum amplitude) of one of the system's modeshapes. Additionally, control of a certain natural frequency can be obtained by adjusting the mass or stiffness at the location of the antinode of the associated modeshape.

Since calculating the dimensions of a brace based on desired natural frequencies was proven to be an ill-posed problem (meaning many solutions exist), it was shown that using an inverse eigenvalue method is preferred over an iterative optimization method, since the latter method only gives one solution when in fact many solutions are available to the designer. The Cayley-Hamilton method was demonstrated to work well when a system needs to be designed based on an entire frequency spectrum. However, the determinant method was shown to be more efficient for partially described problems.

Both methods were successfully applied to the calculation of the dimensions of the brace in a brace-plate system.

The experimental work verified the assumption that relationships can be used to calculate a number of wooden mechanical properties in Sitka spruce and only a few key measurements are necessary in order to establish the entire set of properties required to do a frequency analysis of the plates. Moreover, it was demonstrated that it is possible to experimentally measure the natural frequencies of simply supported rectangular plates, long considered to be difficult. To do so, an experimental setup was designed and built to account for dimensional variations in the plates and to allow the plates to rotate about their line edge while accommodating for span shortening during vibration. Finally, due to the complexity increase by adding the scalloped-shaped brace to the plate, accuracy of both the assumed shape and finite element models was reduced when compared with experimental results. It is important to note that although the finite element method did perform slightly better than the assumed shape method, the discrete solution matrices obtained by the finite element method are significantly larger than those created by a global element method. This significantly increases the difficulty with which the inverse eigenvalue problem can be solved, but without giving the designer any additional solutions which would be considered physically valid.

While much work still needs to be done in order to implement a system into the design of wooden guitar soundboards, overall the work in this thesis lays the foundation and shows promising results for incorporating acoustical consistency into the manufacturing process.

8.3 Recommendations for Future Work

Although the inverse eigenvalue methods proposed in this thesis give exact solutions, these solutions are based on the forward model used to discretize the physical system. Therefore, it would be important to improve on the accuracy of the forward analytical model by incorporating aspects of the physical model which have otherwise been neglected. These include shear deformation and rotary inertia effects, the mass of the air surrounding the braced plate, damping and the addition of glue as the bonding agent between the brace and the plate. In particular, damping seems to have a large effect on

the perceived timbre of the instrument. Therefore, it would be important to study the impact that damping has on the frequencies considered. A study on the best approach to modeling vibratory systems via global element methods should also be performed in order to minimize the size of the mass and stiffness matrices used during the analysis. Furthermore, in order to incorporate this approach into a manufacturing process, it would be necessary to increase the number of braces and dimensions of the plate in order to more accurately reflect the actual soundboard system.

In order to improve the accuracy of the experimental results, it would be important to improve the precision with which the brace is carved into its scalloped-shape. Further investigation of the simply supported experimental setup for measuring natural frequencies should also be performed in order to verify its limitations.

Finally, a study regarding the effects of changes in the mechanical properties and dimensions of the soundboard on the acoustic properties of the instrument's radiated sound should be performed in order to evaluate the necessary accuracy requirements.

Appendix A

Maple Code for the Assumed Shape Method Scalloped Braced-Plate Model

Model

$with(LinearAlgebra)$:

Assumed Shape

$m_1 := 6$

$m_2 := 6$

$\phi_{n_1, n_2} := \sin\left(n_1 \cdot \pi \cdot \frac{x}{Lx}\right) \cdot \sin\left(n_2 \cdot \pi \cdot \frac{y}{Ly}\right)$ $w_o := \sum_{n_1=1}^{m_1} \sum_{n_2=1}^{m_2} \phi_{n_1, n_2} \cdot q_{n_1, n_2}(t)$

$w_d := \dot{w}_o$

$w_x := \frac{\partial}{\partial x} w_o$

$w_y := \frac{\partial}{\partial y} w_o$

$w_{xx} := \frac{\partial^2}{\partial x^2} w_o$

$w_{yy} := \frac{\partial^2}{\partial y^2} w_o$

$w_{xy} := \frac{\partial}{\partial x} \frac{\partial}{\partial y} w_o$

Properties

$c := c$

$h_b := hb$

$Ly := 0.186512$

$Lx := 0.245923$

$Lb := 0.0119$

$r_1 := \frac{Lx}{2} - \frac{Lb}{2}$

$r_2 := r_1 + Lb$

$h_p := 0.00326$

$\mu 1 := 387.26$

$\rho_1 := \mu 1 \cdot h_p$

$Ey1 := 962.83e6$

$Ex1 := 12727.46e6$

$Gxy1 := 653.60e6$

$\nu xy1 := 0.352$

$\nu yx1 := 0.036$

$Sxx1 := \frac{Ex1}{1 - \nu xy1 \cdot \nu yx1}$

$Syy1 := \frac{Ey1}{1 - \nu xy1 \cdot \nu yx1}$

$Sxy1 := \frac{\nu yx1 \cdot Ex1}{1 - \nu xy1 \cdot \nu yx1}$

$dx1 := \frac{Sxx1 \cdot h_p^3}{12}$

$dy1 := \frac{Syy1 \cdot h_p^3}{12}$

$d11 := \frac{Sxy1 \cdot h_p^3}{12}$

$dxy1 := \frac{Gxy1 \cdot h_p^3}{12}$

$Ey2 := 5995.73e6$

$Ex2 := 0.066 \cdot Ey2$

$Gyx2 := 0.057 \cdot Ey2$

$\nu yx2 := 0.394$

$\nu xy2 := 0.042$

$\mu 2 := 467.43$

$$Syy2 := \frac{Ey2}{1 - \nu xy2 \cdot \nu yx2}$$

$$Sxx2 := \frac{Ex2}{1 - \nu xy2 \cdot \nu yx2}$$

$$Sxy2 := \frac{\nu yx2 \cdot Ex2}{1 - \nu xy2 \cdot \nu yx2}$$

Brace

$$y1 := \frac{Ly}{4}$$

$$y2 := \frac{3 \cdot Ly}{4}$$

$$h_{y1} := c \cdot y^2 + h_b + h_p$$

$$h_{y2} := c \cdot \left(y - \frac{Ly}{2} \right)^2 + h_b + h_p$$

$$h_{y3} := c \cdot (y - Ly)^2 + h_b + h_p$$

$$\rho_{y1} := \mu 2 \cdot h_{y1}$$

$$\rho_{y2} := \mu 2 \cdot h_{y2}$$

$$\rho_{y3} := \mu 2 \cdot h_{y3}$$

$$dy21 := \frac{Syy2 \cdot h_{y1}^3}{12}$$

$$dx21 := \frac{Sxx2 \cdot h_{y1}^3}{12}$$

$$d121 := \frac{Sxy2 \cdot h_{y1}^3}{12}$$

$$dxy21 := \frac{Gyx2 \cdot h_{y1}^3}{12}$$

$$dy22 := \frac{Syy2 \cdot h_{y2}^3}{12}$$

$$dx22 := \frac{Sxx2 \cdot h_{y2}^3}{12}$$

$$d122 := \frac{Sxy2 \cdot h_{y2}^3}{12}$$

$$dxy22 := \frac{Gyx2 \cdot h_{y2}^3}{12}$$

$$dy23 := \frac{Syy2 \cdot h_{y3}^3}{12}$$

$$dx23 := \frac{Sxx2 \cdot h_{y3}^3}{12}$$

$$d123 := \frac{Sxy2 \cdot h_{y3}^3}{12}$$

$$dxy23 := \frac{Gyx2 \cdot h_{y3}^3}{12}$$

Kinetic Energy

$$T := \frac{1}{2}\int_0^{r_1}\int_0^{Ly} w_d^2 \cdot \rho_1 \, dy dx + \frac{1}{2}\int_{r_1}^{r_2}\int_0^{y1} w_d^2 \cdot \rho_{y1} \, dy dx + \frac{1}{2}\int_{r_1}^{r_2}\int_{y1}^{y2} w_d^2 \cdot \rho_{y2} \, dy dx + \frac{1}{2}\int_{r_1}^{r_2}\int_{y2}^{Ly} w_d^2$$

$$\cdot \rho_{y3} \, dy dx + \frac{1}{2}\int_{r_2}^{Lx}\int_0^{Ly} w_d^2 \cdot \rho_1 \, dy dx$$

Mass Matrix

$$Q_d := Vector\left(1..m_1 \cdot m_2\right) :$$

$k := 0$:;
for i **from** 1 **by** 1 **to** m_1 **do**
for j **from** 1 **by** 1 **to** m_2 **do**
$k := k + 1$;
$Q_d[k] := \dot{q}_{i,j}(t)$;
$T := subs\left(Q_d[k] = p_k, T\right)$;
end do;
end do;

$k := 0$:;
for i **from** 1 **by** 1 **to** m_1 **do**
for j **from** 1 **by** 1 **to** m_2 **do**
$k := k + 1$;
$g_k := \frac{\partial}{\partial p_k} T$;
end do;
end do;

$$G := \left[seq\left(g_k, k = 1 .. m_1 \cdot m_2 \right) \right]$$

$$P := \left[seq\left(p_k, k = 1 .. m_1 \cdot m_2 \right) \right]$$

$$M, Z := GenerateMatrix\left(G, P \right)$$

Potential Energy

$$V := \frac{1}{2}\int_0^{r_1}\int_0^{Ly} \left(dx1 \cdot w_{xx}^2 + dy1 \cdot w_{yy}^2 + 4 \cdot dxy1 \cdot w_{xy}^2 + 2 \cdot d11 \cdot w_{xx} \cdot w_{yy} \right) \mathrm{d}y\mathrm{d}x + \frac{1}{2}\int_{r_1}^{r_2} \int_0^{y1} \left(dx21 \cdot w_{xx}^2 + dy21 \cdot w_{yy}^2 + 4 \cdot dxy21 \cdot w_{xy}^2 + 2 \cdot d121 \cdot w_{xx} \cdot w_{yy} \right) \mathrm{d}y\mathrm{d}x + \frac{1}{2}\int_{r_1}^{r_2}\int_{y1}^{y2} \left(dx22 \cdot w_{xx}^2 + dy22 \cdot w_{yy}^2 + 4 \cdot dxy22 \cdot w_{xy}^2 + 2 \cdot d122 \cdot w_{xx} \cdot w_{yy} \right) \mathrm{d}y\mathrm{d}x + \frac{1}{2}\int_{r_1}^{r_2}\int_{y2}^{Ly} \left(dx23 \cdot w_{xx}^2 + dy23 \cdot w_{yy}^2 + 4 \cdot dxy23 \cdot w_{xy}^2 + 2 \cdot d123 \cdot w_{xx} \cdot w_{yy} \right) \mathrm{d}y\mathrm{d}x + \frac{1}{2}\int_{r_2}^{Lx}\int_0^{Ly} \left(dx1 \cdot w_{xx}^2 + dy1 \cdot w_{yy}^2 + 4 \cdot dxy1 \cdot w_{xy}^2 + 2 \cdot d11 \cdot w_{xx} \cdot w_{yy} \right) \mathrm{d}y\mathrm{d}x$$

Stiffness Matrix

$$Q_o := Vector\left(1 .. m_1 \cdot m_2 \right) :$$

$k := 0$:;
for i **from** 1 **by** 1 **to** m_1 **do**
for j **from** 1 **by** 1 **to** m_2 **do**
$k := k + 1$;
$Q_o[k] := q_{i,j}(t)$;
$V := subs\left(Q_o[k] = p_k, V \right)$;
end do;
end do;

$k := 0$:;
for i **from** 1 **by** 1 **to** m_1 **do**
for j **from** 1 **by** 1 **to** m_2 **do**
$k := k + 1$;
$g_k := \frac{\partial}{\partial p_k} V$;
end do;
end do;

$$G := \left[seq\left(g_k, k = 1 .. m_1 \cdot m_2 \right) \right]$$

$$P := \left[seq\left(p_k, k = 1 .. m_1 \cdot m_2 \right) \right]$$

$$K, Z := GenerateMatrix\left(G, P \right)$$

save M, K, "M_K_matrices_scalloped.m"

Numerical Solutions

Natural Frequencies

$M2 := evalf(M)$

$K2 := evalf(K)$

$\lambda, A := Eigenvectors(K2, M2)$:

$\lambda := \Re(\lambda)$

$A := \Re(A)$

$\omega := map(\mathrm{sqrt}, \lambda)$

$\omega 2 := evalf\left(\frac{\omega}{2 \cdot \pi}\right)$

Plots

$\Phi := Vector(1..m_1 \cdot m_2)$:

$U := Vector(1..m_1 \cdot m_2)$:

$\psi 2 := Vector(1..m_1 \cdot m_2)$:

for l **from** 1 **by** 1 **to** $m_1 \cdot m_2$ **do**
$k := 0$;
for n_1 **from** 1 **by** 1 **to** m_1 **do**
for n_2 **from** 1 **by** 1 **to** m_2 **do**
$k := k + 1$;
$\Phi[k] := \sin\left(n_1 \cdot \pi \cdot \frac{x}{Lx}\right) \cdot \sin\left(n_2 \cdot \pi \cdot \frac{y}{Ly}\right)$;
$U[k] := A[k, l]$;
end do;
end do;
$\psi 2[l] := \psi[l] = U^{+} . \Phi$;
end do:;

$with(plots)$:

for l **from** 1 **by** 1 **to** $m_1 \cdot m_2$ **do**
$implicitplot3d(\psi 2[l], x = 0..Lx, y = 0..Ly, \psi[l] = -2..2, title = convert(Natural\ Frequency = \omega 2[l], string), titlefont = [TIMES, 12], axes = boxed, orientation = [134, 45])$
end do;

Appendix B

Maple Code for the Cayley-Hamilton Inverse Eigenvalue Method

Matrices

$with(LinearAlgebra):$

read "M_K_matrices_scalloped.m"

Calculate the Cayley-Hamilton Theorem

$$p := expand\left((\lambda - 1.514)\cdot(\lambda - 5.049)\cdot(\lambda - b1)\cdot(\lambda - b2)\cdot(\lambda - b3)\cdot(\lambda - b4)\cdot(\lambda - b5)\cdot(\lambda - b6)\cdot(\lambda - b7)\right)$$

$$I2 := \begin{bmatrix} 1 & 0 & 0 & 0 & 0 & 0 & 0 & 0 & 0 & 0 \\ 0 & 1 & 0 & 0 & 0 & 0 & 0 & 0 & 0 & 0 \\ 0 & 0 & 1 & 0 & 0 & 0 & 0 & 0 & 0 & 0 \\ 0 & 0 & 0 & 1 & 0 & 0 & 0 & 0 & 0 & 0 \\ 0 & 0 & 0 & 0 & 1 & 0 & 0 & 0 & 0 & 0 \\ 0 & 0 & 0 & 0 & 0 & 1 & 0 & 0 & 0 & 0 \\ 0 & 0 & 0 & 0 & 0 & 0 & 1 & 0 & 0 & 0 \\ 0 & 0 & 0 & 0 & 0 & 0 & 0 & 1 & 0 & 0 \\ 0 & 0 & 0 & 0 & 0 & 0 & 0 & 0 & 1 & 0 \\ 0 & 0 & 0 & 0 & 0 & 0 & 0 & 0 & 0 & 1 \end{bmatrix}$$

$$C := coeff(p, \lambda, 9) \cdot (M^{-1}.K)^9 + coeff(p, \lambda, 8) \cdot (M^{-1}.K)^8 + coeff(p, \lambda, 7) \cdot (M^{-1}.K)^7 + coeff(p, \lambda, 6) \cdot (M^{-1}.K)^6 + coeff(p, \lambda, 5) \cdot (M^{-1}.K)^5 + coeff(p, \lambda, 4) \cdot (M^{-1}.K)^4 + coeff(p, \lambda, 3) \cdot (M^{-1}.K)^3 + coeff(p, \lambda, 2) \cdot (M^{-1}.K)^2 + coeff(p, \lambda, 1) \cdot (M^{-1}.K) + coeff(p, \lambda, 0) \cdot I2$$

Solve

$with(DirectSearch):$

$$E := SolveEquations\left(\left[C_{1,1}, C_{2,2}, C_{3,3}, C_{4,4}, C_{5,5}, C_{6,6}, C_{7,7}, C_{8,8}, C_{9,9}\right], \{c = -0.4..2.2, hb = 0.011..0.013, b1 = 2.5..2.8, b2 = 6.6..7.7, b3 = 7.4..8.3, b4 = 9.3..9.9, b5 = 18..20, b6 = 50..62, b7 = 230..260\}, AllSolutions\right)$$

$$c1 := rhs\left(E_{3,8}\right); hb1 := rhs\left(E_{3,9}\right);$$

$$E2 := fsolve\left(\left[C_{1,1}, C_{2,2}, C_{3,3}, C_{4,4}, C_{5,5}, C_{6,6}, C_{7,7}, C_{8,8}, C_{9,9}\right], \{c = -0.4..2.2, hb = 0.011..0.013, b1 = 2.5..2.8, b2 = 6.6..7.7, b3 = 7.4..8.3, b4 = 9.3..9.9, b5 = 18..20, b6 = 50..62, b7 = 230..260\}\right)$$

$$c2 := rhs\left(E2_1\right); hb2 := rhs\left(E2_2\right);$$

$$c := c1$$

$$hb := hb1$$

Verify Solution

$$\lambda, A := Eigenvectors(K, M):$$

$$\lambda := |\Re(\lambda)| \cdot 10^7$$

$$\omega := evalf\left(\frac{map(\mathrm{sqrt}, \lambda)}{2 \cdot \pi}\right)$$

Appendix C

Maple Code for the Determinant Inverse Eigenvalue Method

Matrices

$with(LinearAlgebra)$:

read "M_K_matrices_scalloped.m"

Calculate the Determinant

$P := Determinant(K - \lambda \cdot M)$:

$p1 := subs(\lambda = 1.514, P)$

$p2 := subs(\lambda = 5.049, P)$

Solve

$with(DirectSearch)$:

$e := SolveEquations([p1, p2], \{c = -0.4..2.2, hb = 0.011..0.013\}, AllSolutions)$

$E := e_{2,3}$

$c1 := rhs(E_1)$; $hb1 := rhs(E_2)$;

$E2 := fsolve([p1, p2], \{c = -0.4..2.2, hb = 0.011..0.013\})$

$c2 := rhs(E2_1)$; $hb2 := rhs(E2_2)$;

$c := c1$

$hb := hb1$

Verify Solution

$$\lambda, A := Eigenvectors(K, M):$$

$$\lambda := |\Re(\lambda)| \cdot 10^{7}$$

$$\omega := evalf\left(\frac{map(\mathrm{sqrt}, \lambda)}{2 \cdot \pi}\right)$$

Appendix D

ANSYS Code for the Finite Element Method Scalloped Braced-Plate Model

```
/prep7

!Variables
c1=1
lx=0.245923
ly=0.186512
lb=0.0119
hp=0.00326
hb=0.011
offset=hp/2
h2=hp+hb
r1=lx/2-lb/2
r2=lx/2+lb/2
ep=12727.46e6
eb=5995.73e6
divpm=8
divpx=20
divpy=40
divse=10
divsm=20

!Keypoints
k,1,0,0,-offset
k,2,r1,0,-offset
k,3,r2,0,-offset
k,4,lx,0,-offset
k,5,lx,0,hp-offset
k,6,r2,0,hp-offset
k,7,r1,0,hp-offset
k,8,0,0,hp-offset
k,9,r1,0,h2-offset
k,10,0,ly,-offset
k,11,r1,ly/12,c1*(ly/12)**2+h2-offset
k,12,r1,2*ly/12,c1*(2*ly/12)**2+h2-
offset
k,13,r1,ly/4,c1*(ly/4)**2+h2-offset
k,14,r1,7*ly/20,c1*(7*ly/20-
ly/2)**2+h2-offset
k,15,r1,9*ly/20,c1*(9*ly/20-
ly/2)**2+h2-offset
k,16,r1,11*ly/20,c1*(11*ly/20-
ly/2)**2+h2-offset
k,17,r1,13*ly/20,c1*(13*ly/20-
ly/2)**2+h2-offset
k,18,r1,3*ly/4,c1*(3*ly/4-ly)**2+h2-
offset
k,19,r1,10*ly/12,c1*(10*ly/12-
ly)**2+h2-offset
k,20,r1,11*ly/12,c1*(11*ly/12-
ly)**2+h2-offset
k,21,r1,ly,h2-offset
k,22,r1,ly,hp-offset
k,23,r1,3*ly/4,hp-offset
k,24,r1,ly/4,hp-offset
```

```
!Lines
lstr,1,2
lstr,2,3
lstr,3,4
lstr,4,5
lstr,5,6
lstr,6,7
lstr,7,8
lstr,8,1
lstr,2,7
lstr,3,6
lstr,9,7
lstr,7,24
lstr,24,23
lstr,23,22
lstr,22,21
bsplin,21,20,19,18
bsplin,18,17,16,15,14,13
bsplin,13,12,11,9
lstr,13,24
lstr,18,23
lstr,1,10

!Areas
al,8,1,9,7
al,9,2,10,6
al,10,3,4,5
al,11,12,19,18
al,19,13,20,17
al,20,14,15,16

!Number of elements
lesize,1,,,divpx
lesize,3,,,divpx
lesize,5,,,divpx
lesize,7,,,divpx
lesize,8,,,divpm
lesize,9,,,divpm
lesize,10,,,divpm
lesize,4,,,divpm
lesize,2,,,divpm
lesize,6,,,divpm
lesize,11,,,divpm
lesize,19,,,divpm
lesize,20,,,divpm
lesize,15,,,divpm
lesize,12,,,divse
lesize,13,,,divsm
lesize,14,,,divse
lesize,16,,,divse
lesize,17,,,divsm
lesize,18,,,divse
lesize,21,,,divpy

!Element type
et,1,solid45

!Material Properties of the plate
mp,ex,1,ep
mp,ey,1,962.83e6
mp,ez,1,ep*0.043
mp,gxy,1,653.60e6
mp,gyz,1,ep*0.003
mp,gxz,1,ep*0.061
mp,prxy,1,0.352
mp,pryz,1,0.435
mp,prxz,1,0.467
mp,dens,1,387.26
mat,1
!Make plate 3D
vdrag,1,2,3,,,,21

!Mesh Plate
vmesh,1,3,1

!Material Properties of the brace
mp,ex,2,eb*0.066
mp,ey,2,eb
mp,ez,2,eb*0.043
mp,gxy,2,eb*0.057
mp,gyz,2,eb*0.061
mp,gxz,2,eb*0.003
mp,prxy,2,0.042
mp,pryz,2,0.467
mp,prxz,2,0.435
mp,dens,2,467.43
mat,2
!Make brace 3D
vdrag,4,5,6,,,,6

!Mesh brace
```

```
vmesh,4,6,1

!Coincide node between the plate and
brace
nummrg,node

!Select nodes for boundary conditions
aclear,1,6,1

asel,s,area,,1
asel,a,area,,2
asel,a,area,,3
asel,a,area,,7
asel,a,area,,11
asel,a,area,,15
asel,a,area,,19
asel,a,area,,17
nsla,s,1
nsel,r,loc,z,-0.0001,0.0001
!Boundary conditions
d,all,ux,0
d,all,uy,0
d,all,uz,0

allsel

/PNUM,area,1

!Modal solution
finish
/solu
antype,modal
modopt,lanb,6,0,3000

solve
```

References

[1] Forest Products Laboratory (US), "Wood Handbook, Wood as an Engineering Material," Madison, WI: U.S. Department of Agriculture, Forest Service, 1999, pp. 4.1–13.

[2] Canadian Wood Council, *Wood Design Manual 2010*. Ottawa, ON: Canadian Wood Council, 2010.

[3] R. H. Siminoff, *The Luthier's Handbook: A Guide to Building Great Tone in Acoustic Stringed Instruments*. Milwaukee, WI: Hal Leonard, 2002.

[4] R. B. Hoadley, *Understanding Wood*. Taunton Press, 2000.

[5] P. Dumond, "Towards Improving the Manufactured Consistency of Wooden Musical Instruments through Frequency Matching," Master of Applied Science, University of Ottawa, Ottawa, Canada, 2010.

[6] R. M. French, "Engineering the Guitar: Theory and Practice," in *Engineering the Guitar: Theory and Practice*, 1st ed., New York: Springer, 2008, pp. 159–208.

[7] R. H. Siminoff, *Art of Tap Tuning How to Build Great Sound into Instruments Book*. Milwaukee, WI: Hal Leonard, 2002.

[8] R. Godin, "Godin Guitars Factory Visit, Princeville, QC, Canada," 22-Oct-2007.

[9] G. Caldersmith, "Designing a guitar family," *Applied Acoustics*, vol. 46, no. 1, pp. 3–17, 1995.

[10] E. Jansson, "A Study of Acoustical and Hologram Interferometric Measurements of Top Plate Vibrations of a Guitar," *Acustica*, vol. 25, no. 2, pp. 95–100, 1971.

[11] K. Stetson, "On modal coupling in string instrument bodies," *Journal of Guitar Acoustics*, vol. 3, pp. 23–29, 1981.

[12] I. M. Firth, "Physics of the guitar at the Helmholtz and first top-plate resonances," *J. Acoust. Soc. Am.*, vol. 61, no. 2, pp. 588–593, Feb. 1977.

[13] B. E. Richardson, “Guitar Making - The Acoustician’s Tale,” in *Proceedings of the Second Vienna Talk*, Vienna, Austria, 2010, pp. 125–128.

[14] J. O. Jovicic, “Le role des barres de raidissement sur la table de resonance de la guitare: II. Leur effet sur les nodales de la table (etude holographique),” *Acustica*, vol. 38, pp. 15–16, 1977.

[15] M. Brooke and B. E. Richardson, “Mechanical vibrations and radiation fields of guitars,” *J. Acoust. Soc. Am.*, vol. 94, no. 3, p. 1806, 1993.

[16] M. Brooke and B. E. Richardson, “Numerical modeling of guitar radiation fields using boundary elements,” *J. Acoust. Soc. Am.*, vol. 89, no. 4B, p. 1878, Apr. 1991.

[17] J. C. S. Lai and M. A. Burgess, “Radiation efficiency of acoustic guitars,” *J. Acoust. Soc. Am.*, vol. 88, no. 3, pp. 1222–1227, 1990.

[18] T. Hill, B. Richardson, and S. Richardson, “Acoustical Parameters for the Characterisation of the Classical Guitar,” *Acta Acustica united with Acustica*, vol. 90, no. 2, pp. 335–348, 2004.

[19] B. E. Richardson, “Classical guitar construction: The acoustician’s tale,” *The Journal of the Acoustical Society of America*, vol. 117, no. 4, p. 2589, Apr. 2005.

[20] V. . Howle and L. N. Trefethen, “Eigenvalues and musical instruments,” *Journal of Computational and Applied Mathematics*, vol. 135, no. 1, pp. 23–40, Oct. 2001.

[21] M. J. Elejabarrieta, A. Ezcurra, and C. Santamaría, “Evolution of the vibrational behavior of a guitar soundboard along successive construction phases by means of the modal analysis technique,” *J. Acoust. Soc. Am.*, vol. 108, no. 1, p. 369, 2000.

[22] M. J. Elejabarrieta, A. Ezcurra, and C. Santamaría, “Vibrational behaviour of the guitar soundboard analysed by the finite element method,” *Acta Acustica united with Acustica*, vol. 87, no. 1, pp. 128–136, 2001.

[23] M. J. Elejabarrieta, C. Santamaria, and A. Excurra, “Air Cavity Modes in the Resonance Box of the Guitar: the Effect of the Sound Hole,” *Journal of Sound and Vibration*, vol. 252, no. 3, pp. 584–590, May 2002.

[24] M. J. Elejabarrieta, A. Ezcurra, and C. Santamaria, “Coupled modes of the resonance box of the guitar,” *J. Acoust. Soc. Am.*, vol. 111, no. 5, pp. 2283–2292, May 2002.

[25] A. Ezcurra, M. Elejabarrieta, and C. Santamaria, “Fluid-structure coupling in the guitar box: numerical and experimental comparative study,” *Applied Acoustics*, vol. 66, no. 4, pp. 411–425, Apr. 2005.

[26] R. R. Boullosa, “Vibration measurements in the classical guitar,” *Applied Acoustics*, vol. 63, no. 3, pp. 311–322, Mar. 2002.

[27] R. R. Boullosa, F. Orduña-Bustamante, and A. Pérez López, “Tuning characteristics, radiation efficiency and subjective quality of a set of classical guitars,” *Applied Acoustics*, vol. 56, no. 3, pp. 183–197, Mar. 1999.

[28] J. A. Torres and R. R. Boullosa, “Influence of the bridge on the vibrations of the top plate of a classical guitar,” *Applied Acoustics*, vol. 70, no. 11–12, pp. 1371–1377, Dec. 2009.

[29] A. Chaigne, “Recent advances in vibration and radiation of musical instruments,” *Flow, Turbulence and Combustion*, vol. 61, pp. 31–34, 1999.

[30] E. Bécache, A. Chaigne, G. Derveaux, and P. Joly, “Numerical simulation of a guitar,” *Computers & Structures*, vol. 83, no. 2–3, pp. 107–126, Jan. 2005.

[31] G. Derveaux, A. Chaigne, P. Joly, and E. Becache, “Time-domain simulation of a guitar: Model and method,” *J. Acoust. Soc. Am.*, vol. 114, no. 6, pp. 3368–3383, Dec. 2003.

[32] T. Rossing, *The Science of String Instruments*. Springer Science & Business Media, 2010.

[33] D. W. Fox and V. G. Sigillito, “Bounds for frequencies of rib reinforced plates,” *Journal of Sound and Vibration*, vol. 69, no. 4, pp. 497–507, Apr. 1980.

[34] M. Barrette, A. Berry, and O. Beslin, “Vibration of Stiffened Plates Using Hierarchical Trigonometric Functions,” *Journal of Sound and Vibration*, vol. 235, no. 5, pp. 727–747, Aug. 2000.

[35] L. X. Peng, K. M. Liew, and S. Kitipornchai, “Buckling and free vibration analyses of stiffened plates using the FSDT mesh-free method,” *Journal of Sound and Vibration*, vol. 289, no. 3, pp. 421–449, Jan. 2006.

[36] S. B. Hong, A. Wang, and N. Vlahopoulos, “A hybrid finite element formulation for a beam-plate system,” *Journal of Sound and Vibration*, vol. 298, no. 1–2, pp. 233–256, Nov. 2006.

[37] G. Aksu and R. Ali, “Free vibration analysis of stiffened plates using finite difference method,” *Journal of Sound and Vibration*, vol. 48, no. 1, pp. 15–25, Sep. 1976.

[38] H. Zeng and C. W. Bert, “A differential quadrature analysis of vibration for rectangular stiffened plates,” *Journal of Sound and Vibration*, vol. 241, no. 2, pp. 247–252, 2001.

[39] P. S. Nair and M. S. Rao, “On vibration of plates with varying stiffener length,” *Journal of Sound and Vibration*, vol. 95, no. 1, pp. 19–29, Jul. 1984.

[40] M. Barik and M. Mukhopadhyay, “Free Flexural Vibration Analysis of Arbitrary Plates With Arbitrary Stiffeners,” *Journal of Vibration and Control*, vol. 5, no. 5, pp. 667–683, Sep. 1999.

[41] B. P. Shastry and G. V. Rao, “Vibrations of thin rectangular plates with arbitrarily oriented stiffeners,” *Computers & Structures*, vol. 7, no. 5, pp. 627–629, Oct. 1977.

[42] H. Xu, J. Du, and W. L. Li, “Vibrations of rectangular plates reinforced by any number of beams of arbitrary lengths and placement angles,” *Journal of Sound and Vibration*, vol. 329, no. 18, pp. 3759–3779, Aug. 2010.

[43] L. Dozio and M. Ricciardi, “Free vibration analysis of ribbed plates by a combined analytical–numerical method,” *Journal of Sound and Vibration*, vol. 319, no. 1–2, pp. 681–697, Jan. 2009.

[44] M. Amabili, “Nonlinear vibrations of rectangular plates with different boundary conditions: theory and experiments,” *Computers & Structures*, vol. 82, no. 31–32, pp. 2587–2605, Dec. 2004.

[45] M. Amabili, “Theory and experiments for large-amplitude vibrations of rectangular plates with geometric imperfections,” *Journal of Sound and Vibration*, vol. 291, no. 3–5, pp. 539–565, Apr. 2006.

[46] F. Orduna-Bustamante, “Nonuniform beams with harmonically related overtones for use in percussion instruments,” *J. Acoust. Soc. Am.*, vol. 90, no. 6, pp. 2935–2941, Dec. 1991.

[47] K. Chadan, *An Introduction to Inverse Scattering and Inverse Spectral Problems*. SIAM, 1997.

[48] I. M. Gel'fand and B. M. Levitan, "On the determination of a differential equation from its spectral function," *Izv. Akad. Nauk SSSR Ser. Mat.*, vol. 15, no. 4, pp. 309–360, 1951.

[49] F. R. Gantmakher and M. G. Kreĭn, *Oscillation Matrices and Kernels and Small Vibrations of Mechanical Systems*. Providence, RI: American Mathematical Soc., 2002.

[50] M. T. Chu, "Inverse eigenvalue problems," *SIAM Rev*, vol. 40, pp. 1–39, 1998.

[51] M. T. Chu and G. H. Golub, *Inverse Eigenvalue Problems: Theory, Algorithms, and Applications*. Oxford University Press, USA, 2005.

[52] G. M. L. Gladwell, *Inverse problems in vibration*. Kluwer Academic Publishers, 2004.

[53] H. Hochstadt, "On some inverse problems in matrix theory," *Archiv der Mathematik*, vol. 18, no. 2, pp. 201–207, 1967.

[54] O. H. Hald, "Inverse eigenvalue problems for Jacobi matrices," *Linear Algebra and its Applications*, vol. 14, no. 1, pp. 63–85, 1976.

[55] D. Boley and G. Golub, "Inverse eigenvalue problems for band matrices," in *Numerical Analysis*, vol. 630, G. Watson, Ed. Springer Berlin / Heidelberg, 1978, pp. 23–31.

[56] C. de Boor and E. B. Saff, "Finite sequences of orthogonal polynomials connected by a Jacobi matrix," *Linear Algebra and its Applications*, vol. 75, pp. 43–55, Mar. 1986.

[57] G. M. L. Gladwell, "The Inverse Problem for the Vibrating Beam," *Proc. R. Soc. Lond. A*, vol. 393, no. 1805, pp. 277–295, Jun. 1984.

[58] M. T. Chu, "Numerical Methods for Inverse Singular Value Problems," *SIAM Journal on Numerical Analysis*, vol. 29, no. 3, pp. 885–903, Jun. 1992.

[59] S. Friedland, J. Nocedal, and M. L. Overton, "The Formulation and Analysis of Numerical Methods for Inverse Eigenvalue Problems," *SIAM Journal on Numerical Analysis*, vol. 24, no. 3, pp. pp. 634–667, 1987.

[60] P. Morel, "Des algorithmes pour le problème inverse des valeurs propres," *Linear Algebra and its Applications*, vol. 13, no. 3, pp. 251–273, 1976.

[61] Z. Bohte, “Numerical Solution of the Inverse Algebraic Eigenvalue Problem,” *The Computer Journal*, vol. 10, no. 4, pp. 385–388, Feb. 1968.

[62] V. Pereyra, A. Reinoza, J. Nocedal, and M. Overton, “Numerical methods for solving inverse eigenvalue problems,” in *Numerical Methods*, vol. 1005, Springer Berlin / Heidelberg, 1983, pp. 212–226.

[63] A. C. Downing,Jr. and A. S. Householder, “Some Inverse Characteristic Value Problems,” *J. ACM*, vol. 3, no. 3, pp. 203–207, Jul. 1956.

[64] J. A. Dias da Silva, “On the multiplicative inverse eigenvalue problem,” *Linear Algebra and its Applications*, vol. 78, pp. 133–145, Jun. 1986.

[65] G. N. de Oliveira, “On the multiplicative inverse eigenvalue problem,” in *Canadian Mathematical Bulletin*, Montreal, QC: Canadian Mathematical Society, 1972.

[66] C. de Boor and G. H. Golub, “The numerically stable reconstruction of a Jacobi matrix from spectral data,” *Linear Algebra and its Applications*, vol. 21, no. 3, pp. 245–260, Sep. 1978.

[67] R. Erra and B. Philippe, “On some structured inverse eigenvalue problems,” *Numerical Algorithms*, vol. 15, no. 1, pp. 15–35, 1997.

[68] F. W. Biegler-König, “Construction of band matrices from spectral data,” *Linear Algebra and its Applications*, vol. 40, pp. 79–87, Oct. 1981.

[69] D. Boley and G. H. Golub, “A survey of matrix inverse eigenvalue problems,” *Inverse Problems*, vol. 3, no. 4, p. 595, 1987.

[70] M. T. Chu and J. L. Watterson, “On a Multivariate Eigenvalue Problem: I. Algebraic Theory and a Power Method,” *SIAM J. Sci. Comput.*, vol. 14, pp. 1089–1106, 1993.

[71] X. Chen and M. T. Chu, “On the Least Squares Solution of Inverse Eigenvalue Problems,” *SIAM Journal on Numerical Analysis*, vol. 33, no. 6, pp. 2417–2430, Dec. 1996.

[72] G. M. L. Gladwell and N. B. Willms, “A discrete Gel’fand-Levitan method for band-matrix inverse eigenvalue problems,” *Inverse Problems*, vol. 5, no. 2, pp. 165–179, Apr. 1989.

[73] Y. M. Ram and S. Elhay, “An Inverse Eigenvalue Problem for the Symmetric Tridiagonal Quadratic Pencil with Application to Damped Oscillatory Systems,” *SIAM Journal on Applied Mathematics*, vol. 56, no. 1, pp. 232–244, Feb. 1996.

[74] G. H. Golub and R. R. Underwood, “The block Lanczos method for computing eigenvalues,” in *Mathematical Software III*, J.R. Rice., New York: Springer, 1977.

[75] F. W. Biegler-König, “A Newton iteration process for inverse eigenvalue problems,” *Numerische Mathematik*, vol. 37, no. 3, pp. 349–354, 1981.

[76] W. B. Gragg and W. J. Harrod, “The numerically stable reconstruction of Jacobi matrices from spectral data,” *Numerische Mathematik*, vol. 44, no. 3, pp. 317–335, 1984.

[77] G. M. L. Gladwell, “The application of Schur’s algorithm to an inverse eigenvalue problem,” *Inverse Problems*, vol. 7, no. 4, pp. 557–565, Aug. 1991.

[78] M. T. Chu, “A Fast Recursive Algorithm for Constructing Matrices with Prescribed Eigenvalues and Singular Values,” *SIAM Journal on Numerical Analysis*, vol. 37, no. 3, pp. 1004–1020, Jan. 2000.

[79] C. A. Floudas and P. Pardalos, *Encyclopedia of Optimization*, 2nd ed. 2009.

[80] J. Natelson and W. Cumpiano, *Guitarmaking: Tradition and Technology: A Complete Reference for the Design & Construction of the Steel-String Folk Guitar & the Classical Guitar*. San Francisco, CA: Chronicle Books, 1994.

[81] H. Turnbull, *The Guitar from the Renaissance to the Present Day*. Bold Strummer, 1992.

[82] N. H. Fletcher and T. D. Rossing, *The Physics of Musical Instruments*, 2nd ed. Springer, 1998.

[83] E. Somogyi, “Principles of Guitar Dynamics and Design from the 1992 convention lecture,” *American Lutherie*, vol. 36, 1993.

[84] I. Curtu, M. D. Stanciu, N. C. Cretu, and C. I. Rosca, “Modal analysis of different types of classical guitar bodies,” in *Proceedings of the 10th WSEAS international conference on Acoustics & music: theory & applications*, Stevens Point, Wisconsin, USA, 2009, pp. 30–35.

[85] A. Okuda and T. Ono, “Bracing effect in a guitar top board by vibration experiment and modal analysis,” *Acoustical Science and Technology*, vol. 29, no. 1, pp. 103–105, 2008.

[86] T. Sumi and T. Ono, “Classical guitar top board design by finite element method modal analysis based on acoustic measurements of guitars of different quality,” *Acoustical Science and Technology*, vol. 29, no. 6, pp. 381–383, 2008.

[87] H. C. Jensen, “Production of Chladni Figures on Vibrating Plates Using Continuous Excitation,” *American Journal of Physics*, vol. 23, no. 8, pp. 503–505, Nov. 1955.

[88] R. Lawther, “Assessing how changes to a structure can create gaps in the natural frequency spectrum,” *International Journal of Solids and Structures*, vol. 44, no. 2, pp. 614–635, Jan. 2007.

[89] H. Carrington, “CV. The elastic constants of spruce,” *Philosophical Magazine Series 6*, vol. 45, no. 269, pp. 1055–1057, 1923.

[90] M. E. Haines, “On Musical Instrument Wood,” *J. Catgut Acoustical Society*, vol. 31, pp. 23–32, 1979.

[91] M. E. McIntyre and J. Woodhouse, “On measuring wood properties, Part 3,” *J. Catgut Acoustical Society*, vol. 45, pp. 14–23, 1986.

[92] M. E. McIntyre and J. Woodhouse, “On measuring wood properties, Part 2,” *J. Catgut Acoustical Society*, vol. 43, pp. 18–24, 1985.

[93] M. E. McIntyre and J. Woodhouse, “On measuring the elastic and damping constants of orthotropic sheet materials,” *Acta Metallurgica*, vol. 36, no. 6, pp. 1397–1416, Jun. 1988.

[94] E. Kahle and J. Woodhouse, “The influence of cell geometry on the elasticity of softwood,” *J Mater Sci*, vol. 29, no. 5, pp. 1250–1259, Mar. 1994.

[95] L. Mishnaevsky Jr. and H. Qing, “Micromechanical modelling of mechanical behaviour and strength of wood: State-of-the-art review,” *Computational Materials Science*, vol. 44, no. 2, pp. 363–370, Dec. 2008.

[96] P. Dumond and N. Baddour, “Effects of using scalloped shape braces on the natural frequencies of a brace-soundboard system,” *Applied Acoustics*, vol. 73, no. 11, pp. 1168–1173, Nov. 2012.

[97] P. Dumond and N. Baddour, “Effects of a Scalloped and Rectangular Brace on the Modeshapes of a Brace-Plate System,” *International Journal of Mechanical Engineering and Mechatronics*, vol. 1, no. 1, pp. 1–8, 2012.

[98] P. Dumond and N. Baddour, “A structured approach to design-for-frequency problems using the Cayley-Hamilton theorem,” *SpringerPlus*, vol. 3, no. 1, p. 272, May 2014.

[99] P. Dumond and N. Baddour, “A structured method for the design-for-frequency of a brace-soundboard system using a scalloped brace,” *Applied Acoustics*, vol. 88, pp. 96–103, Feb. 2015.